The role of RNA splicing factors in the regulation of longevity

HARVARD UNIVERSITY
Graduate School of Arts and Sciences

DISSERTATION ACCEPTANCE CERTIFICATE

The undersigned, appointed by the

Committee on Higher Degrees in Biological Sciences in Public Health

have examined a dissertation entitled

The role of RNA splicing factors in the regulation of longevity

presented by Sneha Dutta

candidate for the degree of Doctor of Philosophy and hereby certify that it is worthy of acceptance.

Signature _____

Typed name: Prof. Zachary Nagel

Signature _____

Typed name: Prof. Jean Schaffer

Signature _____

Typed name: Prof. Keith Blackwell

Signature _____

Typed name: Prof. Marian Walhout

Date: July 16, 2021

The role of RNA splicing factors in the regulation of longevity

A dissertation presented

by

Sneha Dutta

to

The Committee on Higher Degrees in Biological Sciences in Public Health

in partial fulfillment of the requirements

for the degree of

Doctor of Philosophy

in the subject of

Biological Sciences in Public Health

Harvard University

Cambridge, Massachusetts

July 2021

Dissertation Advisor: William B. Mair **Sneha Dutta**

The role of RNA splicing factors in the regulation of longevity

Abstract

Geroscience aims to target the aging process to extend healthspan. However, the efficacy of pro-longevity interventions is highly heterogeneous, limiting their translational potential. In my dissertation research, I discovered that activity of RNA splicing factors REPO-1 and SFA-1 early in life, modulates effectiveness of known longevity interventions in *C. elegans*. Inhibition of REPO-1 and SFA-1 during development blocks lifespan extension in genetic mutants of dietary restriction, reduced TORC1 signaling and reduced electron transport chain function. However, they are not required for longevity in the insulin signaling mutants. Strikingly, this is mediated through the regulation of lipid utilization via a POD-2/ACC1 dependent mechanism. The effect on lifespan is seen only when REPO-1 and SFA-1 are inhibited early in life and in the nervous system. Finally, early inhibition of REPO-1 and SFA-1 blocks lifespan extension by late onset suppression of the TORC1 pathway. Together these data highlight how early RNA splicing changes impacts response to longevity interventions and may explain variance in efficacy between individuals.

TABLE OF CONTENTS

List of Figures and Tables

Acknowledgements

My journey to pursue a Ph.D. at Harvard is nothing short of a dream. And there are so many people I met along the way who made it possible to turn this dream into a reality.

I would first like to thank my mentor, Dr. William Mair, without whom, this journey wouldn't have been possible. In the last five years, I have learnt so much from him. His enthusiasm for science is contagious and I cannot remember meeting him to discuss work and not leaving motivated and inspired to do more experiments. He taught me the value of effective science communication which is a virtue I want to take with me wherever I go. I deeply admire Will's 'radical candor' which has truly helped me grow as a scientist. I was fortunate to be part of such a wonderfully collaborative lab environment that he has nurtured. It is hard to miss how much invested Will is in the success of his students and I have been incredibly lucky to have him guide me through my Ph.D.

I am extremely grateful to have been a part of such an amazing lab during my Ph.D. Coming to the United States for the first time, the lab was more than my workplace. It has been my family. A big thank you to all the past and present members of the Mair Lab- Anne, Caroline (Heintz), Kris, Yue, Heather, Caroline (Escoubas), Gio, Pallas, Hannah, Maria, Noel, Arpit, Vanessa, Aditi, Miriam, Sam, Porsha, Malini, Nicole, Emina, Rohan, Andrew, Peter. It was an absolute privilege working with such a hardworking and dynamic team of scientists and they inspired me to give my best every day. A special thank you to Caroline (Heintz) who has been more than a colleague to me. She helped me tremendously in getting my project started and has always been a patient listener and a caring friend during those tough days in the lab. To Anne, I cannot thank her enough for being my biggest support in the lab. She helped me get started during my first days in the country, both in the lab and outside, and patiently answered all my questions. A big thank you to Kris

for teaching me so much when I started in the lab- from how to pick a worm to designing the perfect primer. His mentorship really made me appreciate how fascinating *C. elegans* research is.

I would like to thank members of my qualifying exam and dissertation advisory committee- Marianne Wessling-Resnick, Jay Mitchell, Eric Greer, Frank Slack, Ed Chouchani and Zachary Nagel. Their critical feedback on my work challenged me, gave me direction, and helped me prioritize experiments during my Ph.D. A special thank you to past and present members of the BPH office who helped me navigate through graduate school- Tatevik, Eric, Deirdre and Tom.

I am deeply grateful to have made such wonderful friends at Harvard that made this journey a lot of fun. Special thanks to Rebecca, Aditi, Bobby and Serg for being there for me during grad school.

To all the teachers and mentors who instilled the love for science in me, I am indebted. Words are not enough to thank my first science tutor, Kalyan Sir, who sowed the seeds of scientific curiosity in me. A big thank you to my college professors, particularly Dr. Arup Kumar Mitra who gave me the opportunity to work on my first research project. I am also deeply grateful to Dr. Gotam K. Jarori and Dr. Ullas Kolthur Seetharam for their mentorship during my Master's program that convinced me to pursue a Ph.D.

I feel truly blessed to have so many kind and wonderful people as my friends outside of graduate school. To the old friends I'll always cherish and the new friends I made in Boston- a big thank you for being a part of my journey! I am particularly grateful for my friends Momtanu, Jayeeta and Anwesha for being my constants.

I am incredibly blessed to have the best sister in the world. Thank you, Didi, for those late-night video calls and lengthy conversations where I could bare my heart out. I would not have survived grad school without

you. A big thank you to my brother-in-law, Siddhartha Da, for always being supportive, especially during the time I was applying to graduate school.

To Ma and Baba, I cannot thank you enough. Everything I am today, I owe it to you. I thank you for believing in me, for working so hard to educate me, for motivating me to achieve my goals and putting my dreams and aspirations above everything else. I am incredibly blessed to be your daughter.

Finally, I would like to thank the most incredible man I know, my husband, Ranadeep. I am truly blessed to have met him during my Ph.D. Thank you for being the calming presence in my life and always helping me see things in perspective. You inspire me to be the best that I can be.

P.S. A big shoutout to all the canine friends I made along the way that made this journey beautiful!

CHAPTER 1

Introduction

1.1 Aging is a risk factor for multiple chronic diseases

In the beginning of the 20th century, the average life expectancy in humans was ~47 years (National Center for Health Statistics (US), 2011). Over one hundred years later, this number has almost doubled. This is the result of several contributing factors. Major advances in medical science like the development of vaccines and drugs to prevent and treat infectious diseases to better public health practices have all supported this striking increase in the median lifespan of human beings. This number is further expected to increase, and it is predicted that by 2100, >20% of the world population will be greater than 65 years of age (Escoubas et al., 2017) (**Figure 1.1**).

While reduction in mortality rates have empowered people to live longer lives, there has been a concomitant increase in various non-infectious diseases such as neurodegeneration, metabolic disease, cardiovascular disease, osteoporosis and cancers. In fact, age is the biggest underlying risk factor for these chronic conditions. Often several age-associated diseases often occur as comorbidities and the crippling effect of these conditions drastically reduces the quality of life in the older population (Burkewitz et al., 2016). Most recently, we have seen that the older population has been the hardest hit by the COVID-19 pandemic, further arguing aging as a vulnerability and a major public health concern. As Guy C Brown, Professor of Neuroscience at the University of Cambridge, UK rightly quotes:

"…years are being added to our lives, life is not being added to our years: the extra years are being added at the very end of our lives and are of poor quality".

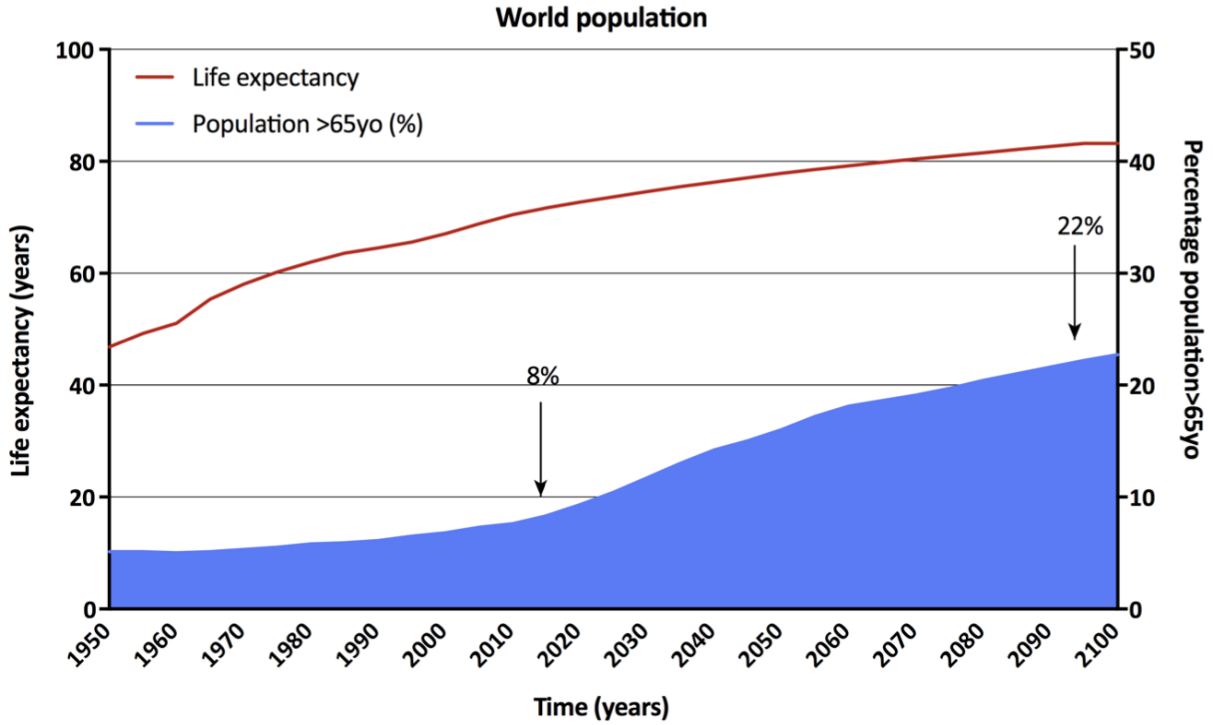

Figure 1.1: Trends in life expectancy and percentage of population >65 years around the world.

Life expectancy has been gradually increasing in the last 70 years. This has resulted in an increase in the percent of people >65 years and the number is expected to rise dramatically in the next century.

Figure adapted from (Escoubas et al., 2017) *with permission.*

1.2 Anti-aging interventions as a strategy to target multiple age-related comorbidities

Age associated diseases like cancer, diabetes and neurodegeneration are caused by multiple genetic and environmental factors, many of which remain to be understood. Efforts in the last three decades have mainly focused on treating each disease in isolation. Patient age is the predominant factor underlying these chronic conditions and more often than not, the elderly population suffer from more than one condition simultaneously (**Figure 1.2**). The hallmarks of aging such as loss of metabolic plasticity, loss of proteostasis, DNA damage and mitochondrial dysfunction are implicated in many of these age-related disorders (López-Otín et al., 2013). Therefore, a more impactful approach might be to classify aging itself as a disease and explore strategies to delay or reverse this process and thereby ameliorate the occurrence of

these chronic conditions. This strategy has been cited as a more efficient way to improve the quality of life and reduce the economic burden associated with late-life illnesses (Goldman et al., 2013).

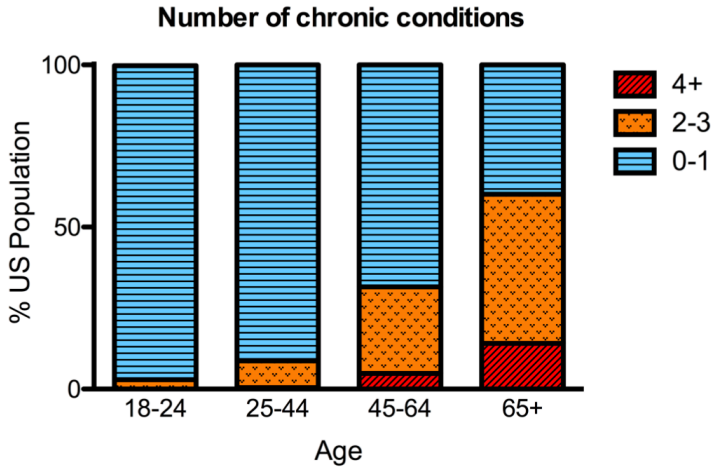

Figure 1.2: Aging leads to the incidence of multiple comorbidities.

With increased biological age, the proportion of population in the US that suffer from multiple chronic conditions increases.

Figure adapted from (Burkewitz et al., 2016) *with permission.*

1.3 Dietary Restriction (DR) is a robust intervention to delay aging

Aging is a malleable process that can be manipulated by various genetic and pharmacological interventions. The most widely studied cellular processes in the context of aging are nutrient signaling pathways, which influence the rate of aging in multiple species. Generally, anabolic processes that lead to excess nutrient and energy, accelerate the rate of aging. In contrast, activation of catabolic processes slows down the aging process. One method of influencing these pathways is by manipulating the diet and the most widely studied regimen is called dietary restriction (DR), which is reduced caloric intake without malnutrition. The reduced energy intake pushes the body to a catabolic state, thus promoting lifespan and healthspan in every organism it has been tested in thus far (Fontana and Partridge, 2015; Mair and Dillin, 2008). Dietary restriction was first documented by Dr. Clive McCay, a biochemistry professor at Cornell University in 1935 (McCay et

al., 1935). He dietary restricted rats and showed that they lived significantly longer than their *ad libitum* fed counterparts. This discovery led him to develop a high protein Cornell bread for the soldiers of World War II, to aid in better rationing of provisions during war. While McCay's DR experiments were severe, subsequent studies over many decades and in multiple species ranging from yeasts to rhesus monkeys have shown that a much milder DR, that does not result in severe deficiencies, can still have a positive effect on lifespan.

While DR extends lifespan, it has also been shown to reduce the incidence of age-related disorders. For example, it was observed in two different ~40 year longitudinal studies in rhesus monkeys (at National Institute of Aging and at the Wisconsin National Primate Research Center) that DR significantly reduced the occurrence of neoplasia, cardiovascular disease and metabolic syndrome (Colman et al., 2009, 2014; Mattison et al., 2012, 2017). DR also improves health outcomes in patients with cancers (Brandhorst and Longo, 2016), neurodegenerative diseases (Fontana and Partridge, 2015; Pani, 2015) and metabolic disorders (Larson-Meyer et al., 2006).

Unfortunately, DR has its side effects. It negatively impacts growth, reproduction, thermoregulation, wound healing and bone density (Dirks and Leeuwenburgh, 2006). It also takes a severe toll on the psychological health. Humans undergoing DR have reported lower cognitive function and a poorer quality of life (Dirks and Leeuwenburgh, 2006; Redman and Ravussin, 2011). Furthermore, the beneficial effects of DR seems to be short-lived. This was shown elegantly in fruit-flies wherein reversing flies on DR to an *ad libitum* fed diet leads to an immediate switch in their mortality rates (Mair et al., 2003). Therefore, a major aim of aging researchers is to unravel the molecular mechanisms underpinning the beneficial effects of dietary restriction. In doing so, the negative side effects can be uncoupled to make DR more translatable to the general population.

1.4 *C. elegans*- A powerful model organism in geroscience

Caenorhabditis elegans has emerged as one of the most versatile and powerful genetic systems to study aging. *C. elegans* are 1mm long, free-living nematodes that were initially isolated from the soil. It was in 1963 when Sydney Brenner proposed the use of this organism to study neuronal development, owing to its simple genetics, for which he was later awarded the Nobel Prize in Physiology and Medicine in 2002. These nematodes quickly became popular and were being used in laboratory research to study different aspects of biology.

What made them particularly popular in aging research was its relatively short lifespan. Wildtype *C. elegans* live for roughly 2-3 weeks (**Figure 1.3**). They live as hermaphrodites and each adult worm can lay 250-300 eggs which also make it possible to grow large number of isogenic populations in a very short amount of time. Hermaphrodites can be easily induced to generate male progeny which can be used for genetic crosses.

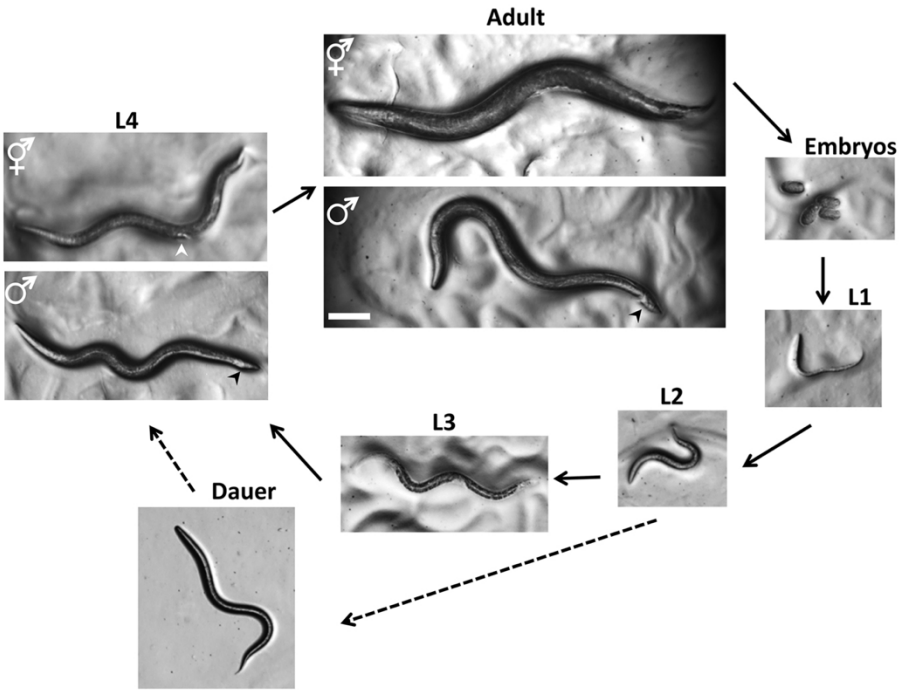

Figure 1.3: *C. elegans* life cycle.

C. elegans go through four larval stages (L1-L4) before reaching adulthood. The cycle takes approximately 72 hours in a wildtype worm. When pre-L2 larvae experience stress such as starvation, they can form the

Figure 1.3 (Continued) dauer larvae. The dauers are highly resilient to stress and can survive under harsh conditions for many months until the ambience is favorable to resume growth.

Figure from (Corsi, 2015).

C. elegans genomes have been fully sequenced and are genetically tractable making it economic and efficient to generate mutations and deletions to study various aging processes. There have been large-scale EMS mutagenesis performed in them that have resulted in a wide array of mutants which are publicly available (Corsi, 2015). Moreover, two RNAi libraries- the Ahringer (Ahringer, 2006) and the Vidal library (Rual et al., 2004), are also available which is a great resource to knockdown almost any gene in these worms. The adult *C. elegans* hermaphrodite has 959 somatic cells and their anatomy has been completely documented. Furthermore, it has a well elucidated network of tissues and robust tissue-specific promoters have been characterized (Okkema and Krause, 2005). More recently, CRISPR has also been successfully implemented making it possible to delete genes at specific loci, generate point mutations as well as tag endogenous genes (Paix et al., 2015). It is interesting to note that the first long-lived genetic mutant was in fact discovered in *C. elegans* (Kenyon, 2011) that set the precedence for aging research in this model organism.

1.5 DR and other longevity paradigms in *C. elegans*

Due to its short lifespan and easy genetics, *C. elegans* has been the model organism of choice among aging researchers for many decades. This has resulted in the discovery of many pathways and cellular processes that contribute to the aging process. Many dietary interventions such as DR as well as genetic and pharmacological interventions have been successfully tested in *C. elegans*.

Dietary Restriction (DR)

Dietary restriction was first demonstrated to extend lifespan in *C. elegans* in the 1970s (Klass, 1977). Since then, researchers have applied DR using multiple different methodologies. *C. elegans* growing in the laboratory use bacteria as their food source and reducing the amount of bacteria available to them is the

most common way of implementing DR. Bacterial Dietary Restriction or bDR was the first protocol used wherein worms were grown in liquid culture containing different concentrations of *E. coli* bacteria (Klass, 1977). Worms generally live on solid matter and growing them in liquid media induces multiple unwanted physiological changes (Lev et al., 2018). Therefore, bDR was adapted to be used on solid agar plates and called solid plate DR (sDR) wherein bacteria are heavily diluted and seeded onto plates in the presence of antibiotics (to prevent further bacterial multiplication), such that less food is available to worms.

A more popular genetic approach to reduce food intake in *C. elegans* are by using the '*eat*' mutants which have reduced rates of pharyngeal pumping, eat less food, and therefore live longer than wildtype worms (Lakowski and Hekimi, 1998). The most widely used *eat* mutant is the *eat-2* worm that have an abnormal acetylcholine-gated cation channel activity resulting in reduced pharyngeal pumping, less food intake and significant increase in lifespan (Lakowski and Hekimi, 1998). Another more radical approach of DR is bacterial deprivation (BD) that involves complete removal of food source during adulthood which also robustly extends lifespan (Kaeberlein et al., 2006). More recently, intermittent fasting (IF) is being applied in worms wherein worms are fed for two days followed by two days of starvation (Honjoh et al., 2009). Time restricted feeding (TRF) is another paradigm of dietary restriction that robustly extends lifespan which is studied in other organisms but is a limitation in *C. elegans* as they do not have a defined circadian rhythm. While several methods of DR are applied in worms, it has been shown that the resulting lifespan extension occur through many unique and some overlapping mechanisms.

Supporting the 'rate of living hypothesis', it was initially believed that DR acts by reducing the metabolic rate of the organism. However, this theory was quickly disproven as measures of metabolic rate such as oxygen consumption did not change in worms subjected to BDR (Houthoofd et al., 2002). Soon, multiple mediators of DR were identified. The most widely studied is the role of DR through reduction of TORC1 function (discussed next). TORC1 is a central nutrient sensing molecule in the cell which is activated in response to nutrient excess. It has been shown that reduction of TORC1 because of DR leads to upregulation

of autophagy which is essential for lifespan induction in DR (Hansen et al., 2008; Jia and Levine, 2007; Tóth et al., 2008). Several transcription factors like PHA-4 (FOXA) (Panowski et al., 2007), HLH-30 (TFEB) (Lapierre et al., 2013) and NHR-62 (Heestand et al., 2013) mediate the increased autophagic flux. Other studies have attributed the requirement of *daf-16*, the worm ortholog of FOXO, essential for longevity in sDR (Greer et al., 2009) and IF (Honjoh et al., 2009). Furthermore, longevity in certain *eat-2* mutants requires sirtuins (Wang and Tissenbaum, 2006) whereas other modes of DR do not (Lamming, 2005).

Reduced TORC1 signaling

TORC1 signaling is a central anabolic pathway whose activity has been implicated in aging and multiple age-associated disorders like cancer. Its activity is regulated by multiple activating and inhibiting proteins, most of which are conserved in *C. elegans*. Inhibiting the activators of this pathway thereby reducing TORC1 signaling, leads to longevity. The most common are the Rag-GTPases RAGA-1 and RAGC-1 which sense the presence of amino acids and activate the TORC1 signaling cascade. Reducing their function by either RNAi or mutation leads to lifespan extension in *C. elegans* (Robida-Stubbs et al., 2012; Schreiber et al., 2010). Pharmacological inhibition of TORC1 signaling using rapamycin has also been shown to robustly increase lifespan in worms, flies and mice (Bjedov et al., 2010; Harrison et al., 2009; Robida-Stubbs et al., 2012). More recently, the effect of rapamycin is being tested on higher vertebrates such as dogs through the Dog Aging Project.

Studies show that longevity through reduced TORC1 is mediated through multiple mechanisms including reduction of protein synthesis (Hansen et al., 2007) and induction of autophagy (Hansen et al., 2008; Lapierre et al., 2013). These are mediated through different transcription such as DAF-16/FOXO SKN-1 (Nrf2) (Robida-Stubbs et al., 2012), PHA-4/FOXA(Sheaffer et al., 2008), Heat Shock Factor HSF-1 (Seo et al., 2013) and Hypoxia Inducible Factor HIF-1 (Chen et al., 2009). While TORC1 is a kinase activated by excess nutrients and growth signals, a similar kinase, AMPK (AMP Activated Protein Kinase) is activated when nutrient availability is low. In fact, reduced TORC1 signaling activates AMPK and

overexpression of the active form of AMPK is sufficient to extend lifespan in *C. elegans* (Apfeld et al., 2004; Mair et al., 2011). Recently, a study published from the Mair lab and pioneered by a former graduate student Yue Zhang, showed that loss of neuronal TORC1 and activation of neuronal AMPK is sufficient for mediating the longevity effects of reduced TORC1 signaling (Zhang et al., 2019). She showed that rescuing TORC1 signaling specifically in the neurons in the otherwise long-lived *raga-1* mutant reverts their lifespan comparable to wildtype worms. This effect is mediated by a cell non-autonomous process wherein loss of neuronal TORC1, through neuropeptides, results in peripheral changes in mitochondrial structure and function. What signals mediate this cell non-autonomous communication remains to be studied.

Reduced Electron Transport Chain (ETC) function

Another broadly studied class of long-lived strains in *C. elegans* are those that have mutations in the electron transport chain components, leading to reduced mitochondrial function. These are broadly classified as the 'Mit' (mitochondrial) mutants. Initially, their longevity was attributed to the fact that reduced ETC resulted in reduced ROS production which would result in lesser cellular damage (Rea, 2005; Sedensky and Morgan, 2006). However, this idea was disproved as oxidative stress did not correlate with lifespan extension in worms with compromised ETC function (Rea et al., 2007). Furthermore, loss of ETC function is required specifically in the larval stages of worm development to mediate longevity (Dillin et al., 2002; Durieux et al., 2011; Rea et al., 2007). Studies showed that upregulation of the mitochondrial UPR because of loss of ETC function is required for their longevity (Durieux et al., 2011). However, contrasting evidence suggest that loss of ATFS-1, the transcriptional factor that mediates the mitoUPR response, does not impact the longevity of ETC mutants (Bennett and Kaeberlein, 2014). Furthermore, it is believed that DR and ETC mutants mediate longevity potentially through similar mechanisms. This is supported by the fact that lifespan extension of the DR mutant *eat-2* and the ETC mutant *clk-1* are not additive. Also, both DR and ETC mutants require AMPK as a mediator (Curtis et al., 2006).

What is particularly interesting is that while mutations in several components of the ETC leads to longevity, mutations in others in fact are lethal and make worms shorter lived. What is the basis of this selectivity is unknown. Therefore, much remains to be understood about the 'Mit' mutants and how they mediate longevity.

Reduced insulin/insulin-like peptide (IIS) signaling

The first long-lived mutants ever discovered were the insulin signaling mutants in *C. elegans* (Friedman and Johnson, 1988; Kenyon, 2011; Kenyon et al., 1993). The most well studied are mutations in genes that code for DAF-2 (insulin receptor) and AGE-1 (PI3K) which live almost twice as long as wildtype worms. The role of IIS in longevity regulation is not limited to *C. elegans* and similar observations have been seen in fruit flies (Clancy, 2001; Tatar, 2001) and mice (Blüher et al., 2003; Holzenberger et al., 2003). Reduced insulin signaling affects lifespan primarily through nuclear localization of DAF-16 (Henderson and Johnson, 2001; Lee et al., 2001; Lin et al., 2001) and activation of transcription factors HSF-1 (Seo et al., 2013) and SKN-1 (Tullet et al., 2008). Longevity of *daf-2* mutants also require the catalytically active subunit of AMPK(Apfeld et al., 2004). Furthermore, just like TORC1 mutants, IIS mutants also require autophagy to extend lifespan (Melendez, 2003). However, IIS and TORC1 affect longevity through distinct mechanisms as mutations in these pathways have an additive effect on lifespan (Chen et al., 2013).

How these different longevity paradigms in *C. elegans* act to regulate lifespan and what are the unique and shared mechanisms at play, that contribute to their positive impact on aging, needs future exploration.

1.6 Role of RNA splicing in aging and longevity

Aging is characterized by a gradual decline in different biological functions that maintain the normal physiology of an organism. It is marked by the incidence of several pathologies like cancers, neurodegenerative disorders, cardiovascular diseases and metabolic syndrome. DR delays or reverses the incidence of several hallmarks associated with aging. At the cellular level, DR improves response to DNA

damage (Haley-Zitlin and Richardson, 1993), delays age-induced mitochondrial deregulation (Ruetenik and Barrientos, 2015; Weir et al., 2017) and improves proteostasis (Matai et al., 2019). At the systemic level, it prevents the occurrence of multiple age-associated disorders like metabolic dysfunction (Colman et al., 2009, 2014; Mattison et al., 2012) and protects against stem cell exhaustion (Mana et al., 2017).

While how aging impacts the cells at the level of DNA and protein is more widely studied, little is known about how it influences the process of transcription and post-transcriptional regulation, thereby affecting cellular RNA. RNA is the critical link between the genetic code and proteins which are the major functional players in a cell. Processing of these RNAs through alternative splicing is also a critical mechanism that allows the building of transcriptomic and proteomic complexity in higher organisms (**Figure 1.4**). There are multiple checkpoints to ensure that the right pool of RNA is maintained in the cells. It comprises of regulation of transcription, capping and polyadenylation of the newly synthesized RNA, splicing of the RNAs and finally, turnover of old or incorrectly synthesized mRNA. With increasing age, disruption of RNA homeostasis can happen due to dysregulation in any of these checkpoints. **Figure 1.5** highlights the points of dysregulation- changes to splicing factor expression and function, aberrant splicing, defective RNA surveillance and aberrant mRNA translation.

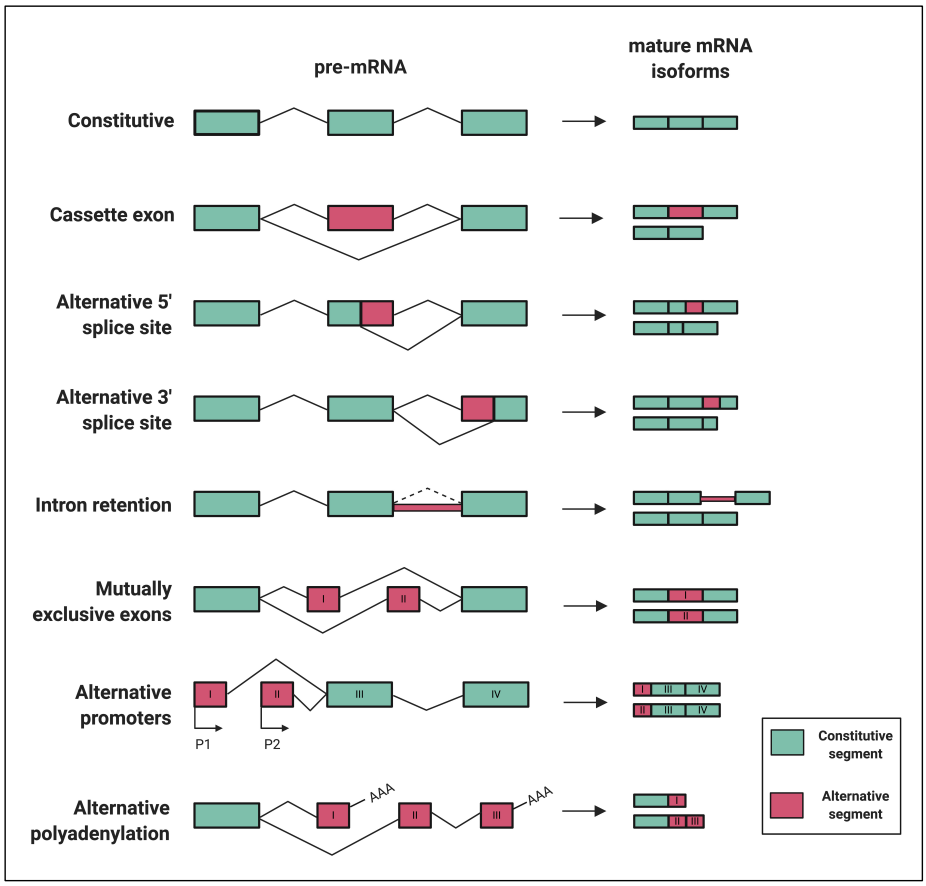

Figure 1.4: Constitutive and alternative splicing events.

Seven types of alternative splicing are cassette exon, alternative 5′ splice site, alternative 3′ splice site, mutually exclusive exons, intron retention, alternative promoter and alternative polyadenylation. Boxes represent exons and lines represent introns.

Figure from "Alternative splicing in aging and longevity" (Bhadra et al., 2020).

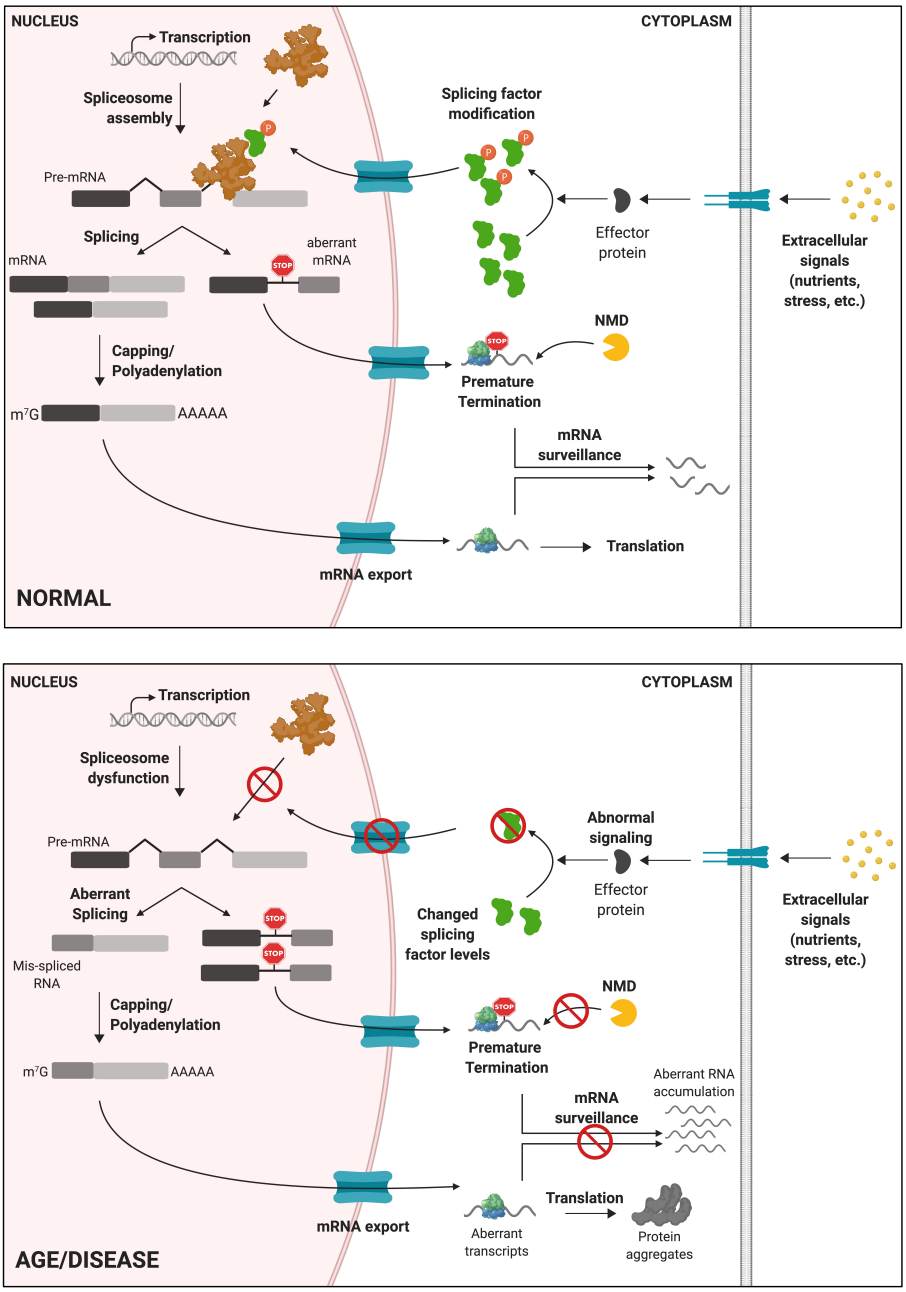

Figure 1.5: Regulation of RNA processing and disruption with age and disease.

RNA processing fidelity is maintained at multiple points between transcription and translation in normal physiology. With advanced age, disruption of RNA homeostasis can compromise cellular/tissue function and contribute to development of age-related diseases. Depicted are some of the points of dysregulation in RNA homeostasis including splicing factor expression changes, and modifications affecting splicing factor localization, spliceosome dysfunction, aberrant splicing, defective RNA surveillance and aberrant mRNA translation.

Figure from "Alternative splicing in aging and longevity" (Bhadra et al., 2020).

Age-associated global changes in alternative splicing events

With the development of more improved, high throughput deep sequencing platforms in the last two decades, the study of changes to cellular RNA at the nucleotide level has been made possible. This has allowed researchers to study the change in RNA not only at the level of expression, but also observe splicing changes with age and in with different treatments. Changes to alternative splicing has been shown with advanced aging in human blood (Harries et al., 2011), senescent fibroblasts and endothelial cells (Holly et al., 2013). In *C. elegans*, a published study pioneered by a postdoctoral fellow in our laboratory, Dr. Caroline Heintz, showed that with age, there is increased aberrant splicing marked by increased reads in introns and unannotated splice junctions (Heintz et al., 2017). Similarly, age-related increases in alternative exon usage have been shown across five different mouse tissues: skin, skeletal muscle, bone, thymus, and white adipose tissue (Rodríguez et al., 2016). Furthermore, alterations to alternative splicing is associated with mouse strain longevity (Lee et al., 2016) (**Figure 1.6**).

Increase in intron retention is emerging as a common feature in aging organisms. As seen in *C. elegans* (Heintz et al., 2017), it was also reported in *Drosophila* heads that with increased age, there was a concomitant increase in intron retention in genes at a global level (Adusumalli et al., 2019). A similar increase was observed in aging mice frontal cortex and hippocampus (Adusumalli et al., 2019).

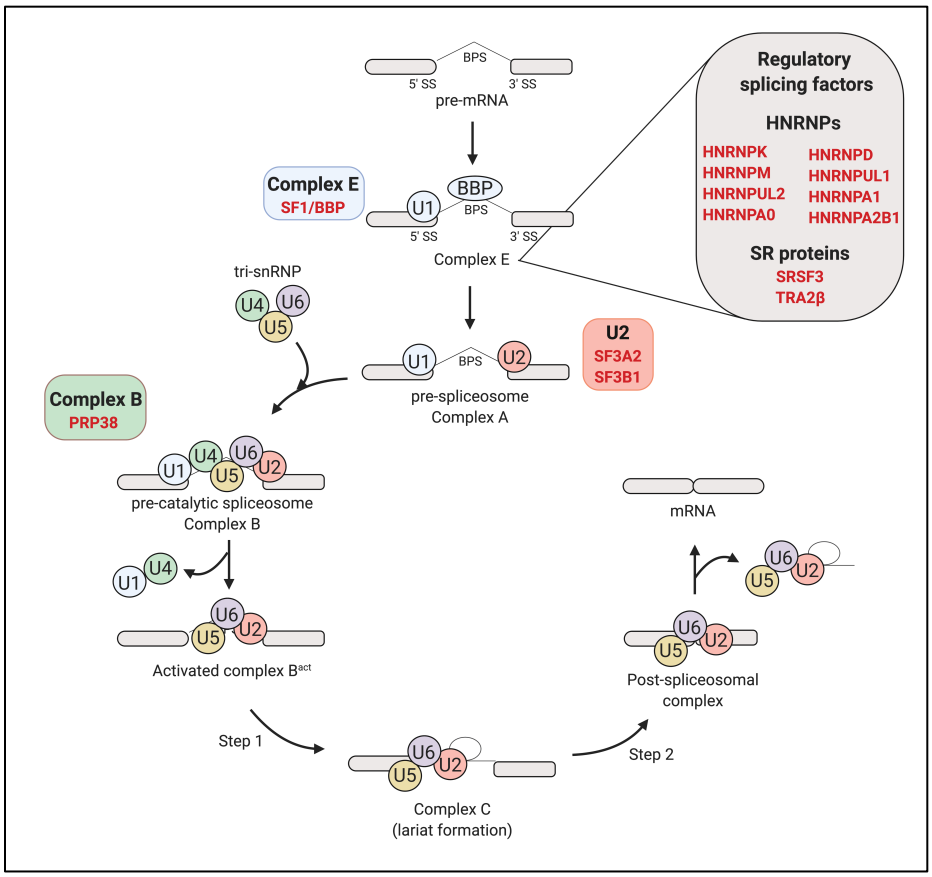

Figure 1.6: Core and regulatory splicing factors are implicated in longevity.

Longevity associated splicing factors participating at different stages of the splicing process are depicted in red. Expression of *Hnrnpk*, *Hnrnpul2*, *Hnrnpm*, *Hnrnpd*, *Hnrnpa0*, *Hnrnpul1*, *Sf3b1*, *Srsf3* and *Tra2β* are associated with strain longevity in mice (Lee et al., 2016). *Hnrnpa1* and *Hnrnpa2b1* levels are associated with strain longevity in mice as well as parental longevity in humans (Lee et al., 2016) while expression of PRP-38 is required for mediating longevity in *C. elegans* (Curran 2007). Notably, splicing factors SF1/SFA-1, SF3A2/REPO-1 (Heintz et al., 2017) and HNRNPUL1/ HRPU-1 (Tabrez et al., 2017) are required for DR-mediated longevity in *C. elegans.*

Figure from "Alternative splicing in aging and longevity" (Bhadra et al., 2020).

Splicing dysregulation in age-associated diseases

Disruptive changes to splicing have also been observed in different chronic conditions associated with aging. A decline in cognitive abilities is one of the most common signs of aging and leads to multiple neurodegenerative pathologies such as Alzheimer's disease (AD) and Parkinson's disease. Interestingly, the nervous system is a hotspot for splicing factor function and therefore, changes to alternative splicing

with advanced age in brains from mice (Stilling et al., 2014) and humans (Mazin et al., 2013; Tollervey et al., 2011) have been studied. It was observed that 95% of changes to splicing events in the human temporal cortex with age was also observed in patients with AD or FTLD (Frontotemporal Lobar Degeneration) (Tollervey et al., 2011). An increase in intron inclusion events was observed) in genes involved in mRNA and protein homeostasis in human prefrontal cortex of patients suffering from AD (Adusumalli et al., 2019).

Besides global effects on splicing, incorrect splicing of individual genes lead to diseases. For example, an exon inclusion event in the pre-mRNA of the TP53 gene leads to generation of an isoform which promotes cellular senescence (Fujita et al., 2009). In another case, an otherwise silent mutation in the Lamin A gene leads to activation of a cryptic 5′ splice site resulting in the formation of a truncated lamin. This leads to the Hutchison Gilford progeria syndrome (McKenna et al., 2014). These are only a few examples, and it is increasingly becoming clear that the root cause of many age-associated disorders lie in isoform level differences of genes as opposed to gene expression changes themselves.

1.7 DR protects against age-induced splicing dysfunction

Since aging results in decline of splicing fidelity and DR ameliorates multiple hallmarks of aging, we asked whether DR protects against age-induced splicing dysfunction. In a study published earlier from our lab, we showed that in *C. elegans*, DR delayed the age-onset dysregulation of global splicing (Heintz et al., 2017). Briefly, RNA-Seq was performed in young (Day 3) and old (Day 15) *C. elegans* to examine global mRNA splicing with age. Day 15 old ad libitum (AL) fed animals showed a modest increase in intron retention and unannotated splice junctions which are indicative of changes in global splicing with age. To test if this process was impacted by DR, a robust paradigm for longevity, the same splicing parameters were analyzed in *eat-2(ad1116)* worms which is a genetic model of DR. Notably, DR reduced the age-associated increase in alternative splicing events that was detected with age in AL fed worms (**Figure 1.7 A,B**).

To examine the role of pre-mRNA splicing in DR using a multicellular system, an in vivo fluorescent alternative splicing reporter in *C. elegans* was used (Kuroyanagi et al., 2013). This reporter strain expresses a pair of *ret-1* exon 5 reporter minigenes with differential frame shifts, driven by the ubiquitous *eft-3* promoter (**Figure 1.7C**). GFP indicates exon 5 has been included whereas expression of mCherry indicates exon 5 has been skipped. While animals fed AL diet show more mCherry expression indicative of exon skipping with age (Day 5) (**Figure 1.7D**), dietary restricted worms maintained a youthful splicing pattern indicated by GFP retention at old age (**Figure 1.7E**). Using this reporter as a readout, it was also shown that early splicing events could serve as a marker of life expectancy (Heintz et al., 2017).

A network-based analysis of the genes most responsive to DR across 17 tissues in mice uncovered a role for RNA processing (Swindell, 2009). More recently, RNA sequencing identified exon skipping and alternate exon usage specifically in lipid genes in livers of rhesus monkeys post two years of DR (Rhoads et al., 2018). Further evidence that RNA processing is linked to DR came from a study in *C. elegans* wherein genes involved in nonsense-mediated RNA decay is required for longevity associated with DR (Tabrez et al., 2017).

Therefore, it is becoming increasingly clear that this link between DR and RNA splicing is a conserved phenomenon. However, how DR affects RNA splicing at the molecular level remains to be understood.

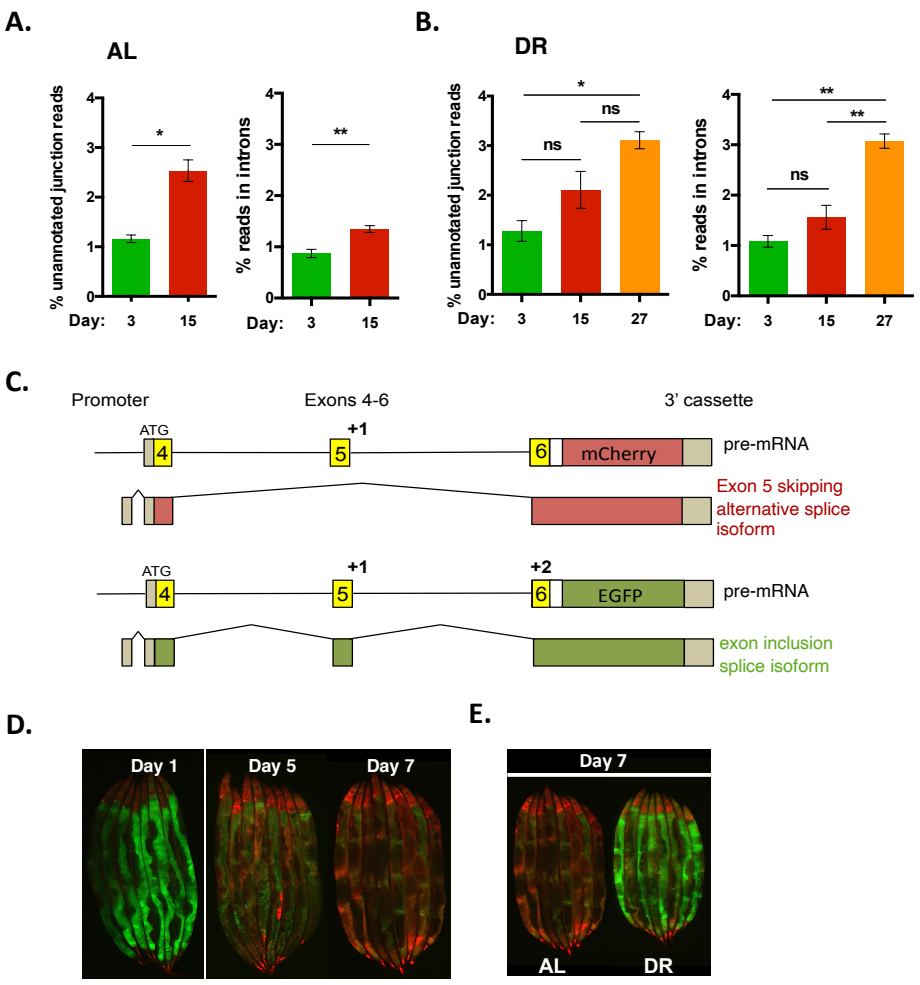

Figure 1.7: Age induces splicing dysfunction and DR protects against it.

A. Percent unannotated junction reads and intron inclusion reads in *ad libitum fed* WT worms at day 3 and day 15.

B. Percent unannotated splice junction reads and intron reads in DR worms at Day 3, 15 and 27. No significant difference is observed between Day 3 and Day 15 worms suggesting DR delays the onset of age-associated splicing dysfunction.

C. Schematic of the *ret-1* minigene reporter construct in *C. elegans*.

D. *ret-1* minigene reporter strain fed ad libitum at Day 1, Day 5 and Day 7. Age induces heterogeneity in splicing pattern by day 5 of adulthood.

E. *ad libitum* fed and dietary restricted *ret-1* minigene reporter strain at Day 7. DR maintains the youthful splicing pattern at Day 7.

Figure adapted from (Heintz et al., 2017).

1.8 REPO-1 and SFA-1 mediate DR longevity in *C. elegans*

To determine whether splicing fidelity contributes to the effect of DR on aging, a targeted reverse genetic screen for spliceosome components that affects lifespan extension in DR was performed by Dr. Caroline Heintz in our lab, using *eat- 2(ad1116)* worms. Knockdown was achieved by feeding worms with bacteria containing dsRNA. Based on the effect of their knockdown on the lifespan of AL and DR fed worms, the splicing factors could be grouped into three categories: I. those which had no effect on the lifespan of AL fed and DR worms (e.g. *rsp-2, rsp-3, hrpf-1*); II. those which reduced lifespan of both AL and DR worms suggesting that they are essential for survival (e.g. *uaf-2, snr-1, snr-2, hrp-2*); III. those that had no effect on the lifespan on AL fed worms but completely abolished DR mediated longevity (*sfa-1, repo 1*) (Heintz et al., 2017) (**Figure 1.8 A,B**). This third class of splicing factors namely SFA-1 and REPO-1 was of particular interest because they potentially play a role in mediating health benefits of DR. Furthermore, the study showed that SFA-1 mediates longevity via reduced TORC1 signaling likely through the same mechanism by which it regulates DR longevity.

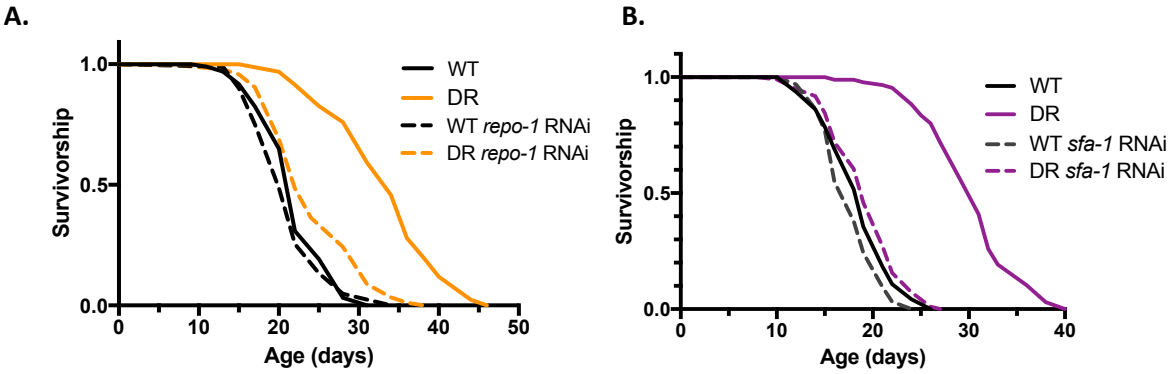

Figure 1.8: Splicing factors REPO-1 and SFA-1 are required for DR-mediated extension of lifespan.

WT and dietary restricted *eat-1(ad1116)* worms fed on control bacteria or bacteria expressing A. *repo-1* RNAi and B. *sfa-1* RNAi.

Figure adapted from (Heintz et al., 2017).

1.9 Open Question- Mechanism underlying REPO-1 and SFA-1 in mediating longevity

While it was clear that REPO-1 and SFA-1 are specifically required to confer DR mediated longevity in *C. elegans* (Fig 1.8 A,B), the mechanism remains unclear. The goal of my thesis is to dissect the mechanism by which these splicing factors mediate the positive impact DR has on lifespan. The central questions I aimed to address are:

(1) Are these splicing factors required specifically for DR mediated longevity or do they function in other longevity paradigms?

(2) What is the molecular mechanism by which REPO-1 and SFA-1 regulate DR longevity?

(3) What is the spatial and temporal requirement of REPO-1 and SFA-1 in mediating lifespan effects?

(4) How do the mammalian orthologs of REPO-1 and SFA-1 (and other splicing factors) change in response to age and DR in mice?

In summary, I discovered that the activity of RNA splicing factors REPO-1 and SFA-1 is important for longevity by dietary restriction, reduced TORC1 and reduced electron transport chain function but is dispensable for longevity in insulin signaling mutants. This is mediated via POD-2/ACC and regulation of lipid utilization. This effect is only seen when REPO-1/SFA-1 are inhibited early in life and in the nervous system. Finally, early inhibition of REPO-1 blocks lifespan extension by late onset suppression of the TORC1 pathway. Together these data highlight how early RNA splicing changes impacts response to longevity interventions and may explain variance in efficacy between individuals.

CHAPTER 2

Splicing factors REPO-1 and SFA-1 are required for lifespan extension in specific longevity paradigms

Introduction

Splicing factors REPO-1 and SFA-1 are required for DR mediated extension of lifespan in *C. elegans* (Heintz et al., 2017). However, it is unclear whether these splicing factors act downstream to DR by maintaining global splicing homeostasis or whether they are required for the processing of specific longevity targets.

REPO-1 and SFA-1 are known to be part of the core spliceosome complex. SFA-1 (or SF1/Branchpoint Binding Protein in mammals) binds to an important sequence, the branch point, which is located around 18 to 40 nucleotides upstream of the 3′ end of an intron that almost always contains an adenine residue. On binding to this site, it recruits U2AF1 (or *uaf-2* in worms) to the 3' splice site of the intron (Krämer, 1992; Ma et al., 2011; Ma and Robert Horvitz, 2009). This is followed by the binding of U2 ribonucleoprotein complex that also contains REPO-1 (or SF3A2 in mammals) which catalyzes the formation of the pre-spliceosome and subsequent steps of the splicing reaction. While these factors appear to be central to processing of all intron-containing genes, there are reports suggesting that they might be selective in the genes they splice. For example, it has been shown that SF1 binds to and is required for the splicing of only a subset of genes (Tanackovic and Krämer, 2005).

We surmised that if REPO-1 and SFA-1 were playing a role in processing of all genes and therefore maintaining global splicing homeostasis, losing these splicing factors would result in a breakdown of the transcriptome that would prevent animals from living beyond a certain point of time. In such a scenario, we might expect it to be required for extending lifespan in all long-lived mutants. Alternatively, if these splicing factors were to specifically process specific mRNA targets, we would expect to see some pathway specificity. The second scenario seems more credible as it was shown that SFA-1 is dispensable for longevity in the insulin signaling mutant *daf-2* (Heintz et al., 2017).

In this chapter, I will describe my work in building RNAi clones that specifically knock down these splicing factors and test their requirement in different longevity paradigms that are known to function through mechanistically distinct nodes.

Results

2.1 REPO-1 and SFA-1 are required for DR mediated longevity

Previously, we demonstrated a requirement for both REPO-1 and SFA-1 in the longevity of *eat-2(ad1116)* mutants- a genetic model of dietary restriction (Heintz et al., 2017). The TORC1 signaling cascade has been implicated as a mediator of the beneficial effects of dietary restriction (Kapahi et al., 2010). Direct suppression of mTORC1 increases lifespan as it mimics the low-energy state in DR (Johnson et al., 2013). To test whether REPO-1 and SFA-1 are required for lifespan extension resulting from loss of TORC1 signaling, we asked whether their knockdown could suppress the long lifespan of animals that are mutant for RAGA-1, an upstream activator of TORC1. While SFA-1 was required for lifespan extension in *raga-1(ok386)* mutants, REPO-1 appeared to be dispensable. Furthermore, both REPO-1 and SFA-1 were shown to be required for longevity in the reduced electron transport chain mutant *isp-1(qm150).*

repo-1 was recently assigned to be part of an operon (CEOP4488), consisting of three genes- *lex-1*, *repo-1* and *rbm-34*. The original RNAi construct (*repo-1*$_{\text{Ahringer}}$) used for knockdown of *repo-1* was obtained from the Ahringer library and its sequence overlapped with the 3' end of the *repo-1* gene and a considerable part of *rbm-34*, the gene downstream of *repo-1* (**Figure 2.1A**). I therefore performed qPCR to test the specificity of knockdown in Day 1 wild type worms fed with *repo-1*$_{\text{Ahringer}}$ from hatch. As expected, *repo-1*$_{\text{Ahringer}}$ knocked down both *repo-1* and *rbm-34* by 50% (**Figure 2.1B**) suggesting it is non-specific. To test if the effects on lifespans were due to knockdown of *repo-1* or *rbm-34*, I designed and cloned three RNAi constructs- *repo-1*$_{\text{FL}}$ and *repo-1*$_{\text{short}}$ that spanned the full length of *repo-1* or the first 403 bp respectively and *rbm-34*$_{\text{FL}}$ that covered the entirety of *rbm-34*. I next examined each construct's specificity by feeding

wild type worms on bacteria containing these RNAi clones from hatch and performing qPCR for *repo-1* and *rbm-34*. Since the full-length RNAi constructs span the whole gene, including the sequences that overlap with the qPCR probe, the misleadingly appear by qPCR as though they result in a massive upregulation rather than knockdown since bacteria amplify these RNAi constructs that interferes with the qPCR probe. However, *repo-1*$_{\text{short}}$ which does not overlap with the qPCR probe binding region shows a ~50-60% knockdown of *repo-1* but has no effect on the levels of *rbm-34,* confirming that this RNAi clone is highly specific to *repo-1* (**Figure 2.1C**). I also tested the effect of each RNAi clone on the lifespan extension of *isp-1(qm150)*. As observed previously, while both *repo-1*$_{\text{FL}}$ and *repo-1*$_{\text{short}}$ suppressed *isp-1(qm150)* longevity comparably to *repo-1*$_{\text{Ahringer}}$ (**Figure 2.1D-F**), *rbm-34*$_{\text{FL}}$ could not (**Figure 2.1G**). Since *repo-1*$_{\text{short}}$ is highly specific (called *repo-1* RNAi henceforth), we tested its role in *eat-2(da1116)* lifespan alongside *sfa-1* RNAi and were able to reconfirm observations made previously (**Figure 2.2 A,B**) (Heintz et al., 2017).

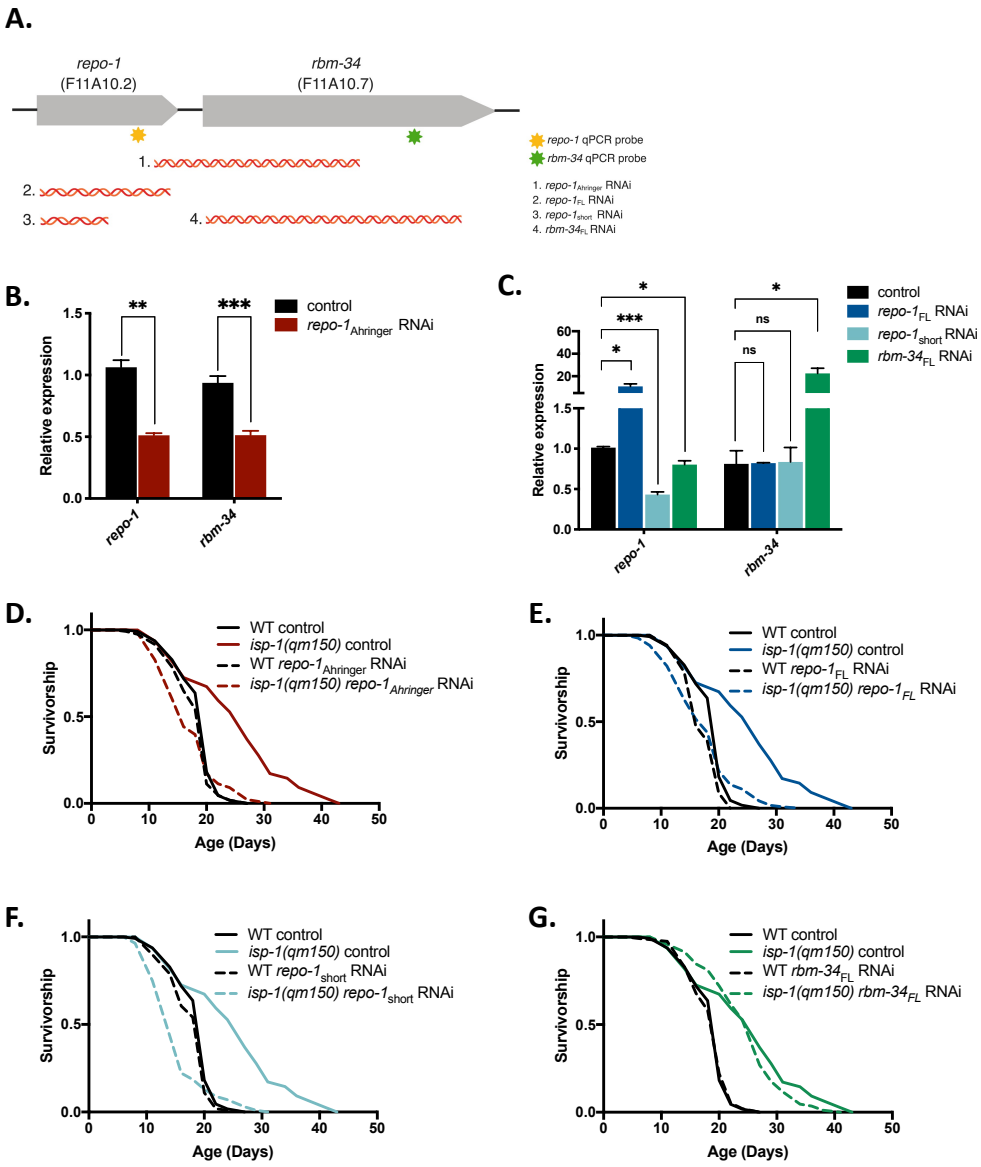

Figure 2.1: Specificity of RNAi to REPO-1.

A. Schematic representing the position of genes *repo-1* and *rbm-34* in the *C. elegans* genome operon CEOP4488 and the target sequences of the old *repo-1* RNAi from the Ahringer library (*repo-1*$_{\text{Ahringer}}$ RNAi) and the newly constructed *repo-1*$_{\text{FL}}$, *repo-1*$_{\text{short}}$ RNAi and *rbm-34*$_{\text{FL}}$ RNAi. Approximate positions of the qRT- PCR probes are marked.

B. *repo-1*$_{\text{Ahringer}}$ RNAi knocks down both *repo-1* and *rbm-34*. qRT-PCR of *repo-1* and *rbm-34* expression in Day 1 wildtype worms on control and *repo-1*$_{\text{Ahringer}}$ RNAi from hatch.

C. qRT-PCR of *repo-1* and *rbm-34* expression in Day 1 wildtype worms fed with control, *repo-1*$_{\text{FL}}$, *repo-1*$_{\text{short}}$ and *rbm-34*$_{\text{FL}}$ RNAi from hatch (****$P\leq0.0001$, ***$P\leq0.001$, **$P\leq0.01$, *$P\leq0.05$; ns $P>0.05$). *P*-values calculated with unpaired, two-tailed Welch's t-test. qRT–PCR data are mean + s.e.m. of 3 biological replicates. Increased signal of *repo-1* and *rbm-34* on treatment with *repo-1*$_{\text{FL}}$ and *rbm-34*$_{\text{FL}}$ RNAi

Figure 2.1 (Continued) respectively is likely due to non- specific signals from the siRNAs produced by bacteria that are ingested by the worms. Note that *repo-1*$_{\text{short}}$ RNAi is able to knockdown *repo-1* with equal efficiency as *repo-1*$_{\text{Ahringer}}$ RNAi but has no effect on *rbm-34* expression.

D-G. Knockdown of *repo-1* and not *rbm-34* blocks lifespan extension in a *C. elegans* model of longevity. Survivorship of wildtype (WT) and *isp-1(qm150)* worms with or without D. *repo-1*$_{\text{Ahringer}}$ (*P*=0.5434), E. *repo-1*$_{\text{FL}}$ (*P*=0.1228), F. *repo- 1*$_{\text{short}}$ RNAi (*P*=0.0006, shorter-lived) and G. *rbm-34*$_{\text{FL}}$ RNAi (*P*= <0.0001) (*P*-values are comparing wildtype RNAi vs *isp-1(qm150)* RNAi in each case).

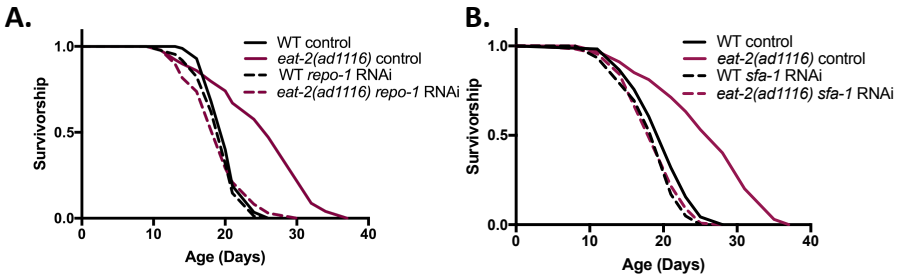

Figure 2.2: REPO-1 and SFA-1 are required for lifespan extension in DR.

A,B. Survivorship of wild-type (WT) and *eat-2(ad1116)* worms -/+ *repo-1* RNAi (*P*=0.8753) and *sfa-1* RNAi (*P*=0.5658) (*p*-values comparing wildtype N2 on RNAi versus *eat-2(ad1116)* on RNAi, ≥3 replicates).

2.2 REPO-1 and SFA-1 are required for TORC1 mediated longevity

Since TORC1 directly plays a role in DR mediated extension of lifespan, we next tested the role of REPO-1 and SFA-1 knockdown in lifespan extension via suppression of the TORC1 pathway. While knockdown of SFA-1 blocks *raga-1(ok386)* as shown previously (**Figure 2.3B**) (Heintz et al., 2017), knockdown of REPO-1 using the new specific *repo-1* RNAi clone was also able to suppress lifespan extension in these mutants (**Figure 2.3A**). Similarly, a knockdown of REPO-1 and SFA-1 completely suppress the lifespan extension exhibited by *rsks-1(ok1255), a* mutation of the S6 kinase ortholog that lies downstream of TORC1 (**Figure 2.3 C,D**). Together, these data suggest that both REPO-1 and SFA-1 are required for lifespan extension in the DR mutant *eat-2(ad1116)* and reduced TORC1 signaling mutants.

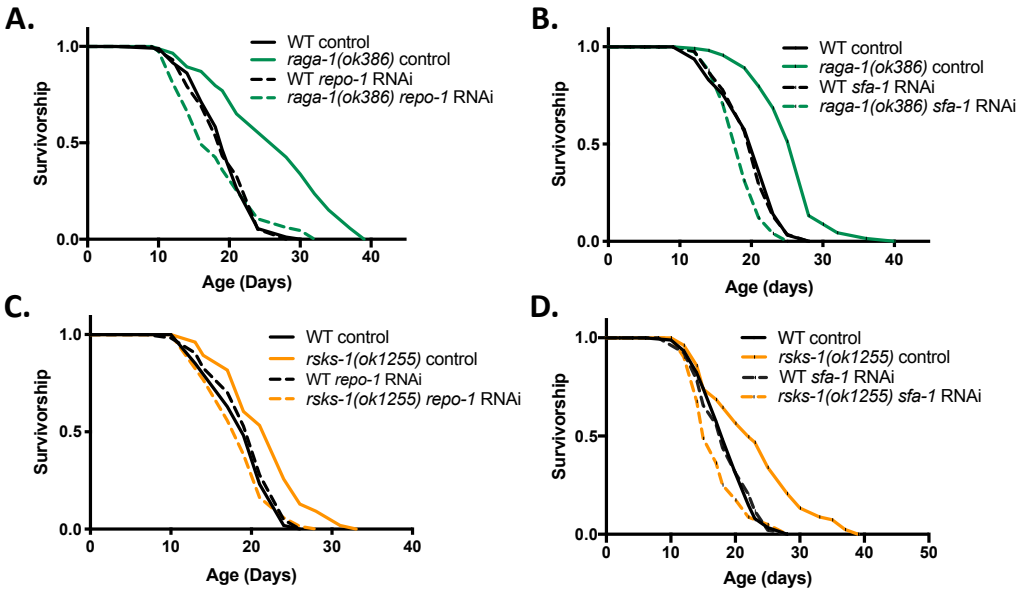

Figure 2.3: REPO-1 and SFA-1 are required for TORC1 longevity.

A, B. Survivorship of WT and *raga-1(ok386)* worms -/+ *repo-1* RNAi (*P*=0.5407) and *sfa-1* RNAi (*P*=0.002) (*p*-values comparing wildtype N2 on RNAi versus *raga-1(ok386)* on RNAi, ≥3 replicates).

C, D. Survivorship of wild-type (WT) and *rsks-1(ok1255)* C. -/+ repo-1 RNAi (P=0.0803) and *sfa-1* RNAi* (*P*= 0.0406) (*p*-values comparing wildtype N2 on RNAi versus *rsks-1(ok1255)* on RNAi, 2 replicates).
*Data for *rsks-1(ok1255)* on *sfa-1* RNAi from (Heintz et al., 2017)

2.3 REPO-1 and SFA-1 are required for longevity in different mutants of ETC

Another broadly studied class of long-lived genetic mutants in worms are the electron transport chain mutants that have reduced mitochondrial respiration and are resistant to multiple stresses (Rea, 2005). As shown previously, knockdown of both REPO-1 and SFA-1 blocks lifespan extension in *isp-1(qm150),* a hypomorphic mutation in the Rieske Fe-S protein of Complex III (**Figure 2.4 B**,**E**). To test if this effect is conserved across mutants of different ETC complexes, I assessed lifespans of *clk-1(qm30)* and *nuo-6(qm200)* upon knockdown of REPO-1 and SFA-1. While *clk-1(qm30)* is a deletion mutation in demethoxyubiquinone (DMQ) hydroxylase that helps in the synthesis of ubiquinone, *nuo-6(qm200)* is a point mutation in the NADH-ubiquinone oxidoreductase of complex I both of which reduce ETC function. Subjecting both these mutants to *repo-1* and *sfa-1* RNAi treatment from hatch completely suppress their

lifespan extension (**Figure 2.4 A,D** and **Figure 2.4 C,F**) suggesting that the requirement of REPO-1 and SFA-1 in longevity is conserved across ETC mutants.

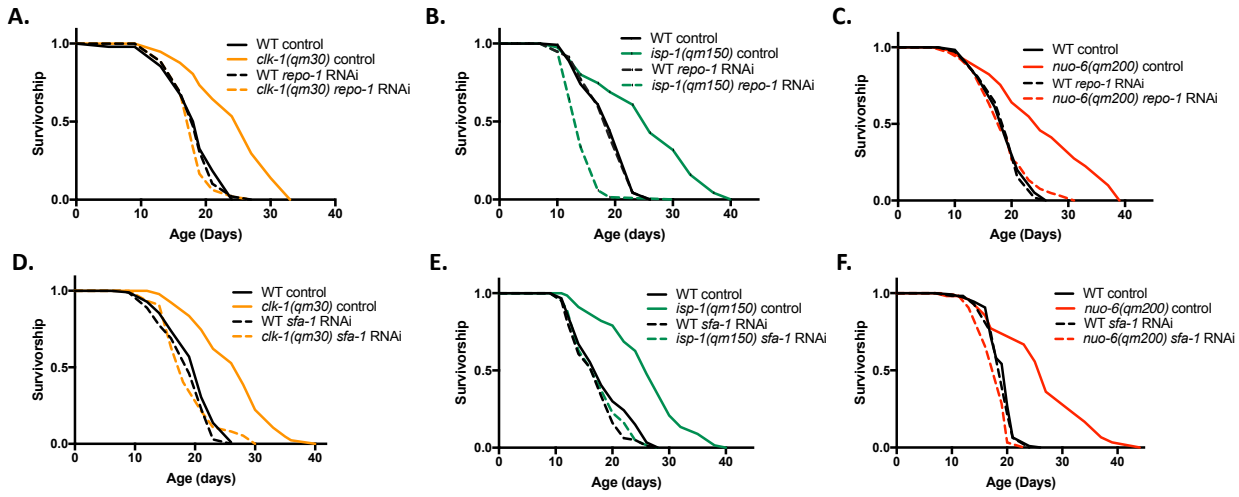

Figure 2.4: REPO-1 and SFA-1 are required for ETC longevity.

A, D. Survivorship of wild-type (WT) and *clk-1(qm30)* worms -/+ *repo-1* RNAi (P = 0.1838) and *sfa-1* RNAi (P=0.86) (p-values comparing wildtype N2 on RNAi versus *clk-1(qm30)* on RNAi, >=3 replicates).

B, E. Survivorship of wild-type (WT) and *isp-1(qm150)* worms -/+ *repo-1* RNAi (P<0.0001) and *sfa-1* RNAi* (P=0.1050) (p-values comparing wildtype N2 on RNAi versus *isp-1(qm150)* on RNAi, 2 replicates).
*Data for *isp-1(qm150)* on *sfa-1* RNAi from (Heintz et al., 2017).

C, F. Survivorship of wild-type (WT) and *nuo-6(qm200)* worms -/+ *repo-1* RNAi (P=0.9116) and *sfa-1* RNAi (P<0.0001) (p-values comparing wildtype N2 on RNAi versus *nuo-6(qm200)* on RNAi, 2 replicates).

2.4 REPO-1 and SFA-1 are dispensable for rIIS longevity

The first discovered class of long-lived genetic mutants were the reduced insulin and insulin-like growth factor signaling (rIIS) mutants (Kenyon, 2011). These mutants are believed to extend lifespan robustly through mechanisms that are distinct from DR and reduced TORC1 signaling. Consistent with our previous findings, the new *repo-1* RNAi and *sfa-1* RNAi did not block the IIS pathway mutant *daf-2(e1370)* mediated lifespan (**Figure 2.5 C,D**). *daf-2(e1370)* is a hypomorphic mutation in the insulin receptor. To confirm that REPO-1 and SFA-1 is dispensable for longevity in other mutants of the IIS pathway, I tested

their role in another IIS mutant- *age-1(hx546)* which is the worm PI3K that acts downstream to *daf-2*, mutation in which also leads to robust lifespan extension. Interestingly, REPO-1 and SFA-1 is dispensable for longevity in *age-1(hx546)* mutants as well (**Figure 2.5 A,B**) suggesting that rIIS evokes lifespan benefits independent of REPO-1 and SFA-1 function.

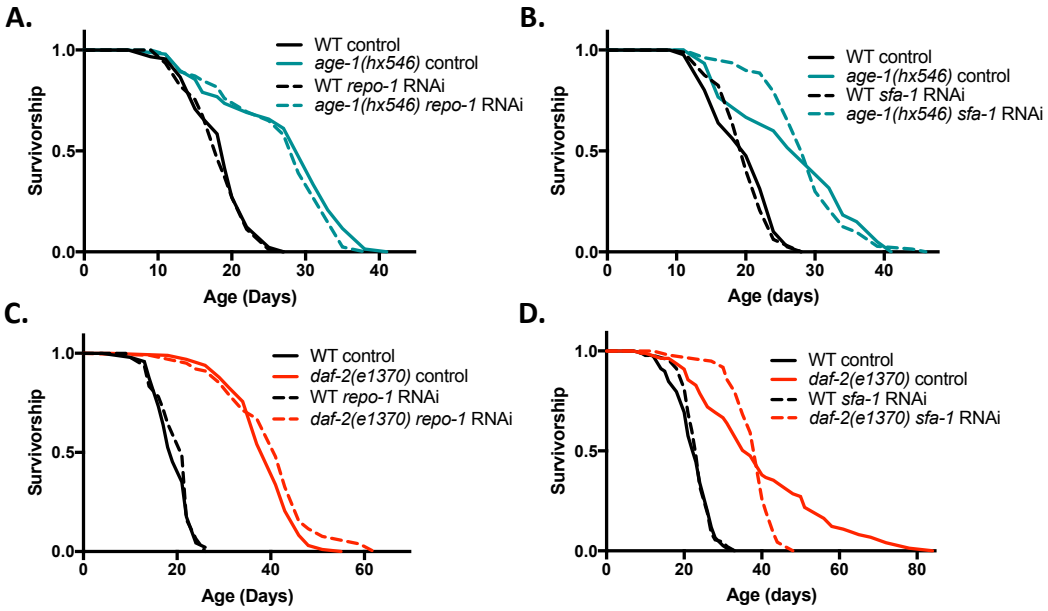

Figure 2.5: REPO-1 and SFA-1 are dispensable for rIIS longevity.

A, B. Survivorship curve of wild-type (WT) and *age-1(hx546)* worms -/+ *repo-1* RNAi (P<0.0001) and *sfa-1* RNAi (P<0.0001) (p-values comparing wildtype N2 on RNAi versus *age-1(hx546)* on RNAi, >=3 replicates).

C, D. Survivorship of wild-type (WT) and *daf-2(e1370)* -/+ *repo-1* RNAi (P<0.0001) and -/+ *sfa-1* RNAi (P<0.0001) (p-values comparing wildtype N2 on RNAi versus *daf-2(e1370)* on RNAi, >=3 replicates).
*Data for *daf-2(e1370)* on *sfa-1 RNAi* from (Heintz et al., 2017).

DAF-16, the worm ortholog of mammalian FOXO, is activated on suppression of the rIIS pathway and is the known mediator of lifespan extension in the insulin signaling mutants. It has been shown that overexpression of DAF-16 is sufficient to extend lifespan (Henderson and Johnson, 2001; Lin et al., 2001). Interestingly, in long-lived worm strains overexpressing the DAF-16a/b, loss of REPO-1 and SFA-1 completely suppresses lifespan comparable to wildtype worms (Fig 2.6 A,B). This suggests that REPO-1

and SFA-1 are dispensable for longevity in IIS longevity, however, this mechanism is independent of their role downstream to DAF-16.

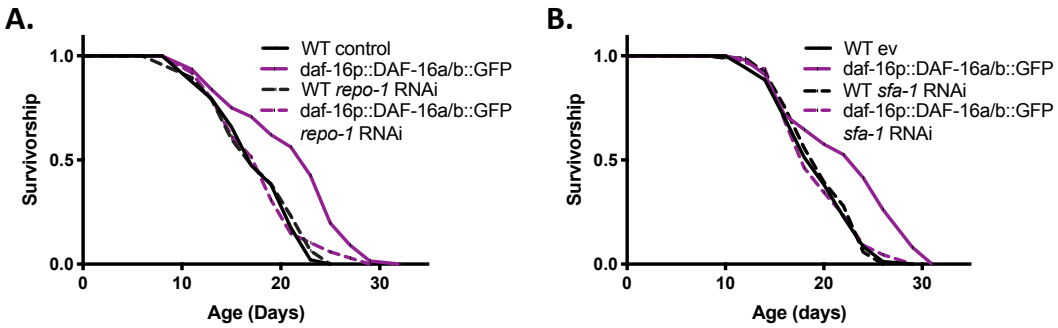

Figure 2.6: REPO-1 and SFA-1 are required for lifespan extension in DAF-16 overexpressors.

A, B. Survivorship of wild-type (WT) and DAF-16a/b overexpressor worms (*daf-16p*::DAF16a/b::GFP) -/+ *repo-1* RNAi (P=0.8994) and *sfa-1* RNAi (P=0.8718) (P-values are comparing WT on RNAi vs mutant on RNAi, 2 replicates).

2.5 REPO-1 is suppressed in different longevity mutants with equal efficiency

To rule out the possibility that differences in sensitivity to RNAi and knockdown efficiency of *repo-1* in different genetic backgrounds is underlying the differences in lifespan effects, we performed qPCR on strains belonging to different longevity pathways with and without *repo-1* knockdown. **Figure 2.7** shows that irrespective of the genetic background, the *repo-1* RNAi clone can efficiently knockdown *repo-1* levels by ~50%. The fact that loss of REPO-1 and SFA-1 are able to suppress DR, reduced TORC1 and reduced ETC mediated lifespan but is unnecessary for rIIS suggests that it is required for the processing of a shared set of genes that are important for longevity.

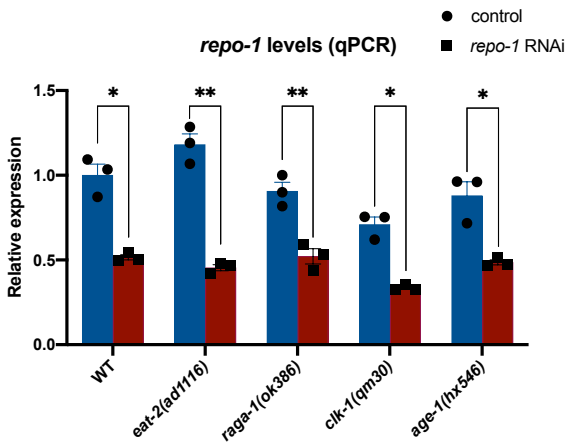

Figure 2.7: REPO-1 is knocked down in different mutants with equal efficiency.

qPCR showing ~50% knockdown of *repo-1* in different longevity mutants fed with empty vector and *repo-1* RNAi from hatch and collected at Day 1 of adulthood (****$P \leq 0.0001$, ***$P \leq 0.001$, **$P \leq 0.01$, *$P \leq 0.05$; ns $P > 0.05$). *P*-values calculated with unpaired, two-tailed Welch's t-test. qRT–PCR data are mean + s.e.m. of 3 biological replicates.

2.6 Effect of REPO-1 and SFA-1 on lifespan can be uncoupled from known downstream mediators of DR, TORC1 and ETC mediated longevity

Previous reports suggest mitochondrial UPR as a known mediator of longevity in the ETC and *eat-2* mutants (Durieux et al., 2011). However, contrasting evidence imply that this might not be the case as knocking down *atfs-1*, the key transcriptional regulator of mitoUPR, does not block ETC longevity (Bennett and Kaeberlein, 2014). To test the role of splicing factors in ETC mutants and whether they affect mitoUPR, I crossed the mitochondrial UPR transcriptional reporters *hsp-6p::gfp* and *hsp-60p::gfp* into the ETC mutant *isp-1(qm150)*. While mitoUPR is highly upregulated in the mutants, knocking down *repo-1* in this background does not suppress or exacerbate this induction (**Figure 2.8 A,B**). Further, I tested whether oxidative stress could be linked to the longevity phenotype in the DR, TORC1 and ETC mutants. *sod-3* is a superoxide dismutase responsible for clearing superoxide radicals and relieving oxidative stress. qPCR results show that while *repo-1* knockdown induces *sod-3* expression in *eat-2(ad1116)* and *raga-1(ok386)*, it does not increase the *sod-3* expression in *clk-1* mutants which already has an upregulated *sod-3* expression

pattern (**Figure 2.8C**). This suggests that change in oxidative stress is unlikely to be causal to the longevity phenotype.

We next tested if changes in beta oxidation played a role in REPO-1/SFA-1 dependent longevity. To do that, we crossed the *isp-1(qm150)* ETC mutant to the strain expressing a transcriptional reporter of *acs-2* (*acs-2p::gfp*). ACS-2 or acyl-CoA synthetase plays a role in breakdown of fatty acids and is upregulated to promote beta-oxidation. While the ETC mutant *isp-1(qm150)* shows a massive upregulation of *acs-2*, loss of REPO-1 does not reverse it (**Figure 2.8D**). Furthermore, *acs-2* transcript levels across different longevity mutants with and without REPO-1 do not get altered (**Figure 2.8E**) suggesting that rate of beta-oxidation and fat mobilization is unlikely to be the mechanism by which REPO-1 and SFA-1 regulate DR, TORC1 and ETC longevity.

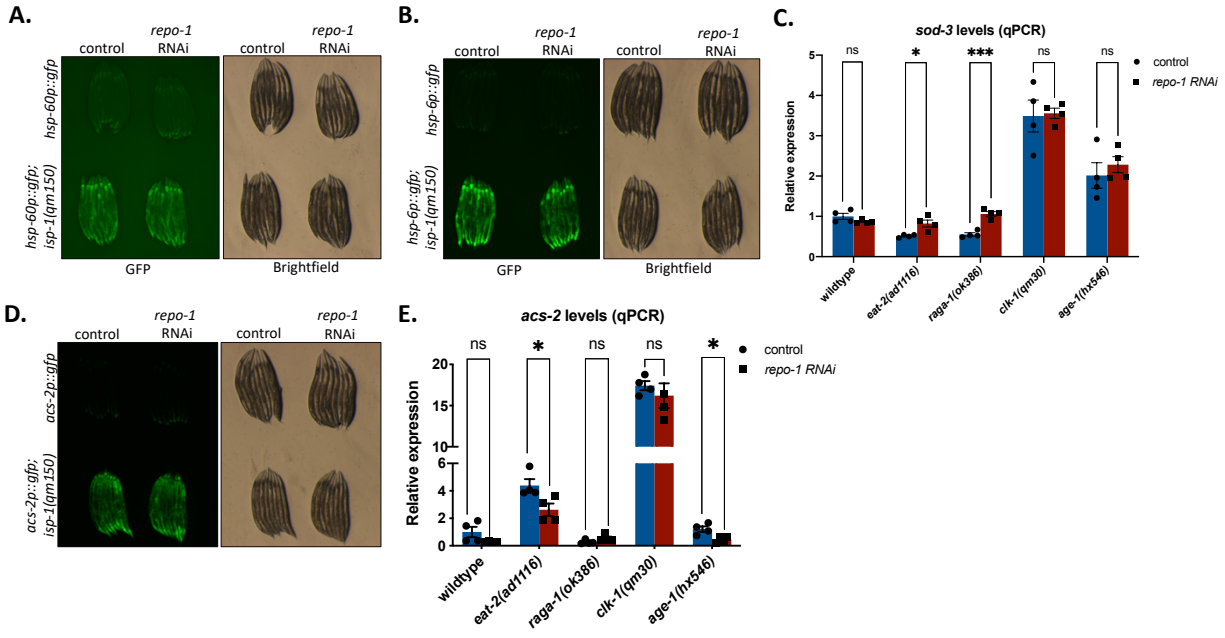

Figure 2.8: Knockdown of REPO-1 does not abrogate mitoUPR or beta-oxidation.

A,B. Transcriptional induction of mitochondrial chaperones *hsp-6p::GFP and hsp-60p::GFP* in wildtype N2 and ETC mutant *isp-1(qm150)* without or with *repo-1* RNAi from hatch and imaged at Day 1 of adulthood.

C. RT-qPCR of *sod-3* in Day 1 WT and longevity mutants fed on control bacteria or *repo-1* RNAi from hatch. (****$P \leq 0.0001$, ***$P \leq 0.001$, **$P \leq 0.01$, *$P \leq 0.05$; ns $P > 0.05$). *P*-values calculated with unpaired,

Figure 2.8 (Continued) two-tailed Welch's t-test. qRT–PCR data are mean + s.e.m. of 4 biological replicates. Samples here are the same as used in RNA-Seq (Chapter 3).

D. Knockdown of REPO-1 does not abrogate *acs-2* induction in ETC mutants. Day 1 imaging of *acs-2p::GFP* in wildtype N2 and *isp-1(qm150)* background without or with *repo-1* RNAi from hatch.

E. RT-qPCR of *acs-2* in Day 1 WT and longevity mutants fed on control bacteria or *repo-1* RNAi from hatch. (****$P \leq 0.0001$, ***$P \leq 0.001$, **$P \leq 0.01$, *$P \leq 0.05$; ns $P > 0.05$). *P*-values calculated with unpaired, two-tailed Welch's t-test. qRT–PCR data are mean + s.e.m. of 4 biological replicates. Samples here are the same as used in RNA-Seq (Chapter 3).

Discussion

In this chapter, I show that REPO-1 and SFA-1 are required for lifespan extension downstream of DR, TORC1 and ETC longevity specifically but is unessential for longevity driven by reduced insulin signaling. Although REPO-1 and SFA-1 are a part of the core splicing machinery, the fact that they exhibit pathway specificity suggests that these factors splice specific RNA targets, whose function is important for mediating longevity in DR, TORC1 and ETC mutants.

This finding is particularly interesting because of two reasons: 1. It suggests that longevity via *eat-2* mediated dietary restriction, reduced TORC1 and reduced ETC mediate lifespan extension likely through some shared mechanism that requires REPO-1 and SFA-1 activity; 2. It also implies that the components of the spliceosome while important for splicing of some targets, are dispensable for others. This opens a completely new avenue of research in RNA biology where specific splicing factors process only a subset of all genes. This selectivity could be regulated by availability of binding site, splicing factor expression and/or their post-translational modifications.

It is also possible that signals originating from DR, reduced TORC1 and reduced ETC signaling, modulate expression/modification of these splicing factors which impacts their splicing function. There are reports that have linked metabolic signals directly modulating the activity of splicing factors and upstream kinases. For example, AKT might indirectly impact splicing function by affecting splicing factor expression (Latorre

et al., 2019). AKT directly regulates splicing by modulating SR proteins (Blaustein et al., 2005) or SR protein-specific kinase activity and localization (Zhou et al., 2012). mTORC1 activation has been shown to phosphorylate leading to the activation and nuclear translocation of SRPK2, that further promotes splicing of lipogenic genes (Lee et al., 2017). Whether DR, reduced TORC1 and reduced ETC directly influences SFA-1 and REPO-1 activity remains to be understood.

CHAPTER 3

Loss of REPO-1 and SFA-1 remodels lipid metabolism to affect longevity

Introduction

Metabolic pathways are highly complex and significantly crosstalk with each other. While the effects of DR, TORC1, ETC and rIIS longevity are mediated through regulation of interconnected pathways, there is evidence suggesting that distinct non-overlapping mechanisms might be at play to promote lifespan extension. For example, it has been shown that lifespan extension by reduction of TORC1 as well as IIS require *daf-16,* the *C. elegans* ortholog of FOXO (Jia et al., 2004; Kenyon et al., 1993; Robida-Stubbs et al., 2012). However, longevity from mutations in *rsks-1* and *daf-2* leading to reduced TORC1 and insulin signaling, respectively, is additive (Chen et al., 2013). While common molecular players might impact lifespan downstream to these pathways, such synergy suggests that TORC1 and IIS might act in complex parallel pathways to regulate longevity.

Such a complex interaction is also seen in the case of longevity induced by DR and TORC1. It has been shown that in the DR mimetic *eat-2* mutant in *C. elegans*, additional inhibition of components of the TORC1 pathway does not result in further extension of lifespan (Hansen et al., 2007). This is supported by observation in *Drosophila* that lifespan extension resulting from restricting dietary yeast is not further increased by inhibition of the TOR pathway (Kapahi et al., 2004). However, other reports in flies have shown that rapamycin and DR can have additive effects on lifespan as compared to individual treatments in flies (Bjedov et al., 2010).

Thus, there is growing literature on the process by which lifespan extension is mediated by these seemingly converging but distinct metabolic pathways. How REPO-1 and SFA-1 affects the longevity of some pathways and not others remain to be established.

In this chapter, I describe my work to identify mechanisms underlying REPO-1 and SFA-1's role in regulating lifespan extension in DR, TORC1 and ETC mutants. By undertaking an unbiased RNA-Sequencing approach, I sought to identify shared underlying transcriptomic changes that occur on loss of

REPO-1 in the different longevity mutants. Further, using SRS microscopy and enhanced crosslinking immunoprecipitation (eCLIP), I provide evidence that suggests these splicing factors in regulate longevity through the remodeling of lipid metabolism.

Results

3.1 Loss of splicing factor REPO-1 specifically affects lipid metabolism in splicing factor dependent longevity pathways

Since REPO-1 and SFA-1 loss affected DR, TORC1 and ETC mediated longevity and had no effect on IIS longevity, we leveraged this finding to design an RNA-Seq experiment to explore underlying transcriptional changes that correlate with the longevity phenotype. N2, *eat-2(ad1116), raga-1(ok386), clk-1(qm30)* and *age-1(hx546)* were grown on control empty vector or repo-1 RNAi from hatch and collected them at Day 1 of adulthood. We surmised that since REPO-1/SFA-1 acts during the developmental stages (see Chapter 4) to regulate lifespan, early transcriptional changes that might be causal to longevity could be captured at Day 1. Four biological replicates for each sample were collected and 75-bp paired-end RNA-Seq was performed at the Dana Farber Genomics Core. Subsequent analysis of the data was done in collaboration with Mary Piper from the Harvard Chan Bioinformatics Core. Principal component analysis in PC1 and PC2 showed that WT, *age-1(hx546)* and *raga-1(ok386)* are relatively similar compared to *eat-2(ad1116)* and *clk-1(qm30)* worms. Interestingly, *repo-1* RNAi drove significant changes specifically in the splicing factor dependent (SF-dependent) longevity mutants *eat-2(ad1116)*, *raga-1(ok386)* and *clk-1(qm30)* mutants but had less prominent effects on wildtype and splicing factor independent (SF-independent) mutant *age-1(hx546)* which correlated well with the longevity effect on *repo-1* knockdown (Fig 3.1A). We next explored the differential effect of *repo-1* knockdown on each long-lived mutant relative to wild-type worms. In other words, we looked for genes that responded differently to *repo-1* knockdown in a mutant compared to WT. These genes were clustered in an UpSet plot based on the mutant they were differentially responsive in (Fig 3.1B). Interestingly, only 6 genes responded differently on *repo-1* knockdown in the SF-

independent mutant *age-1(hx546)* compared to WT worms compared to thousands of genes in the SF-dependent mutants. These data suggest that loss of *repo-1* has a different effect on the physiology of the SF-dependent longevity mutants compared to WT and *age-1(hx546)* worms.

We further probed the 620 shared differentially expressed genes that that were common in the SF-dependent longevity mutants *eat-2(ad1116)*, *raga-1(ok386)* and *clk-1(qm30)* (**Appendix II- Supplementary table 8.1**). I used the WormCat platform built specifically to annotate and visualize enriched gene sets in *C. elegans* datasets (Holdorf et al., 2020) to identify signatures in these shared 620 differentially responsive genes. Interestingly, metabolism was one of the most significant terms with 'lipid metabolism' being the most enriched sub-category (Fig 3.1C). Another interesting category was 'mRNA processing' suggesting that there might be indirect or compensatory changes in the post-transcriptional machinery on loss of REPO-1 specifically in these longevity pathways.

We clustered the 620 genes to identify whether lipid metabolism genes have a specific pattern of expression. **Figure 3.2A** shows the 23 clusters from this analysis. I focused our analysis on clusters 5, 6, 14, 20 and 23 where *eat-2(ad1116)*, *raga-1(ok386)* and *clk-1(qm30)* responded alike on *repo-1* RNAi whereas N2 and *age-1(hx546)* responded differently. Cluster 6, which showed a class of genes that were upregulated in the SF-sensitive mutants on loss of *repo-1*, was particularly interesting because it was enriched for genes in fatty acid metabolism (**Figure 3.2B**). These include genes like *cpt-5* which is predicted to have acyl transferase activity and *fat-3* that is a stearoyl-CoA desaturase. qPCR of these genes in independent samples further validated that they are upregulated in the SF-dependent mutants on loss of *repo-1* and *sfa-1* but not in WT and *age-1(hx546)* mutants (**Figure 3.2 C,D**).

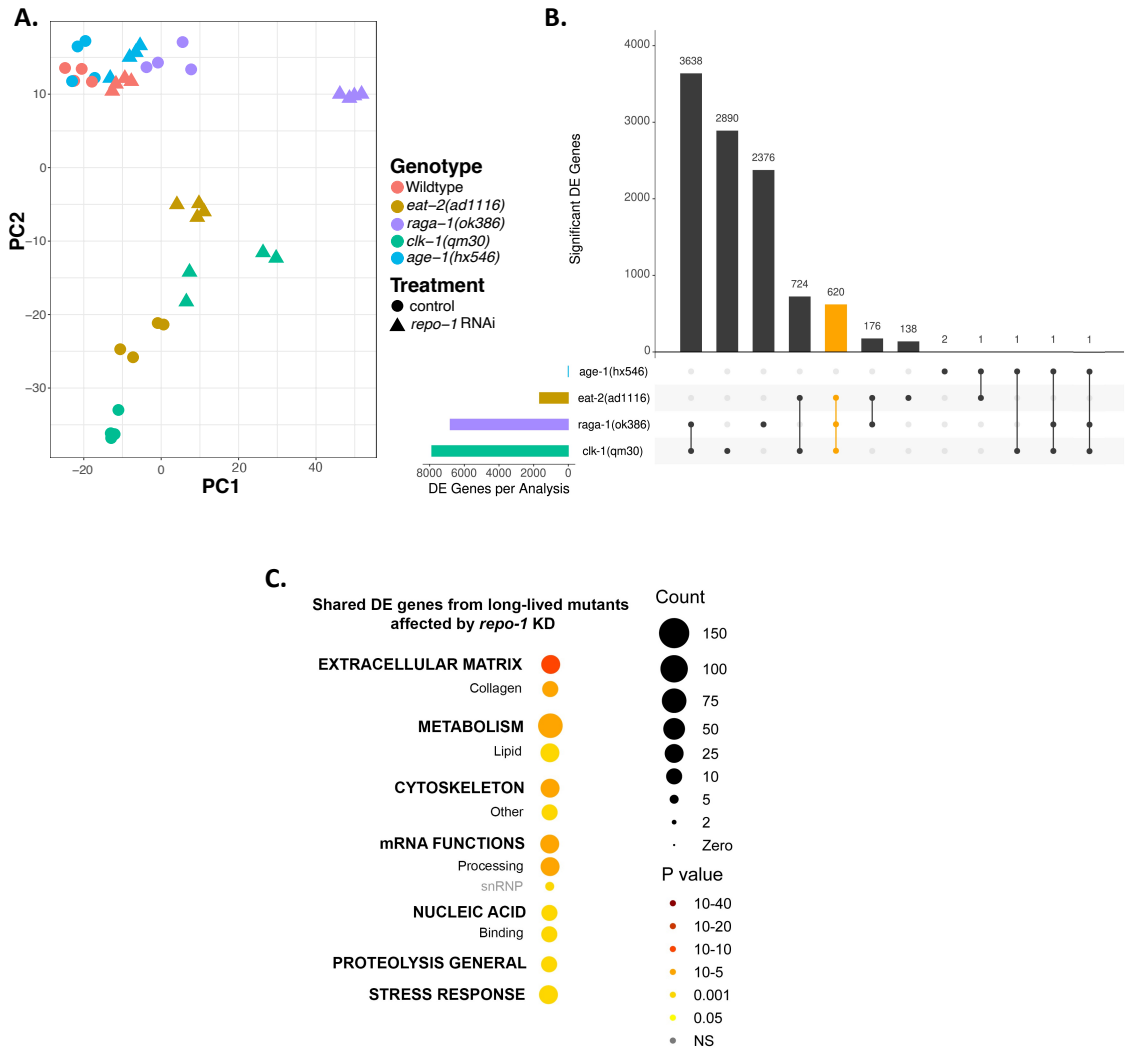

Figure 3.1: Loss of splicing factor REPO-1 causes widespread changes in splicing factor dependent longevity mutants.

A. Principal Component Analysis of RNA Seq Samples in different longevity mutants -/+ *repo-1* RNAi.

B. UpSet plot (UpSetR R package) quantifying genes in different longevity mutants that respond differently on *repo-1* knockdown compared to wildtype N2 worms.

C. WormCat visualization of categories enriched in 620 shared genes that are differentially affected on loss of REPO-1 in splicing factor-dependent pathways compared to wildtype N2 worms.

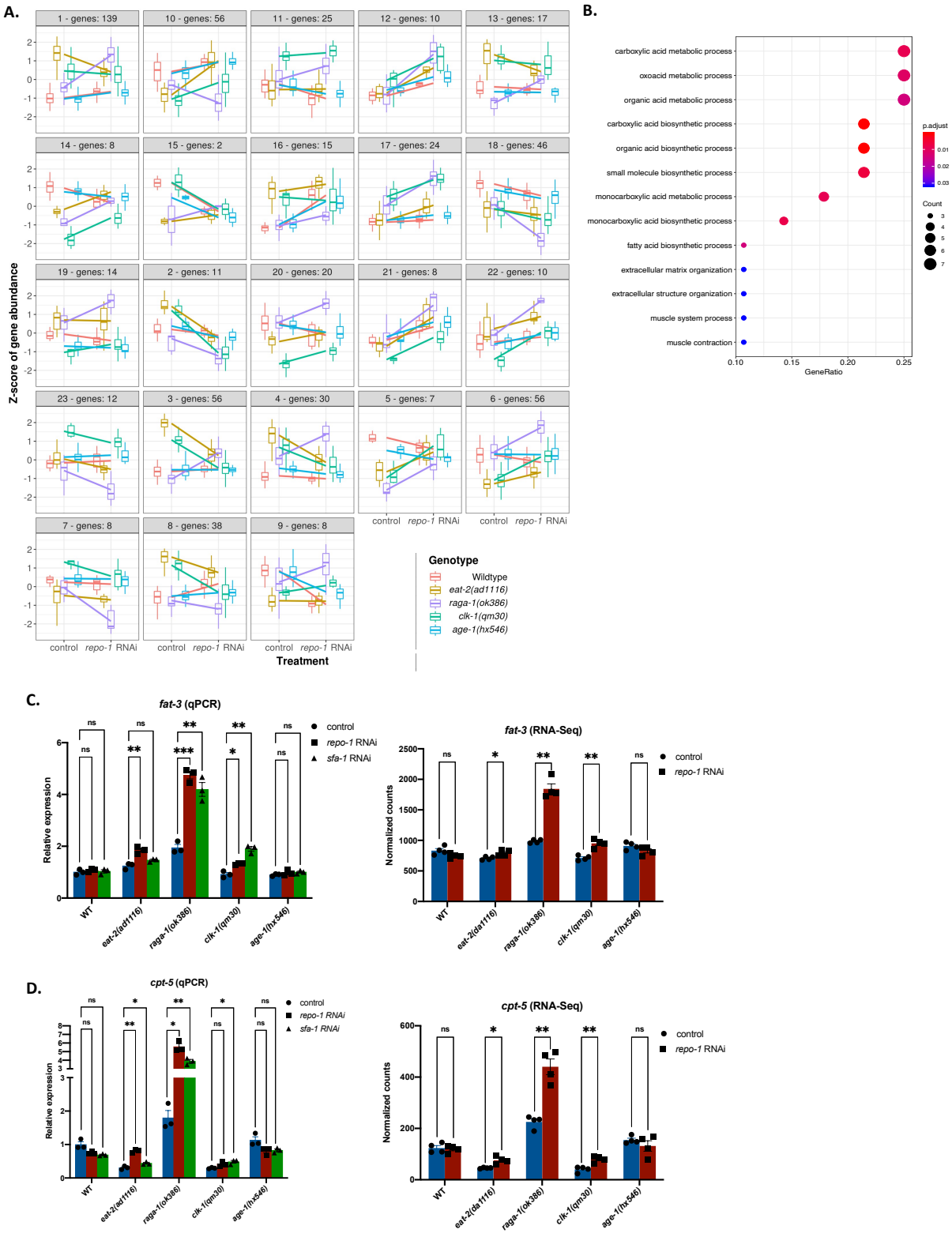

Figure 3.2: Loss of REPO-1 specifically affects lipid metabolism in splicing factor dependent longevity pathways.

Figure 3.2 (Continued) A. Cluster analysis of 620 shared genes in REPO-1 dependent mutants based on expression pattern

B. GO term enrichment of Cluster 6 (56 genes) shows upregulation of genes some of which are enriched in fatty acid metabolism.

C. Expression of *fat-3* by qRT-PCR in wildtype and different mutants -/+ *repo-1* and *sfa-1* RNAi at Day 1; Normalized counts of *fat-3* transcript in RNA-Seq of wildtype and different mutants -/+ *repo-1* RNAi at Day 1.

D. Expression of *cpt-5* by qRT-PCR in wildtype and different mutants -/+ *repo-1* and *sfa-1* RNAi at Day 1; Normalized counts of *cpt-5* transcript in RNA-Seq of wildtype and different mutants -/+ *repo-1* RNAi at Day 1.

(****$P \leq 0.0001$, ***$P \leq 0.001$, **$P \leq 0.01$, *$P \leq 0.05$; ns $P > 0.05$). *P*-values calculated with unpaired, two-tailed Welch's t-test. RNA-seq data are mean + s.e.m. of normalized read counts of 4 biological replicates. qRT–PCR data are mean + s.e.m. of 3 biological replicates.

Changes in the expression of lipid genes, while suggestive of changes to lipid metabolism, cannot dissect the direction of change in these animals. We therefore sought to visualize lipids in these worms in the presence and absence of splicing factors.

3.2 Loss of SFA-1 and REPO-1 increases lipid content in DR and TORC1 mutants

Many staining techniques like Nile Red staining, Oil Red O staining have been adopted to visualize lipid content in worms. However, one major drawback is that these techniques tend to non-specifically stain other organelles in worms besides lipid droplets (Escorcia et al., 2018) resulting in artifacts. Stimulated Raman Scattering (SRS) Microscopy is a non-invasive label-free method of imaging molecules in living tissue that has been adapted to visualize neutral lipids in *C. elegans* (Wang et al., 2011). In collaboration with Dr. Sena Mutlu in Prof. Meng Wang's lab at Baylor College of Medicine, Texas, we performed SRS microscopy in WT, *eat-2(ad1116)*, *raga-1(ok386)*, *clk-1(qm30)* and *age-1(hx546)* on control and *repo-1/sfa-1* RNAi. As expected and consistent with previous findings, *eat-2(ad1116)* worms reared on control plates had reduced lipid content in the intestine compared to WT animals, whereas lipids were increased in *raga-1(ok386)* and *age-1(hx546)* mutants (Watts and Ristow, 2017). Upon loss of REPO-1 and SFA-1,

lipid content remained unchanged in the WT background, yet was significantly increased in the SF-dependent mutants *eat-2(ad1116)* and *raga-1(ok386)* (**Figure 3.3 A,B**). This increase was not observed in the SF-independent IIS mutant *age-1(hx546)*. Strangely, *repo*-1 and *sfa-1* RNAi also had no obvious impact on intestinal lipid content in the splicing dependent mutant *clk-1(qm30)* (**Figure 3.3B**). ETC mutants have impaired mitochondrial function and it is possible that the lipid phenotype in the other SF-dependent mutants is linked to mitochondrial function. Thus, SRS microscopy suggests that these splicing factors not only regulate the expression of lipid metabolic genes in SF-dependent longevity mutants but can also alter their lipid content.

Accumulation of lipids can be a result of increased storage, reduced breakdown or both. A previous study in the lab had shown that loss of *sfa-1* using RNAi blocked fasting induced beta-oxidation in worms (Heintz et al., 2017). To test whether this phenomenon is conserved on loss of *repo-1* as well, I used the strain expressing the transcriptional reporter of *acs-2* (*acs-2p::gfp*) and fed them with control bacteria or *repo-1* RNAi from hatch. At Day 3, I either kept them fed or fasted them for 16hours followed by imaging. **Figure 3.3C** shows that similar to SFA-1 loss, worms with a loss of REPO-1 were unable to induce beta-oxidation and *acs-2* synthesis to the same degree as control worms on fasting. This suggests that disrupted beta-oxidation could have a role in the accumulation of lipids we observe in the SF-dependent longevity mutants.

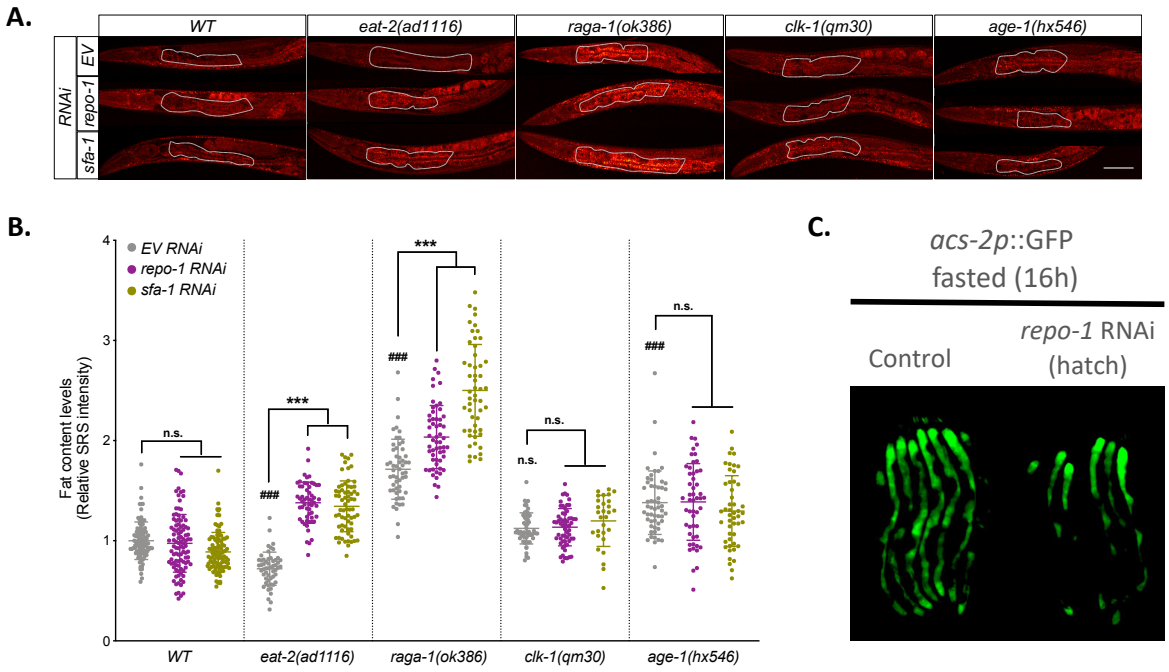

Figure 3.3: Loss of REPO-1 and SFA-1 leads to accumulation of lipids in DR and TORC1 mutants.

A. Representative images of SRS microscopy showing fat levels in wildtype N2, *eat-2(ad1116)*, *raga-1(ok386)*, *clk-1(qm30)* and *age-1(hx546)* on control, *repo-1* and *sfa-1* RNAi. Worms were fed on RNAi from hatch and imaged 24 hours post L4 stage.

B. Quantification of SRS signal using ImageJ (pooled data quantifying anterior intestine of n=20-30 worms, N=3; ### $P<0.001$ long-lived mutant vs wildtype on control EV RNAi; *** $P<0.001$ control EV vs *repo-1/sfa-1* RNAi; n.s. $P>0.05$).

C. Fluorescence images of the *acs-2* transcriptional reporter worm *acs-2p::GFP* on control bacteria and *repo-1* RNAi from hatch followed by fasting for 16 hours at Day 3. Images captured at ~Day 4 of adulthood.

3.3 SFA-1 and REPO-1 have shared conserved mRNA targets that play a role in lipid biosynthesis

To understand how SFA-1 and REPO-1 modulate lipid metabolism, I set out to identify their direct RNA targets. We speculated that true targets that impinge on longevity might be highly conserved. We therefore performed enhanced cross-linking immunoprecipitation (eCLIP) in two different systems- in whole worms and in mouse embryonic fibroblast cell lines (MEFs). For worms, we generated two worm strains containing CRISPR tagged endogenous SFA-1 and REPO-1 with 3X FLAG. We used eCLIP services of Eclipse

Bioinnovations Inc. San Diego that have a standardized eCLIP workflow for RNA binding proteins in cells and tissues from different species (Van Nostrand et al., 2016). We UV-crosslinked wildtype N2 (control), 3XFLAG::REPO-1 and 3XFLAG ::SFA-1 and shipped snap-frozen samples. FLAG antibody was used to pull down SFA-1:RNA and REPO-1:RNA complexes (**Figure 3.4A**). Contrary to what we expected, we identified very few targets of SFA-1 and REPO-1. Using a log2 fold change >= 1 and -log10(p-value) >= 1 over input as a cutoff, we identified binding peaks in 196 and 289 genes respectively for REPO-1 and SFA-1 with 43 overlapping target genes (**Figure 3.4B**) (**Appendix II- Supplementary table 8.3)**. Interestingly, several binding peaks were identified on the *tos-1* gene for both SFA-1 and REPO-1. *tos-1* is a previously established target of SFA-1 (Ma et al., 2011; Ma and Robert Horvitz, 2009) and we further confirmed that loss of both SFA-1 and REPO-1 changed the splicing pattern of *tos-1* in *C. elegans* (**Figure 3.4C**). This gave us further confidence that true peaks were identified using the eCLIP approach.

For eCLIP in MEFs, we crosslinked cells followed by IP with SF1 (mammalian SFA-1) and SF3A2 (mammalian REPO-1) antibodies (**Figure 3.4D**). Interestingly, we identified a lot more peaks in MEFs compared to worms. True peaks were defined as those showing enrichment of log2 fold change >= 2 and -log10(p-value) >= 2 over input. Sequencing identified ~964 and ~841 genes targeted by SF1 and SF3A2 in MEFs, respectively. 424 genes, representing ~50% of total targets, are shared (**Figure 3.4E**) (**Appendix II-Supplementary table 8.2)**. Exact hypergeometric probability analysis revealed that the overlap of genes was highly significant (representation factor = 10.5) and unlikely to be a chance event, suggesting that SF1 and SF3A2 might act together to regulate splicing.

Interestingly, in both MEFs and in *C. elegans,* we find an enrichment of shared target genes involved in RNA processing and in lipid metabolism. One such target involved in lipid metabolism is Acetyl CoA Carboxylase 1 (ACC1), the rate-limiting enzyme of the fatty acid biosynthetic pathway. ACC1 is a target of both SF1 and SF3A2 in MEFs, and the pre-mRNA for POD-2, the *C. elegans* orthologue of ACC1, was identified as a shared target of SFA-1 and REPO-1 in *C. elegans*.

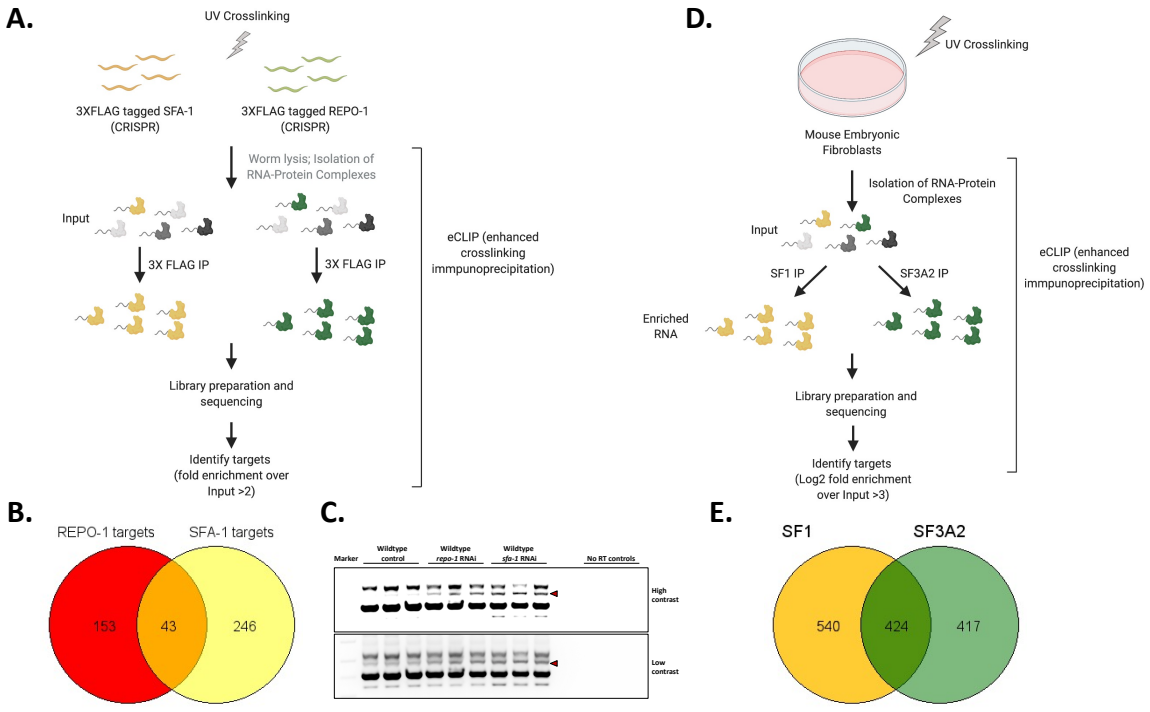

Figure 3.4: Enhanced crosslinking immunoprecipitation (eCLIP) in MEFs and *C. elegans* identifies shared conserved targets of REPO-1 and SFA-1

A. Schematic of eCLIP in *C. elegans*.

B. Venn diagram displaying the overlap of RNA targets with enrichment >2 fold (log2 fold change >1, IP vs Input) in SFA-1 and REPO-1.

C. Validation of *tos-1* as a target of SFA-1 and REPO-1. Semi-quantitative PCR showing differential isoforms of *tos-1* in Day 1 worms on loss of *repo-1* and *sfa-1* using RNAi. Red arrow marks the appearance of a different isoform of *tos-1* on loss of *repo-1* and *sfa-1*.

D. Schematic of eCLIP in Mouse Embryonic Fibroblasts (MEFs).

Figure 3.4 (Continued)

E. Venn diagram showing targets of SF1 (mammalian SFA-1 ortholog) and SF3A2 (mammalian REPO-1 ortholog) and their overlap in MEFs. True gene targets identified as peaks in IP over input sample that had a log2fold enrichment>2 and -log10(p-value)>2, N=2. Plot generated using GeneVenn.

3.4 Loss of POD-2 mimics loss of splicing factor SFA-1 and REPO-1 in different longevity pathways

POD-2/ACC1 converts acetyl-CoA to malonyl CoA, thus catalyzing the first step in the formation of *de novo* lipids. Previously, it has been shown that loss of POD-2 blocks *eat-2(ad1116)* mediated lifespan extension but had no effect on WT lifespan (Yuan et al., 2012). We therefore reasoned that dysfunctional POD-2/ACC1 would alter lipid stores in SFA-1 and REPO-1 depleted animals, and that this might modulate the aging effects in SF-sensitive pro-longevity mutants.

To test if POD-2 plays a role, we inhibited lifespan extension of SF-dependent and SF-independent mutants with and without RNAi of ACC1/POD-2. We observed that worms on *pod-2* RNAi from hatch leads to larval arrest suggesting *pod-2* and lipid biosynthesis is crucial for normal worm development. We therefore initiated *pod-2* RNAi from Day 1 of adulthood. Strikingly, inhibition of POD-2 mimicked the longevity intervention specificity of SFA-1 and REPO-1. *pod-2* RNAi from day 1 of adulthood fully suppresses lifespan extension of *eat-2(ad1116), raga-1(ok386),* and *clk-1(qm30)* mutants but does not suppress lifespan in the SF-resistant *age-1(hx546)* (Fig 3.5 A-D) mutants. These data suggest that SFA-1 and REPO-1 modulate responses to specific longevity interventions via lipid remodeling and POD-2 dependent disruption of *de novo* lipid biosynthesis.

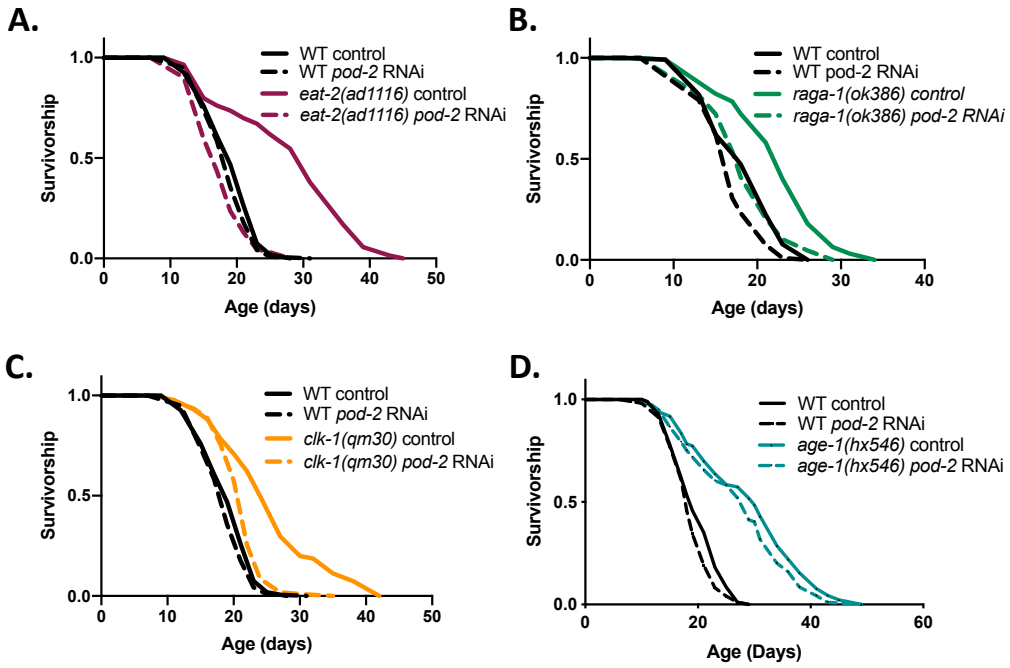

Figure 3.5: Loss of POD-2 suppresses DR, TORC1 and ETC longevity but is not required for IIS longevity

Survivorship curves -/+ *pod-2* RNAi of wildtype (WT) and A. *eat-2(ad1116)* (P=0.057, 2 replicates); B. *raga-1(ok386)* (P=0.1923, 4 replicates); C. *clk-1(qm30)* (P<0.0001, 2 replicates) and D. *age-1(hx546)* (P<0.0001, 3 replicates). RNAi initiated at Day 1 of adulthood. p-values reflect comparison of wildtype N2 fed with *pod-2* RNAi versus long-lived mutant with *pod-2* RNAi.

Discussion

Previous studies from our lab have shown that while DR in *C. elegans* leads to multiple changes at the level of gene expression, loss of SFA-1 specifically reversed expression of lipid metabolism genes that is induced by DR (Heintz et al., 2017). Therefore, it is likely that changes in lipid metabolism on loss of splicing factor could be the underlying mechanism driving the longevity suppression in SF-dependent mutants.

In this chapter, I have shown that loss of REPO-1 causes widespread changes in the SF-dependent longevity mutants and particularly affects lipid metabolism genes. Moreover, these changes translate to alterations in

actual levels of lipid as seen by SRS microscopy. Using eCLIP, I identified POD-2/ACC1 as a highly conserved target of both SFA-1 (SF1 in mammals) and REPO-1 (SF3A2 in mammals) in worms and MEFs. Strikingly, POD-2 mimics SFA-1/REPO-1's requirement in longevity of DR, TORC1, ETC and IIS. Together, these findings hint at the causal role of lipid metabolism in longevity mediated by REPO-1 and SFA-1.

There are several reports linking the causal role of lipid metabolism in mediating lifespan extension in different species (Papsdorf and Brunet, 2019). DR for example, has been shown to remodel lipid profiles and components of lipid metabolism pathway are required for longevity in *C. elegans* and *Drosophila* (Heestand et al., 2013; Katewa et al., 2012). Upregulation of autophagy through reduced TORC also contributes to lipid homeostasis through HLH-30/TFEB in worms (O'Rourke and Ruvkun, 2013). More recently, it has been shown that short term caloric restriction in rhesus monkeys leads to upregulation of spliceosome components in their livers. This is coupled to massive post-transcriptional changes in genes involved particularly in lipid metabolism (Rhoads et al., 2018). This suggests that lipid metabolism is a central process modulated by different metabolic inputs and its regulation might be key in extending lifespan and healthspan in different organisms. This regulation might be brought about at a post-transcriptional level by splicing factors such as REPO-1 and SFA-1. It is possible that alternative splicing of genes involved in fat metabolism leads to specific splice isoforms which are required for mediating longevity in DR, TORC1 and ETC mutants. Which lipid genes undergo differential splicing in these different longevity paradigms and in what tissues, is yet to be characterized. Furthermore, how these splice isoforms functionally impact lipid metabolism and aging remains to be investigated.

CHAPTER 4

REPO-1 is required in early life and in the neurons to mediate longevity

Introduction

REPO-1 and SFA-1 regulate DR, TORC1 and ETC longevity by modulating lipid metabolism. However, to completely understand how they mediate this response, it is imperative to study their spatial and temporal requirement. This is particularly interesting considering the tissue and timing requirement of the longevity pathways themselves. For example, there is evidence suggesting that knockdown of electron transport chain complexes specifically during the L3-L4 larval stages of worm development is sufficient for longevity, whereas knockdown in adulthood has no effect on lifespan (Dillin et al., 2002). Conversely, interventions such as DR and TORC1 knockdown/pharmacological inhibition can be initiated later in life to obtain longevity benefits (Vellai et al., 2003).

There have been several reports elucidating the key tissues that mediate the benefits of DR, TORC1 and ETC mutation. For example, a previous study from our lab has shown that neuronal TORC1 is important for longevity (Zhang et al., 2019). More specifically, rescuing TORC1 activity only in the neurons in an otherwise long-lived TORC1 mutant is sufficient to suppress lifespan. It has also been shown that ETC knockdown in intestinal and neuronal tissues is required for increased longevity (Durieux et al., 2011). Furthermore, downstream mediators of DR longevity show tissue-specific expression pattern. For example, *skn-1* activation is required in a specific class of neurons (ASI neurons) to mediate DR longevity (Bishop and Guarente, 2007).

Since the longevity pathways that are regulated by REPO-1 and SFA-1 have complex spatial and temporal dynamics, we sought to understand when these splicing factors are required in determining lifespan of these long-lived mutants. In this chapter, I address the timing and tissue requirement of REPO-1 and SFA-1 to better understand their role in DR, TORC1 and ETC longevity.

Results

4.1 REPO-1 and SFA-1 are ubiquitously expressed in all tissues throughout life but shows an elevated expression at larval stages

To get a deeper insight into how these splicing factors might act to regulate longevity, I investigated the expression pattern of REPO-1 and SFA-1 and whether it is limited to a particular tissue or life stage in *C. elegans*. Using CRISPR technology, I inserted a C-terminal GFP tag in the endogenous locus of *repo-1* to express a fusion REPO-1::GFP line. Similarly, Caroline Heintz, a postdoctoral fellow, inserted an N-terminal wrmScarlet tag on SFA-1 to express wrmScarlet::SFA-1. We crossed these two strains to generate a single line expressing fluorescently tagged REPO-1 and SFA-1 and imaged different stages under the fluorescence scope. As expected of splicing factors, REPO-1 and SFA-1 expression was nuclear with a strong co-localization in most major tissues and life stages (**Figure 4.1 A,**B). A more detailed examination of SFA-1 and REPO-1 expression in the germline revealed that SFA-1 expression is suppressed in the maturing oocytes and during fertilization (**Figure 4.1A**, white arrows), after which it starts to express again in the hatched eggs (**Figure 4.1B**), likely from newly produced zygotic mRNA. REPO-1 on the other hand, continues to be expressed during this time and maternal transcripts might contribute to its expression. A previous report showed that a semi-dominant mutation in REPO-1 (also called SF3a66) causes anterior-posterior axis reversal in one-cell stage embryos, suggestive of its requirement in early embryogenesis in *C. elegans* (Keikhaee et al., 2014). This was further validated by using the Auxin Inducible Degron System (AID), to suppress REPO-1 function. Using CRIPSR, I generated *repo-1::gfp::degron* worms that were crossed to TIR1 expressing worms which is a plant derived E3-ubiquitin ligase. These strains when exposed to auxin at low (0.025 mM) or high 1mM) concentrations, catalyzed the degradation of degron tagged REPO-1. I observed that in the presence of auxin, eggs could not hatch or were arrested at the L1 stage in some cases further supporting the idea of REPO-1 as a major player in early development (**Figure 4.1C**). Very recently there has been a report showing SF3A2, the mammalian ortholog of REPO-1, to be important

for chromosome segregation in *Drosophila* and human cells (Pellacani et al., 2018). This function of REPO-1 could be conserved and essential for its role in mitotic tissues in *C. elegans*.

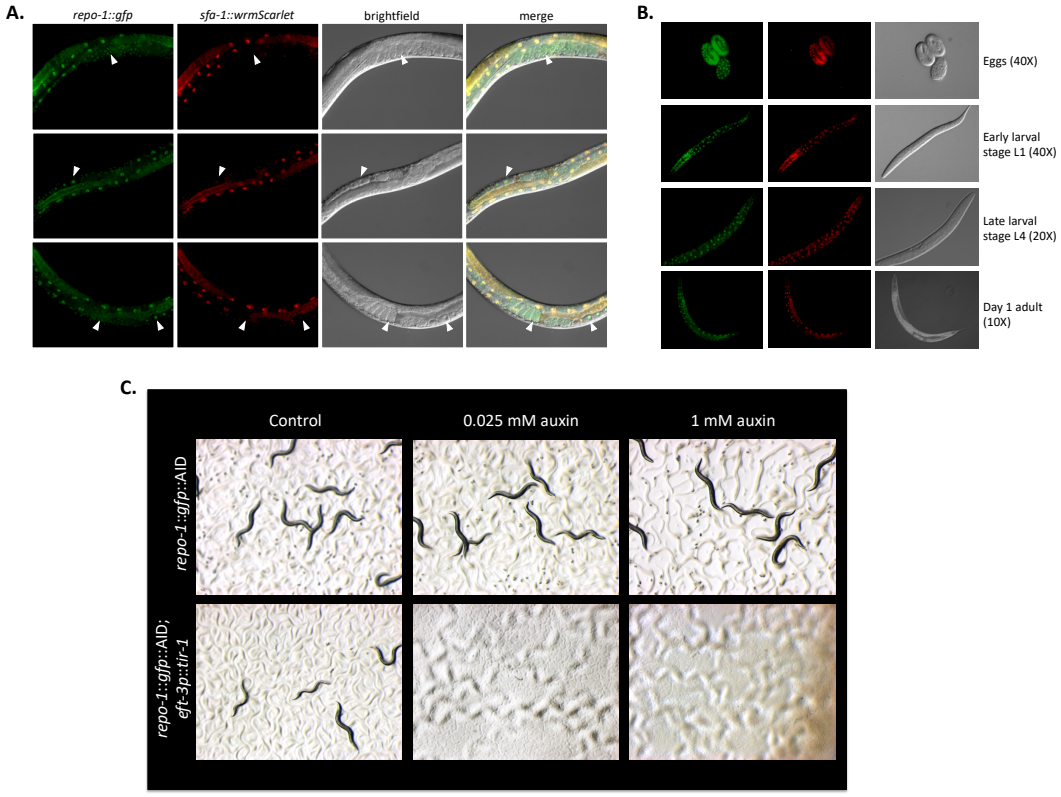

Figure 4.1: SFA-1 and REPO-1 are expressed across all worm life stages and in different tissues and is required for development.

A. Worms with CRISPR tagged REPO-1::GFP and CRISPR tagged SFA-1::wrmScarlet at Day 1. White arrows mark the presence of REPO-1 and absence of SFA-1 in early embryos.

B. Microscopic images of CRISPR tagged REPO-1 fused to GFP and CRISPR tagged SFA-1 fused to wrmScarlet from the egg stage to Day 1 of adulthood.

C. REPO-1 is an essential gene. Auxin inducible degradation of REPO-1 leads to lethality.

I next tested the expression levels of SFA-1 and REPO-1 across all stages of life. I first queried a data set published from our lab in which young and old wild type and *eat-2(ad1116)* worms were sequenced (Heintz et al., 2017). I found that neither *repo-1* nor *sfa-1* mRNA levels changed between young (day 3) and old (day 15) worms either in the wild type (WT) or in the *eat-2(ad1116)* background (**Figure 4.2 A,B**). To observe protein level changes across different life stages, I used CRISPR to generate N terminal 3XFLAG-

tagged REPO-1. I did extended egg lays and collected worms after 24 hours (L1-L2s), 48 hours (L3-L4s) and also adult worms at Day 1, 5, 10 and 15. Westerns using anti-FLAG antibody revealed elevated, almost double the expression of REPO-1 at early larval stages as compared to Day 1 of adulthood (**Figure 4.2 E,F**). However, with age, the level of REPO-1 does not alter significantly (**Figure 4.2 C,D**). These findings hint at the fact that splicing factors such as REPO-1 could play an important role in early life stages of *C. elegans*.

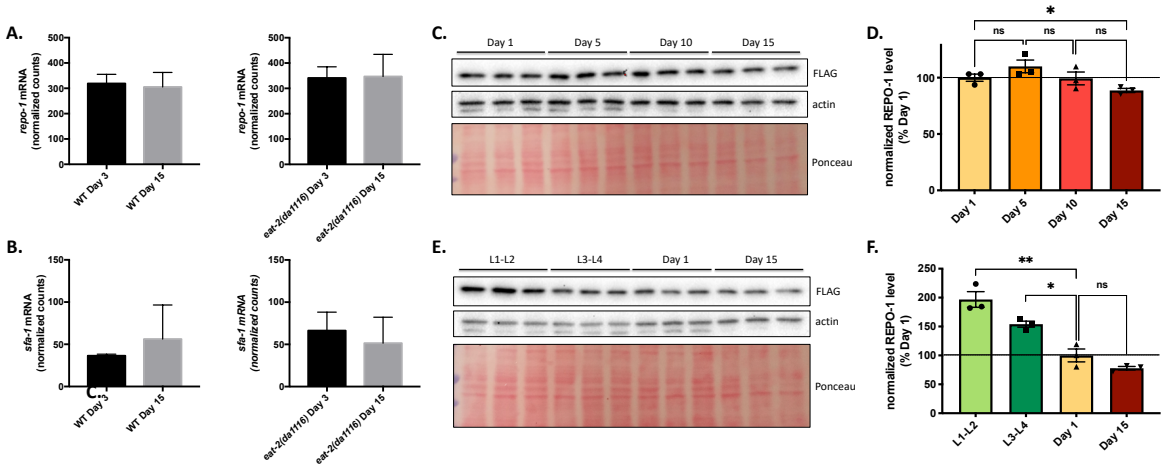

Figure 4.2: REPO-1 is expressed at elevated levels in early larval stages of worm development and might be crucial for its function in this time window.

A, B. Normalized counts of *repo-1* transcripts at Day 3 and Day 15 in WT and *eat-2(ad1116)* worms. Normalized counts of *sfa-1* transcripts at Day 3 and Day 15 in WT and *eat-2(ad1116)* worms. Transcript counts obtained from previously published RNA-Seq data (Heintz et al. Nature 2017).

C, D. Western blot of CRISPR tagged endogenous 3XFLAG::REPO-1 worms at Day1, Day 5, Day 10 and Day 15 of adulthood. Blots probed with 3XFLAG and actin antibodies. Ponceau staining of the blot shows equal loading. Quantification of 3XFLAG:REPO-1 normalized to actin. Blots quantified using ImageJ and represented as percent of expression at Day 1 of adulthood. (**** P≤0.0001, *** P≤0.001, ** P≤0.01, * P≤0.05; ns P>0.05; n=3).

E, F. Western blot of CRISPR-tagged endogenous 3XFLAG::REPO-1 worms at early (L1-L2) and late (L3-L4) larval stages and at Day1 and Day 15 of adulthood. Blots probed with 3XFLAG and actin antibodies. Quantification done using ImageJ, normalized to intensity of actin band and plotted as percent of expression at Day 1 of adulthood (**** P≤0.0001, *** P≤0.001, ** P≤0.01, * P≤0.05; ns P>0.05; n=3).

4.2 REPO-1 and SFA-1 are required in early life to extend lifespan in long-lived mutants

To test when REPO-1 and SFA-1 are required to mediate lifespan extension in different longevity paradigms, I used the RNA interference approach wherein we fed wildtype and long-lived strains with *repo-1* and *sfa-1* RNAi from hatch or from Day 1 of adulthood. In this regard, *eat-2(ad1116)*, *raga-1(ok386)* and *clk-1(qm30)* worms were either grown on *repo-1* and *sfa-1* RNAi from hatch or were transferred from control bacteria to RNAi containing bacteria on Day 1 of adulthood (D1-onset). I first compared the efficiency of knockdown between hatch vs D1-onset RNAi treatment. Western analysis on worms using RNAi from adulthood shows knockdown of REPO-1 and SFA-1 by Day 3 comparable to worms treated with RNAi from hatch (**Figure 4.3 A-D**). Subsequently, lifespan analysis was performed to measure survivorship over the next 3 weeks. While *clk-1(qm30)* worms grown on *repo-1* or *sfa-1* RNAi from hatch exhibited a complete suppression of lifespan extension, worms that were depleted of REPO-1 from adulthood were not able to abolish lifespan extension (**Figure 4.3 I,J**). This was also true for DR mutant *eat-2(ad1116)* and TORC1 mutant *raga-1(ok386)* (**Figure 4.3 E,F** and **Figure 4.3 G,H** respectively). These data suggests that REPO-1 and SFA-1 are required during the larval developmental phase of the worm life cycle irrespective of the longevity intervention. Together with observations showing elevated REPO-1 levels in early larval stages, these findings point towards an important role of splicing factors SFA-1 and REPO-1 in modulating longevity targets very early on in life.

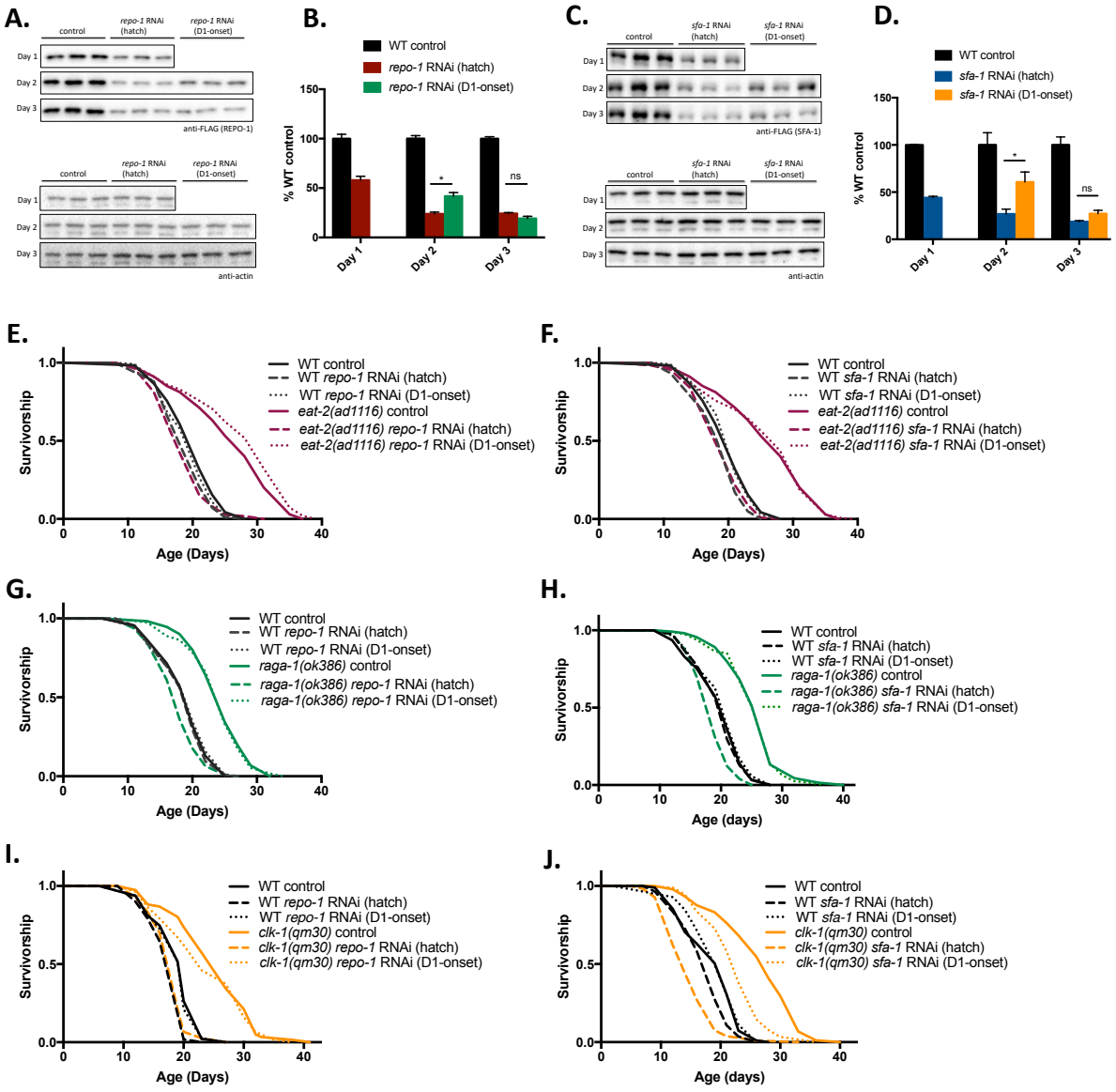

Figure 4.3: REPO-1 and SFA-1 creates a permissive landscape during the early stages of development to mediate longevity benefits later in life.

A-D. Adult-onset RNAi efficiently knocks down REPO-1 and SFA-1 comparable to RNAi from hatch. Western blotting of CRISPR tagged endogenous A. 3XFLAG::REPO-1 worms -/+ *repo-1* RNAi; C. 3XFLAG::SFA-1 worms -/+ *sfa-1* RNAi from hatch or Day 1 of adulthood (D1-onset). Samples collected on Day 1, Day 2 and Day 3 to measure efficiency of knockdown. Lysates probed for 3XFLAG as a readout of REPO-1/SFA-1 and actin as loading control. Quantification of knockdown of B. REPO-1 and D. SFA-1 normalized to actin. Blots quantified using ImageJ and represented as percent of RNAi untreated control. (****$P \leq 0.0001$, ***$P \leq 0.001$, **$P \leq 0.01$, *$P \leq 0.05$; ns $P > 0.05$). *P*-values calculated with unpaired, two-tailed Welch's t-test.

E, G, I. Survivorship of wild-type (WT) and long-lived mutants E. *eat-2(ad1116)*; G. *raga-1(ok386)* and I. *clk-1(qm30)* -/+ *repo-1* from hatch (- - -) or Day 1 of adulthood (D1-onset) (…). P = 0.5315, 0.0285,

Figure 4.3 (Continued) 0.2672 for WT *repo-1* RNAi hatch vs *eat-2(da1116)*, *raga-1(ok386)* and *clk-1(qm30)* mutants on *repo-1* RNAi hatch respectively). P = <0.0001, <0.0001, <0.0001 for WT *repo-1* RNAi D1-onset vs *eat-2(da1116)*, *raga-1(ok386)* and *clk-1(qm30)* mutants on *repo-1* RNAi D1-onset respectively).

F, H, J. Survivorship of wild-type (WT) and long-lived mutants F. *eat-2(ad1116)*; H. *raga-1(ok386)* and J. *clk-1(qm30)* -/+ *sfa-1* from hatch (- - -) or Day 1 of adulthood (D1-onset) (…). P = 0.5658, 0.002, <0.0001 for WT *sfa-1* RNAi hatch vs *eat-2(da1116)*, *raga-1(ok386)* and *clk-1(qm30)* mutants on *sfa-1* RNAi hatch respectively). P = <0.0001, <0.0001, <0.0001 for WT *sfa-1* RNAi D1-onset vs *eat-2(da1116)*, *raga-1(ok386)* and *clk-1(qm30)* mutants on *sfa-1* RNAi D1-onset respectively).

4.3 REPO-1 is required in neuronal tissues to mediate TORC1 longevity

To better understand which pathways or genes are important for REPO-1 and SFA-1 to promote lifespan extension, I assessed the tissue in which REPO-1 acts to mediate longevity in the *raga-1(ok386)* mutant. Since REPO-1 is an essential gene, loss of which leads to lethality (**Figure 4.1C**), a gene knockout and tissue specific rescues could not be used. Traditionally, tissue-specific RNAis are used wherein worms are fed with shRNA expressed under a tissue-specific promoter. This system however tends to be leaky. We therefore used RNAi combined with the SKILODGE system (Silva-Garcia et al. G3, 2019) to address this question (**Figure 4.4A**).

I CRISPR tagged endogenous *repo-1* with an N-terminal *gfp* tag and crossed this line to long-lived *raga-1* worms [Fig 4.4B, *raga-1(ok386)* control]. Feeding these worms *gfp* RNAi acts as a surrogate for knockdown of endogenous *repo-1*, that suppresses the lifespan extension of *raga-1(ok386)* worms [Fig 4.4B, *raga-1(ok386); repo-1* knockdown (endo)]. In this background, I expressed single copy knock-ins of *repo-1* in safe harbor loci in the worm genome under tissue specific promoters- *eft-3p* (ubiquitous), *rab-3p* (neuronal) and *myo-3p* (muscle). This copy of *repo-1* was tagged to wrmScarlet and hence resistant to *gfp* RNAi. As expected, ubiquitous SKILODGE expression of *repo-1* was able to rescue *raga-1* longevity in the background of endogenous *repo-1* knockdown (**Figure 4.4C**). Rescuing *repo-1* expression in the muscle was not able to rescue the longevity (**Figure 4.4E**). Strikingly, neuronal rescue of *repo-1* was able to completely rescue the lifespan extension (**Figure 4.4D**), suggesting that neuronal REPO-1 is required to

facilitate lifespan extension in the TORC1 mutant *raga-1*. This finding is particularly intriguing in the light of a previous study in our lab showing that neuronal TORC1 suppression is required to extend lifespan in *C. elegans* (Zhang et al., 2019). It is possible that REPO-1 regulates proximal longevity signals downstream of TORC1 which originate in the neurons that thereby control downstream processes cell autonomously or non-autonomously.

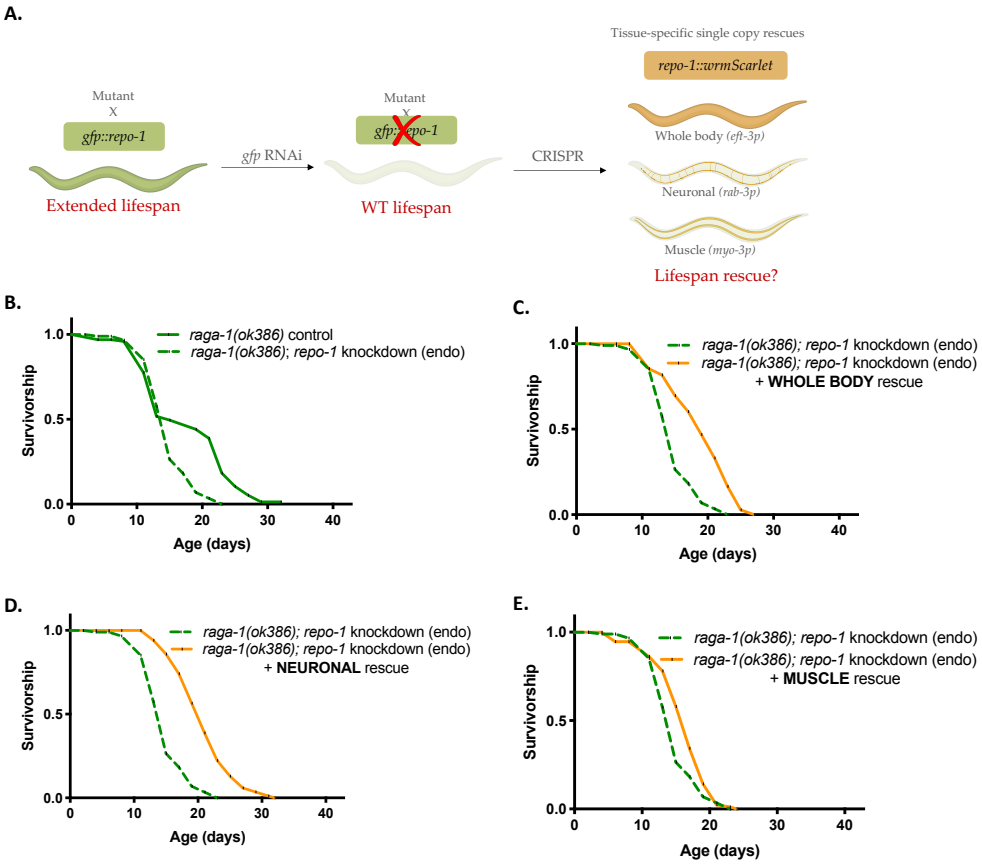

Figure 4.4: Neuronal REPO-1 is required for TORC1 longevity.

A. Schematic of altered RNAi approach used for whole body knockdown and tissue-specifc rescue of REPO-1.

B. Survivorship of *raga-1(ok386);gfp::repo-1* [*raga-1(ok386)* control] with knockdown of endogenous *repo-1* using *gfp* RNAi [*raga-1(ok386)*; *repo-1* knockdown (endo)] (*P*=<0.0001).

C-E. Survivorship of *raga-1(ok386)* with knockdown of endogenous *repo-1* (whole body) and tissue-specific rescue. *raga-1(ok386);gfp::repo-1* on *gfp* RNAi from hatch [*raga-1(ok386)*; *repo-1* knockdown (endo)] with tissue specific rescue of *repo-1* in C. whole body (driven by *eft-3p::repo-1::wrmScarlet*; *P*=

Figure 4.4 (Continued) <0.0001, 3 replicates), D. neurons (driven by *rab-3p::repo-1::wrmScarlet*; *P*= <0.0001, 3 replicates) and E. muscle (driven by *myo-3p::repo-1::wrmScarlet*; *P*= 0.0039, 3 replicates).

4.4 Early loss of SFA-1 and REPO-1 blocks longevity in a model of late onset TORC1 suppression

Interventions like dietary restriction and drugs such as rapamycin and metformin have been shown to have beneficial effects on lifespan and healthspan when administered late in life (Vellai et al., 2003). Such late-onset treatments are very important for their clinical translatability in treating age-related diseases and ameliorating health decline. Since loss of SFA-1 and REPO-1 early in life blocks lifespan extension in genetic models of DR and TORC1 longevity, I asked whether this loss has any bearing on the efficacy of adult-onset longevity treatments. To address this question, I used *raga-1* RNAi to knockdown the activator of TORC1 signaling, RAGA-1, during adulthood. This intervention has been shown to robustly extend lifespan in *C. elegans* (Zhang et al., 2019). I either pre-fed worms on control bacteria or *repo-1*/*sfa-1* RNAi containing bacteria during larval stages and transferred them to *raga-1* RNAi in adulthood to observe their response. I found that while *raga-1* RNAi treatment from adulthood robustly extended lifespan, knocking down either REPO-1 or SFA-1 during development renders this adult-onset intervention ineffective (**Figure 4.5 A,B**).

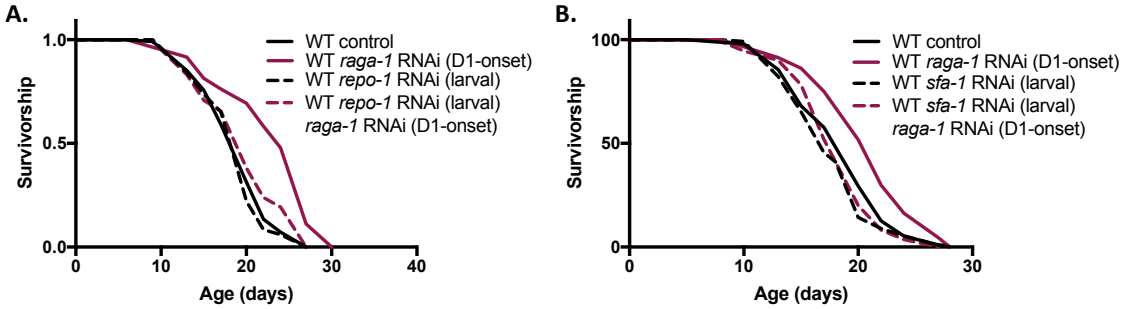

Figure 4.5: Efficacy of late-onset longevity interventions is dependent on early life activity of REPO-1 and SFA-1.

A. Survivorship curve of wildtype N2 worms -/+ *repo-1* RNAi in the larval stages -/+ *raga-1* RNAi from Day 1 of adulthood (*P*= 0.0244 wildtype N2 on *repo-1* RNAi (larval) versus wildtype N2 on *repo-1* RNAi (larval) + *raga-1* RNAi (D1-onset), 3 replicates).

Figure 4.5 (Continued) B. Survivorship curve of wildtype N2 worms -/+ *sfa-1* RNAi in the larval stages -/+ *raga-1* RNAi from Day 1 of adulthood (*P*= 0.2480 wildtype N2 on *sfa-1* RNAi (larval) versus wildtype N2 on *sfa-1* RNAi (larval)+ *raga-1* RNAi (D1-onset), 2 replicates).

Discussion

In this chapter, I show that irrespective of the longevity pathway, REPO-1 and SFA-1 act early during worm development to mediate longevity benefits later in life. Furthermore, I show that neuronal REPO-1 is required for lifespan extension, at least in the TORC1 mutant *raga-1(ok386)*. Finally, suppressing the activity of these splicing factors early makes worms resistant to longevity interventions administered later in life.

These findings have important implications on our ability to translate anti-aging therapeutics to humans. Increasing evidence shows that the same pro-longevity intervention can be beneficial, ineffective, or worse, harmful to different individuals of a population. For example, dietary restriction has different effects on longevity in different genotypes of *C. elegans* (Lucanic et al., 2017) or mice (Mitchell et al., 2016). In the case of methionine restriction, which is known to extend lifespan, while the intervention benefits a major population of mice and rats, a significant sub-population die sooner than non-restricted controls (Miller et al., 2005). If we were able to predict an individual's response to different treatment, we could inch a step closer to precision medicine. My work shows that the activity of splicing factors REPO-1 and SFA-1 sets a permissive landscape early in life which makes late-onset longevity interventions efficacious. Whether the activity of these splicing factors are heterogenous in each population and is the underlying cause of heterogeneity in response to treatments remains to be understood.

Furthermore, it is interesting to note that at least for TORC1 longevity, the function of these splicing factors is important in the neuronal tissue. It is well known that the central nervous system is a hotspot of splicing factor activity and the most striking changes to alternative splicing with age happen in the brain (Mazin et al., 2013; Raj and Blencowe, 2015; Stilling et al., 2014; Tollervey et al., 2011). Which genes and/or

pathways in the nervous system are regulated by the activity of these splicing factors and how they translate to longevity is an open question. Furthermore, we need to experimentally demonstrate that manipulating the function of these splicing factors in the neuronal tissue only in development results in effects on longevity. Besides, while I have shown that loss of REPO-1 and SFA-1 influences lipid metabolism and stored lipid levels, whether this process is regulated cell autonomously or non-autonomously remains to be studied. I attempted to address this question using the AID tagged REPO-1 worm where I crossed it to a strain expressing TIR-1 (the E3 ubiquitin ligase) exclusively in the neurons such that exposing these worms to auxin would result in degradation of the splicing factor only in the neurons. However, these worms display a phenotype where they climb the walls of culture plates and desiccate, making them unfit for lifespan studies. Current efforts are being made to standardize this system by using different versions of TIR1, to alleviate this technical difficulty. In doing so, we will have a more refined system to better control the spatial and temporal activity of these splicing factors and hopefully be able to address some of these questions in the near future.

CHAPTER 5

Components of the spliceosome change with age and caloric restriction in mice

(The introduction and discussion in this chapter draws heavily from the review "Alternative Splicing in Aging and Longevity" written by Malini Bhadra, Porsha Howell, Sneha Dutta, Caroline Heintz and William Mair for Human Genetics, 2019).

Introduction

Dietary restriction affects RNA splicing fidelity. However, if and how changes to nutrients influence the levels and/or post-translational modification of splicing factors, ultimately affecting their function, is only beginning to be studied. It has been shown that changes in expression or activity of splicing factors correlate with aging and longevity in humans, mice and *C. elegans* (Curran and Ruvkun, 2005; Heintz et al., 2017; Holly et al., 2013; Lee et al., 2016; Tabrez et al., 2017). In a study characterizing changes in gene expression of splicing factors with age in human blood, ~ 30% of the analyzed transcripts showed expression changes. Some of these splicing factor changes were also shown to be linked to cellular senescence in human fibroblasts and endothelial cells. Gene expression differences were observed in core spliceosomal components like *Sf3b1, Lsm2, Lsm5* and regulatory splicing factors such as *Srsf1, Srsf6, Srsf14, Hnrnpab, Hnrnpd* and *Hnrnph3* (Holly et al., 2013). Changes to splicing factor expression with age was also observed in humans leading to speculations that changes to splicing factor expression and activity could be a driver of the aging process (Lee et al., 2019). The expression of *HNRNPM* and *HNRNPA0* correlated with cognitive decline while *AKAP17A* expression levels correlated with cognitive as well as physical function decline. Age-related changes in expression of other splicing factors including *PTBP1/2*, *RAVER1* and *ROD1* were identified in the human temporal cortex (Tollervey et al., 2011).

Splicing factor expression changes are also associated with strain longevity in mice (Lee et al., 2016). These include core splicing factors such as *Sf3b1* and regulatory splicing factors like *Hnrnpa1, Hnrnpa2b1*, *Hnrnpk*, *Hnrnpul2*, *Hnrnpm*, *Hnrnpd*, *Hnrnpa0*, *Hnrnpul1*, *Srsf3* and *Tra2β*. Very interestingly, *Hnrnpa1 and Hnrnpa2b1* also correlate with parental longevity in humans (Lee et al., 2016). However, there is no consensus about which splicing factors correlate with age in different settings. Differences in identity and the direction of expression of splicing factors are seen between different human cohorts, tissues and cell types (Holly et al., 2013; Lee et al., 2016). Therefore, although there is a marked pattern of splicing factor expression changes associated with aging in different settings, functional studies are needed to determine if they are causally linked to longevity. In *C. elegans*, the branch point binding protein SFA-1 is required

for DR and TORC1-mediated extension of lifespan. Overexpression of SFA-1 increases lifespan, supporting a causal and sufficient role in DR longevity (Heintz et al., 2017) (**Figure 5.1A**). I also observed that overexpression of REPO-1 using extrachromosomal arrays resulted in a small, but significant lifespan extension was observed (*unpublished*) (**Figure 5.1B**). However, what the precise mechanism by which DR modulates SFA-1 and REPO-1 activity remains unclear.

We have observed that the levels of SFA-1 and REPO-1 do not change significantly with age or in the different longevity mutants (described in Chapter 4). However, my previous work has also shown that these splicing factors are important in specific tissues such as neurons to mediate longevity benefits. This encouraged us to examine the expression and activity of splicing factors tissue specifically. I wanted to assess changes that are highly conserved in higher organisms. I therefore used the mouse model to address this question. Moreover, using mice have an advantage in this regard wherein tissues can be harvested easily for transcriptomic and proteomic analysis.

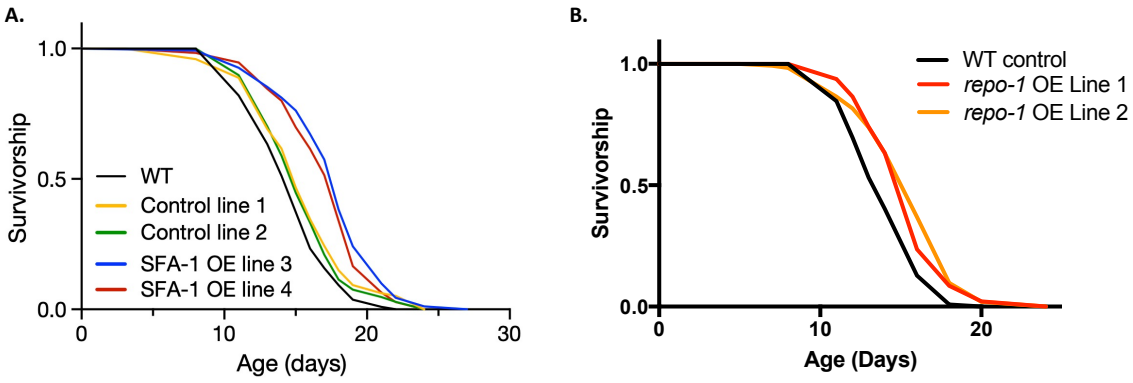

Figure 5.1: Overexpression of SFA-1 and REPO-1 in *C. elegans* extends wildtype lifespan.

A. Overexpression (OE) of SFA-1 increases wild-type lifespan ($P<0.0001$).

Figure adapted from (Heintz et al., 2017).

B. Overexpression of REPO-1 using extrachromosomal arrays driven by the ubiquitous *eft-3* promoter increases median wild-type lifespan ($p<0.0001$).

In this chapter, I describe my work with young and old, *ad libitum* fed and caloric-restricted mice obtained from the National Institute of Aging (NIA) from which I isolated tissues and characterized splicing factor expression changes using NanoString. These experiments were done in collaboration with my colleagues, Dr. Anne Lanjuin (Research Scientist) and Dr. Caroline Heintz (Research Fellow).

Results

5.1 Caloric Restriction in mice

Four cohorts of C57BL/6 male mice were obtained from the National Institute of Aging. They were 4 months and 18 months of age and either *ad libitum* fed (AL) or calorie restricted (CR). We obtained 5 animals belonging to each group. Both CR and AL are individually housed. CR is initiated at the NIA at 14 weeks of age at 10% restriction, increased to 25% restriction at 15 weeks, and to 40% restriction at 16 weeks where it is maintained throughout the life of the animal. Survival curves, food intake curves and body weights of the NIA strains are published (Turturro et al., 1999). We chose 4 months and 18 months of age because they represent young and old age population in these mice strains. At 18 months, differences in the physiological age of the AL and CR group begin to appear. While the CR group is at 100% survivorship, the AL group begin to die at this point and is at around the ~90% survivorship mark.

After arriving at the mouse facility, the mice were housed in the rodent facility at Harvard Chan School of Public Health in accordance with HCCM guidelines. To acclimate to the new environment, they were kept on the AL and CR diet for one month before being sacrificed. The food was obtained from the NIA wherein chunk diet was fed to the AL group. One pellet of the fortified diet was fed to the CR group between 6:00 and 8:00 AM every morning shortly before the 'lights on' phase i.e. right before their rest cycle begins. The whole experiment was repeated twice such that we had n=10 mice for each group.

On the day of tissue harvesting, food was removed from all the groups at 10AM after the CR group finished their food pellet for the day. Animals were sacrificed after 6 hours of food removal. Mice were weighed before dissection. As expected, body weights increased over age and CR mice had significantly lower weights than AL fed mice (Fig 5.2A). Mice were euthanized in a CO_2 chamber, followed by cervical dislocation, cardiac puncture to collect serum from the blood, and tissue harvest. Tissues harvested included hypothalamus-enriched sample of the brain (and other regions of the brain collected separately), gastrocnemius and soleus muscle, gonadal and inguinal fat pads, heart, testes and the pituitary gland. Observation of the livers in mice from each of the experimental groups revealed that while age-associated fatty liver was observed in the AL group, the livers in old CR mice were protected from it (**Figure 5.2B**). Finally, primary dermal fibroblasts were cultured from mouse tails by Dr. Porsha Howell, a former postdoctoral fellow in the lab, and stored at -80°C.

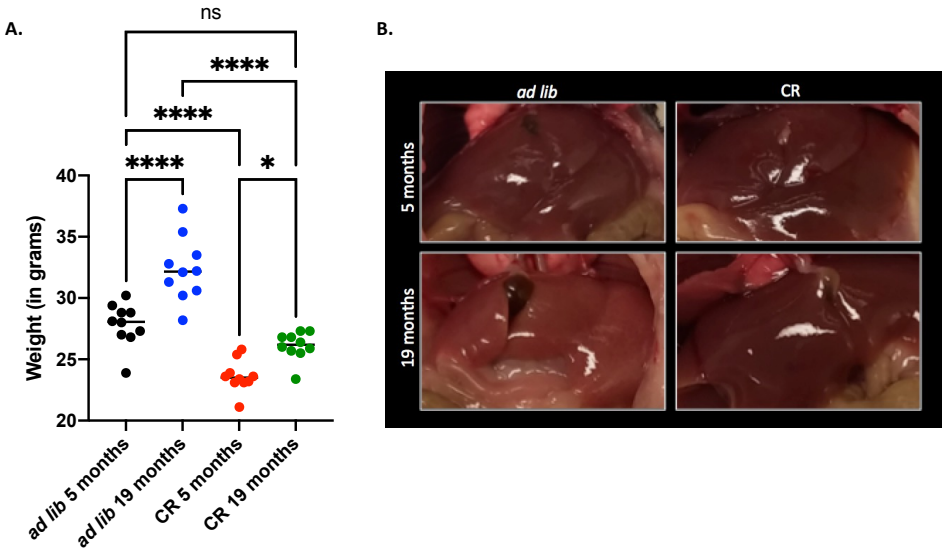

Figure 5.2: Characterization of young/old *ad libitum* and caloric-restricted C57BL/6 mice.

A. Weights of young 5 month and old 19 month old *ad libitum* fed and calorie-restricted C57BL/6 mice. Data pooled from 2 biological replicates (n=5 per treatment per replicate).

B. Representative images of livers of young 5 month and old 19 month old *ad libitum* fed and calorie-restricted C57BL/6 mice. Note the appearance of fatty liver in *ad libitum* fed old mouse unlike its CR counterpart.

5.2 Using NanoString to study transcriptional changes in spliceosome components

To assess differences in the expression of the mammalian orthologs of SFA-1 and REPO-1 in different tissues with age and on caloric restriction along with other splicing factors, I used the NanoString platform (Geiss et al., 2008) (**Figure 5.3**). NanoString is a patented technology that allows us to quantify the amounts of RNA of multiple genes in the same mix. In principle, this technology is used to measure differences proteins, RNA, DNA as well as other biomolecules depending upon the recognition probes being used. NanoString uses two probes to capture each gene of interest. The first probe, also called the 'capture probe', contains a 35- to 50-base sequence complementary to a particular target mRNA plus a short common sequence coupled to an affinity tag such as biotin. The second probe, 'the reporter probe', contains a second 35- to 50-base sequence complementary to the target mRNA, which is coupled to a color-coded tag that provides the signal for detection. The tag consists of ssDNA that is attached to a series of complementary *in vitro* transcribed RNA segments each labeled with a specific fluorophore. Hybridization results in the formation of a tripartite structure comprising of the target mRNA, its reporter probe and the specific capture probe (**Figure 5.3A**). The linear order of these differently colored RNA segments creates a unique barcode for each gene we are interested to quantify (**Figure 5.3C**).

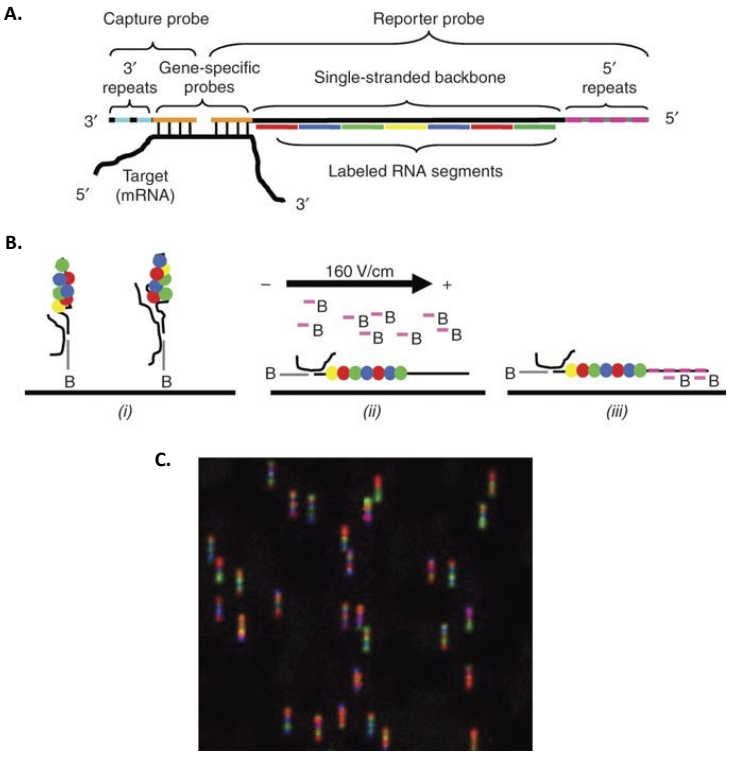

Figure 5.3: Schematic of the NanoString nCounter gene expression system.

A. Schematic representation of the hybridized complex with a tripartite structure.

B. Schematic of the (i) binding (ii) electrophoresis and (iii) immobilization of the probes bound to the target mRNA.

C. False-color image of immobilized reporter probes that is detected by the nCounter platform.
Figure adapted from (Geiss et al., 2008).

Depending on the number of genes to be analyzed, we can procure a custom reporter probe set that can detect and quantify up to ~800 genes in a single mix of a given sample. We therefore designed a custom probe set of ~60 genes including *Sf1* (*sfa-1* in worms) and *Sf3a2* (*repo-1* in worms) based on available published literature and specifically our own RNA seq datasets (Heintz et al., 2017) (Table 5.1). The expression of these splicing factors either respond to change in age or upon CR or are implicated to be associated with longevity (Holly et al., 2013; Latorre et al., 2019; Lee et al., 2016; Rhoads et al., 2018; Swindell, 2009; Tabrez et al., 2017).

Table 5.1: Genes detected by the custom reporter probe set using NanoString.

Splicing Factors				
Celf2	*Ctnnbl1*	*Ddx23*	*Hnrnpa0*	*Hnrnpa1*
Hnrnpa2b1	*Hnrnpd*	*Hnrnph3*	*Hnrnpk*	*Hnrnpm*
Hnrnpr	*Hnrnpul2*	*Hnrnpab*	*Imp3*	*Lsm2*
Mbnl1	*Nono*	*Nova1*	*Prpf18*	*Prpf3*
Prpf38a	*Prpf4*	*Prpf4b*	*Prpf8*	*Ptbp1*
Rbfox1	*Rbfox2*	*Rbfox3*	*Sf1*	*Sf3a1*
Sf3a2	*Sf3b1*	*Sf3b4*	*Slu7*	*Smn1*
Srpk2	*Srrm2*	*Srrm3*	*Srsf1*	*Srsf18*
Srsf2	*Srsf3*	*Srsf4*	*Srsf5*	*Srsf6*
Srsf7	*Tdp43*	*Tra2b*	*Zcchc8*	*Sf3a3*
Snrpg				
Cr control				
Sgk1				
Age control				
Grn	*Cdkn2a*			
Reference genes				
Ube2d2	*Cyc1*	*rpl13*	*β2m*	*Ppia*
Hmbs				

5.3 Splicing factors and splicing factor kinases demonstrate tissue specific changes in expression in response to age and caloric restriction

To assess differences in splicing factor expression, I performed NanoString analysis of gene expression on RNA samples from three tissues: liver (n=5), gastrocnemius muscle (n=3) and hypothalamus (enriched) (n=3). Counts for the splicing factor targets were analyzed using nSolver 4.0 software.

I first looked at the expression of *Sf1* and *Sf3a2* mRNA in the three tissue types (**Figure 5.4**). From the normalized counts, it was evident that *Sf1* mRNA was more abundantly expressed in the hypothalamus enriched brain region as compared to liver and muscle (**Figure 5.4C**). On the other hand, *Sf3a2* mRNA showed lower expression in the liver compared to muscle and hypothalamus (**Figure 5.4D**). Interestingly, *Sf1* mRNA levels showed mild but significant changes in response to caloric restriction. In the muscle, I observed an upward trend in response to CR which is significant at 19 months of age (**Figure 5.4B**). In the

hypothalamus, *Sf1* mRNA levels were significantly upregulated in response to CR in young 5 month old mice but remained elevated in the old mice in either diet groups (**Figure 5.4C**). In contrast, in the liver, *Sf1* mRNA levels are downregulated in response to CR in young mice (**Figure 5.4A**). Dynamic changes in *Sf1* mRNA levels in the early timepoint in response to CR perhaps hint at the fact that early life changes in *Sf1* can occur in response to diet, which might lead to long-term impacts on the organism. *Sf3a2* on the other hand did not show significant changes at the level of mRNA with age or diet in any of the tissues. However, there was an upward trend in their expression in response to CR in the liver (**Figure 5.4D**). This corroborates with similar upward trends (not significant) in the expression of *Sf3a2* in the liver of rhesus monkeys fed a CR diet for 2 years (Rhoads et al., 2018).

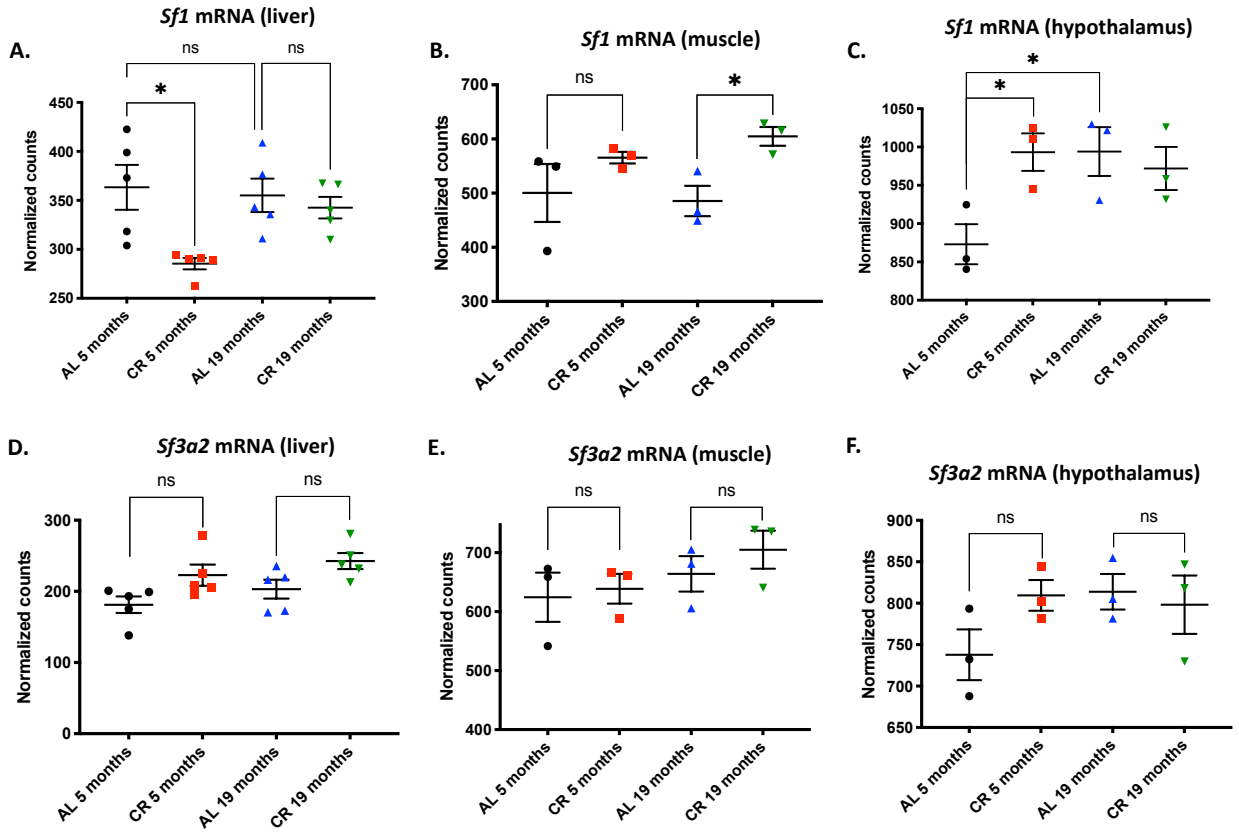

Figure 5.4: Expression of *Sf1* and *Sf3a2* mRNA in three different tissues of young/old and AL/CR mice using NanoString.

A, B, C. Expression of *Sf1* (mammalian *sfa-1*) in liver, gastrocnemius muscle and hypothalamus enriched brain region.

Figure 5.4 (Continued) D, E, F. Expression of *Sf3a2* (mammalian *repo-1*) in liver, gastrocnemius muscle and hypothalamus enriched brain region.

Counts are normalized to *β2m, Cyc1, Hmbs, Ppia* mRNA in liver; *Cyc1*, *Hmbs* mRNA in the muscle; *β2m, Cyc1, Hmbs, Ppia, Rpl13* mRNA in the hypothalamus. Normalization is done on the nSolver software wherein these transcripts showed a stable expression pattern in the different tissue types.

(****$P \leq 0.0001$, ***$P \leq 0.001$, **$P \leq 0.01$, *$P \leq 0.05$; ns $P > 0.05$). *P*-values calculated with unpaired, two-tailed Welch's t-test.

More generally, splicing factor mRNA levels stayed constant across age and diet in the three tissues tested. However, some splicing factors changed either in response to age or diet. Of special interest were changes to *Hnrnpa1* mRNA in the liver and hypothalamus (**Figure 5.5A; 5.7A**). They were both upregulated with age. In the hypothalamus, *Hnrnpa1* mRNA was significantly increased with age in *ad libitum* fed group but not in the CR group (**Figure 5.7A**). This is particularly interesting because previous reports suggest that *Hnrnpa1* mRNA expression correlates to parental longevity in humans and strain longevity in mice (Lee et al., 2016). Further it was shown that the expression of *Hnrnpa1* increases with rising passage numbers of fibroblasts cultured *in vitro* linking the expression level to the onset of senescence (Holly et al., 2013). Other splicing factors and regulatory proteins that responded to CR are *Sf3b1, Prpf18, Imp3* and *Mbnl1* in the liver (**Figure 5.5**), *Hnrnph3, Prpf4b* and *Srsf7* in the muscle (**Figure 5.6**), *Prpf4b, Hnrnpnm* and *Rbfox2* in the hypothalamus-enriched brain region (**Figure 5.7**).

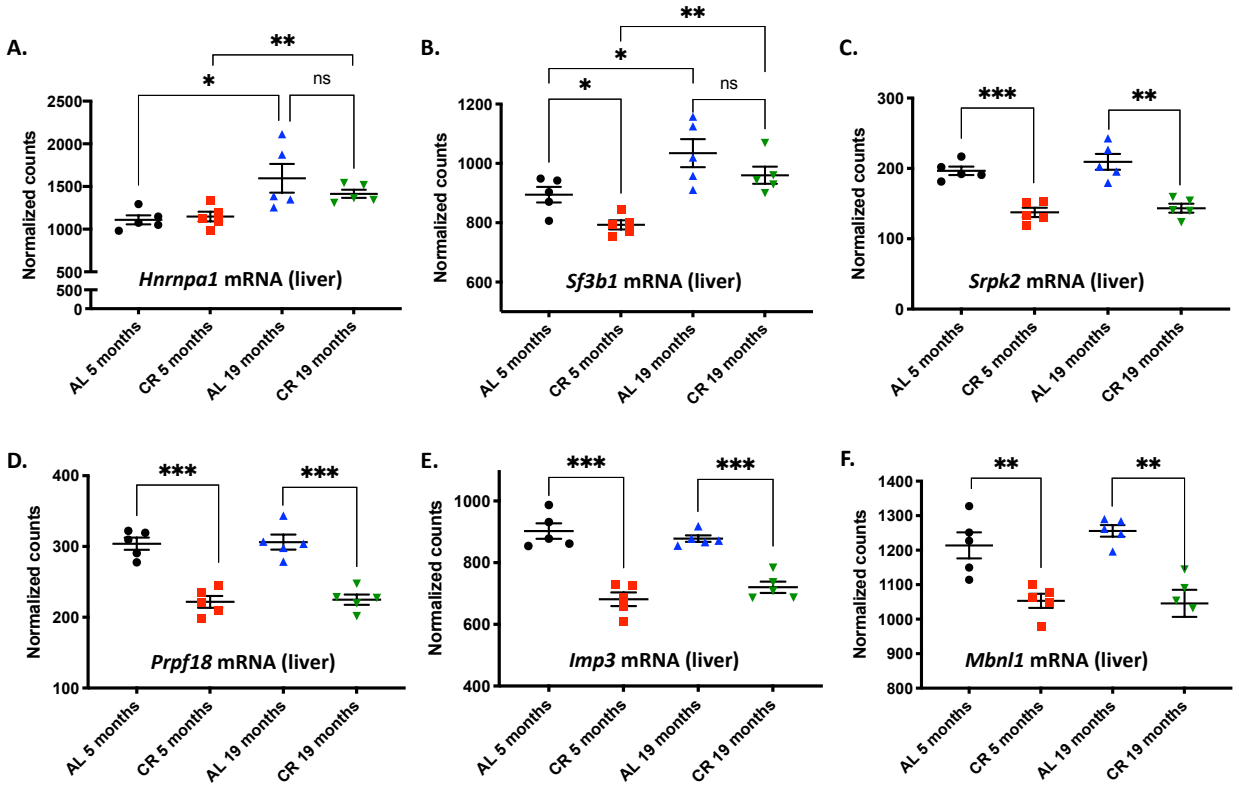

Figure 5.5: Expression of splicing factors and splicing factor kinase mRNA in liver of young/old and AL/CR mice using NanoString.

Counts are normalized to *β2m, Cyc1, Hmbs, Ppia* mRNA. Normalization is done on the nSolver software wherein these transcripts showed a stable expression pattern in the liver.

(****$P \leq 0.0001$, ***$P \leq 0.001$, **$P \leq 0.01$, *$P \leq 0.05$; ns $P > 0.05$). *P*-values calculated with unpaired, two-tailed Welch's t-test.

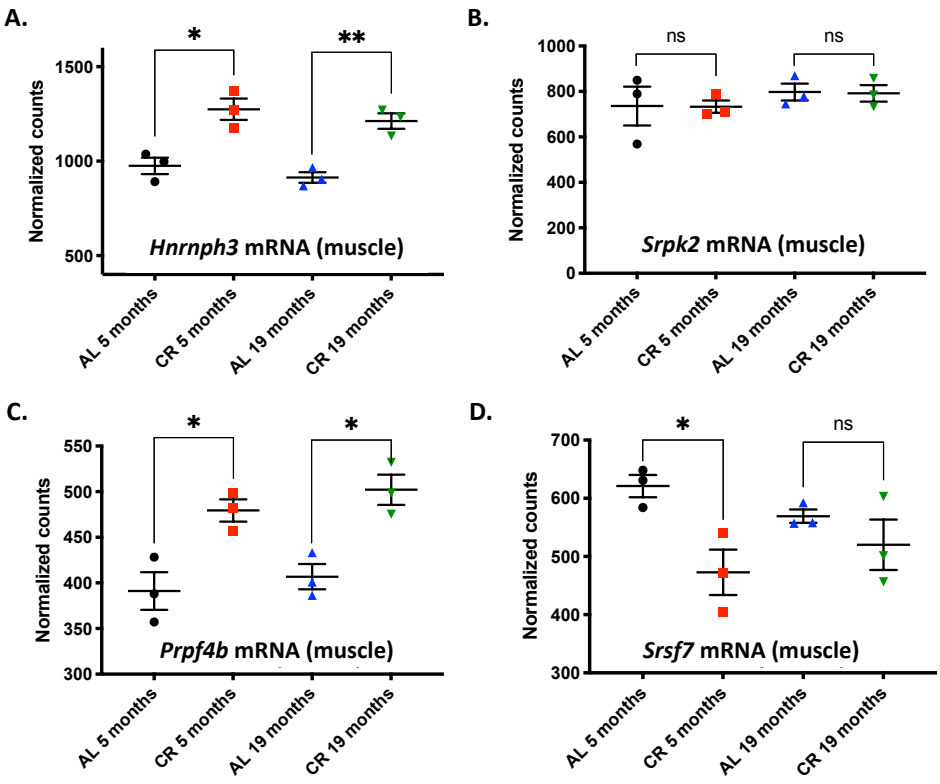

Figure 5.6: Expression of splicing factors and splicing factor kinase mRNA in gastrocnemius muscle of young/old and AL/CR mice using NanoString.

Counts are normalized to *Cyc1* and *Hmbs* mRNA. Normalization is done on the nSolver software wherein these transcripts showed a stable expression pattern in the muscle.

(****$P \leq 0.0001$, ***$P \leq 0.001$, **$P \leq 0.01$, *$P \leq 0.05$; ns $P > 0.05$). *P*-values calculated with unpaired, two-tailed Welch's t-test.

Another interesting observation was the upregulation of *Srpk2* mRNA in the liver of CR mice (**Figure 5.5C**) which was not observed in muscles or hypothalamus (**Figure 5.6B; 5.7B**). SRPK2 is a serine/threonine kinase which phosphorylates SR proteins that are essential components of the pre-mRNA splicing machinery. Some of its well-known substrates include SF2/SRSF1. A recent report showed SRPK2 function is tightly coupled to the metabolic signal integrator mTORC1. It demonstrates that SRPK2 is a direct substrate of S6K that lies downstream to mTORC1 (Lee et al., 2017). In response to nutrient signals, S6K phosphorylates SRPK2 at Ser494. This predisposes it to phosphorylation by casein kinase 1 (CK1) on Ser497. These two phosphorylation events cause SRPK2 shuttling from the cytoplasm to the nucleus, where

it can phosphorylate SR proteins, causing them to splice mRNAs, particularly those that belong to lipogenic genes, thus generating stable mRNAs. In the absence of nutrient signals, lipid genes remain unspliced making them prone to nonsense mediated mRNA decay. They also show this regulation to be essential for growth of cancer cells, as they need to integrate anabolic signals for lipid synthesis. The downregulation of *Srpk2* mRNA in the liver in CR animals suggests that it could be controlled transcriptionally by the action of transcription factors that play a role in mediating catabolic responses.

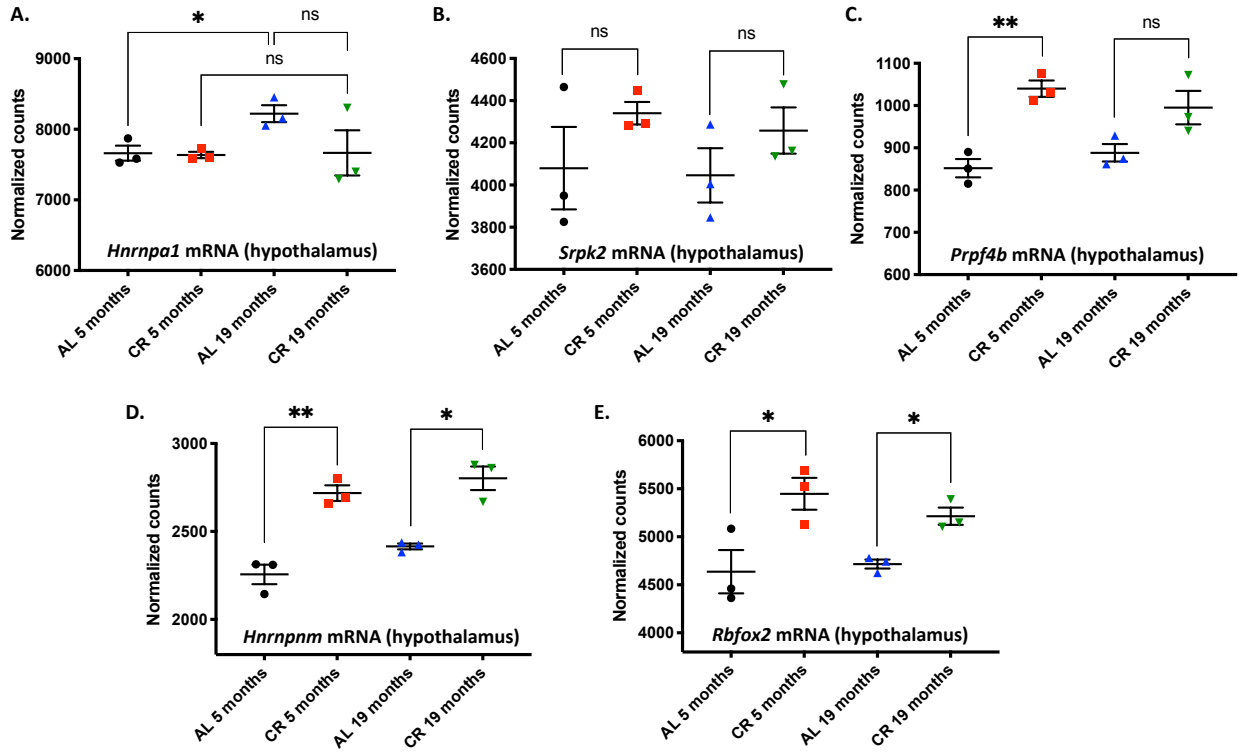

Figure 5.7: Expression of splicing factors and splicing factor kinase mRNA in hypothalamus-enriched brain region of young/old and AL/CR mice using NanoString.

Counts are normalized to *β2m, Cyc1, Hmbs, Ppia* and *Rpl13* mRNA. Normalization is done on the nSolver software wherein these transcripts showed a stable expression pattern in the hypothalamus.

(****$P \leq 0.0001$, ***$P \leq 0.001$, **$P \leq 0.01$, *$P \leq 0.05$; ns $P > 0.05$). *P*-values calculated with unpaired, two-tailed Welch's t-test.

Discussion

Age and diet are critical factors that impact the cellular mRNA landscape. While changes to gene expression and function at the transcriptional level are widely studied, how post-transcriptional control such as splicing is also affected is only beginning to be understood. It is becoming increasingly clear that aging and longevity paradigms such as CR affect splicing through changes to the spliceosome at multiple levels (Heintz et al., 2017; Lee et al., 2016; Rhoads et al., 2018; Swindell, 2009; Tabrez et al., 2017).

In this chapter, I used NanoString technology to identify differences in expression of specific splicing factor mRNAs in several mouse tissues with change in age and CR. While interesting changes were observed, they were rather mild. It is likely that splicing factors are stably expressed and regulated at the level of their activity rather than expression.

Several lines of evidence suggest that signaling through nutrient sensing pathways can affect the activity of splicing factors. For example, activation of AKT downstream of insulin and growth factor signals has been shown to impact splicing both directly and indirectly. AKT can impact splicing indirectly through modulation of splicing factor expression (Latorre et al., 2019), or directly through the regulation of SR proteins that bind RNA and impact splicing (Blaustein et al., 2005) or SR protein-specific kinase (SRPK) activity and localization (Zhou et al., 2012). A phosphoproteomic screen of the three AKT isoforms identified 25 RNA processing proteins including multiple splicing factors and splicing regulatory proteins, that are modulated by AKT (Sanidas et al., 2014), suggesting that extracellular signals, through AKT, can influence alternative splicing through post-translational modification of specific splicing factors. AKT has also been shown to phosphorylate several SR proteins including SRSF4 and SRSF6 in mammalian cell lines (Jiang et al., 2009). This is potentially through SRPKs, since growth factor-stimulated cells promote SRPK phosphorylation and translocation to the nucleus, SR protein phosphorylation and subsequent changes to alternative splicing through a mechanism involving AKT (Zhou et al., 2012). Recent work also suggests a functional role for AKT regulation of splicing factor activity in age-associated phenotypes such

as senescence and cancer. Inhibition of AKT and/or ERK leads to an upregulation of splicing factor expression and alleviation of senescent phenotypes in human fibroblast (Latorre et al., 2019). Furthermore, pharmacological inhibition of PI3K/AKT/mTOR upregulates splicing regulatory protein, HNRNPM-dependent splicing regulation, which plays a role in cancer treatment (Passacantilli et al., 2017). Further research is needed to determine whether AKT generally acts a mediator between nutrient signaling, splicing factor activity and age-associated phenotypes.

Recent data have also revealed a connection between mTORC1 signaling and alternative splicing. mTORC1 activation of S6K1 leads to phosphorylation of splicing factor kinase SRPK2, which translocates to the nucleus and activates SR protein binding to the U1–70 K spliceosome component to promote splicing of lipogenesis-related transcripts to fuel cancer cell growth (Lee et al., 2017). mTORC1 activation also influences 3′ splice site utilization and alternative exon usage of components of the spliceosome to regulate the transcriptome, which may serve as another mechanism for mTOR-regulated translational control (Chang et al., 2015, 2019).

While multiple reports are emerging suggesting that various nutrient signaling pathways change splicing factor activity or expression and therefore, affect alternative splicing of specific genes, whether they are causal to longevity remains to be understood. With advanced proteomics and deep sequencing technologies available to us, future studies on regulation of splicing factor activity and generation of alternative splice isoforms will greatly advance our understanding on how these might play a role in aging and age-related diseases.

CHAPTER 6

Discussion, Significance and Future directions

Aging research in the last few decades has shown that environmental conditions and genetic manipulation can strongly influence the rate of physiological aging. The most widely studied anti-aging intervention is dietary restriction (DR) which has been shown to positively impact nearly every organism in which it has been tested to date, not only increasing longevity but also protecting against many chronic diseases. However, DR is coupled to clinically undesirable side effects such as stunted growth, poor immunity and reproductive capacity. Therefore, harnessing the molecular and cellular processes mediating the beneficial responses of DR has the potential to yield novel therapeutics that can reduce the incidence of multiple age-associated chronic illnesses in the elderly.

Geroscience has focused so far on studying mechanisms by which the longevity of model organisms can be improved and the onset of chronic diseases delayed. In this regard, various longevity inducing pharmacological and dietary interventions are being studied. However, there are two outstanding questions that remain to be understood completely.

1. Why do individuals age at different rates?

2. How can we predict the response of individuals to longevity interventions such as DR?

6.1 Individuals show heterogeneity in their natural aging rates

Aging is an extremely complex process. The trajectory of a person's health as they move through the course of their life varies drastically. While race, gender (National Center for Health Statistics (US), 2011), socio-economic status and income heavily influence our life expectancy (Chetty et al., 2016), it is becoming clear that there are genetic and environmental determinants play a major role in how well we age (**Figure 6.2**). However, there is still a contributing factor(s), that has an impact on our aging rates even when all other factors are controlled for. The simplest example comes my experience during my dissertation work where I cultured isogenic, wild type *C. elegans* worms and used them for lifespan measurements. What really stood out to me was that while these worms had the same DNA and were exposed to the same food and other growth conditions, some lived for 10-12 days whereas others lived for 25-27 days, most averaging at roughly 3 weeks. The sigmoidal nature of survivorship curves (accounting for death due to natural causes) in a population is almost always true, whether in a laboratory setting or in the wild. What causes some individuals to die sooner whereas others to live exceptionally long? Are there stochastic gene expression or epigenetic differences in a population that underlie this variation? Can these differences be captured early in life and used as a "biomarker" of life expectancy?

Understanding the mechanism underlying this heterogeneity has become a compelling question in aging research. *C. elegans* is an excellent model to address this question owing to their short lifespan and ease of growing isogenic worm populations, that age at different rates. In *C. elegans*, natural heterogeneity in the expression of a stress-sensitive gene, *hsp-16.2*, predicts lifespan (Rea et al., 2005). In another report, it has been shown that a stochastic early life increase in ROS in a sub-population of worms, sets a cascade of events in motion that improve stress resistance and prolong lifespan in those animals (Bazopoulou et al., 2019). Data published from our own lab has shown that the splicing pattern of specific genes can be a predictor of life expectancy. Fluorescent mini gene reporters of a single exon 5 skipping event in *ret-1* (Kuroyanagi et al., 2013) (**Figure 6.1A**) in *C. elegans* can be used to sort isogenic animals at day 6 of adulthood into subpopulations with short (SL) or long life-expectancies (LL), identifying animals that are

naturally aging poorly or well (Heintz et al., 2017) (**Figure 6.2 B,C**). Animals with prevalent *ret-1* exon 5 inclusion (GFP) at day 6 show lifespan extension compared to isogenic animals with exon 5 skipping (mCherry). Dr. Caroline Heintz, a Research Associate in our lab, isolated six biological replicates of LL and SL subpopulations at day 6 and performed 75-bp paired-end RNA-Seq. In collaboration with Mary Piper from the Harvard Chan Bioinformatics Core and Maria Perez-Matos, a graduate student in our laboratory, we analyzed gene expression and differential isoform usage differences between LL and SL worms, in an attempt to understand the nature of the early changes occurring in individuals of an isogenic population, that otherwise age differently.

First, we used WormCat (Holdorf et al., 2020) to identify functional signatures in genes significantly up or downregulated in the long life-expectancy animals (**Figure 6.1D**). LL animals have decreased expression of multiple functional categories including genes regulating 'signaling' and the 'proteosome', while genes required for 'stress response/detoxification' and 'proteolysis', processes known to be longevity-related, are increased. LL animals also show widespread changes in genes required for lipid metabolism, with subsets of lipid metabolic genes showing increased expression, suggesting differences in their lipid metabolism or composition (**Figure 6.1D**). Differential isoform usage between LL and SL animals is enriched for pathways implicated in aging such as 'signaling', 'proteolysis' and 'lipid metabolism' further suggesting that splicing of pre-mRNAs specifically linked to these pathways is coupled to life expectancy (**Figure 6.1E**). Instead of a generalized loss of splicing fidelity in animals that are aging poorly, these data suggest that heterogeneity in expression and splicing of genes in specific functional categories, including lipid metabolism and proteolysis, early in the life of an individual is coupled to life expectancy.

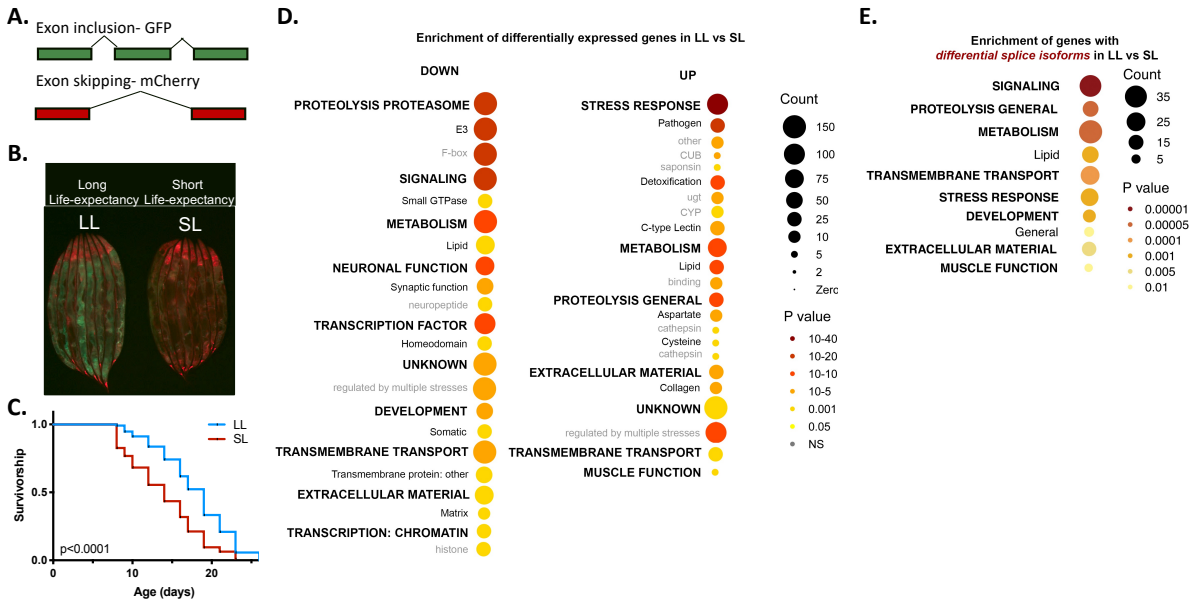

Figure 6.1: Early life alternative splicing of mRNAs related to lipid metabolism and known longevity pathways correlate with subsequent life expectancy in *C. elegans.*

A. Schematic illustrating the fluorescence expression pattern of *ret-1* splicing reporter worm. Inclusion/exclusion of exon 5 results in GFP/mCherry expression respectively.

B. Representative images of *ad-libitum* fed *ret-1* reporter worms segregated at Day 6 based on their splicing pattern.

C. Survivorship of the worm sub-populations separated at Day 6 (P<0.0001, 1 of 6 replicates). Worms that age slowly are marked 'LL' (Long Life-expectancy) and worms that age rapidly as 'SL' (Short Life-expectancy).

Results (B, C) published in Heintz et al. Nature, 2017

D. WormCat visualization of categories enriched in down and upregulated genes in LL vs SL worms. padj<0.01 and fold change>1.5 was used as cutoff to mark differentially expressed genes.

E. WormCat visualization of categories enriched in genes that exhibit differential isoform usage in LL vs SL worms.

Results (D, E) obtained in collaboration with Maria Perez-Matos (Graduate student, Mair Laboratory) and Mary Piper (Bioinformatician, Harvard Chan Bioinformatics Core)

Since inter-individual splicing differences occur early, it is plausible to think that differences in the activity of splicing factors early in life could be responsible for these stochastic changes, which could ultimately impact the rate of aging. I have shown that in *C. elegans*, early life SFA-1 and REPO-1 is required for

longevity in DR, TORC1 and ETC mutants. Furthermore, overexpression of SFA-1 (Heintz et al., 2017) and REPO-1 (unpublished) is sufficient to increase median lifespan in wildtype worms. Furthermore, there is an elevated expression of REPO-1 protein in early life. Interestingly, the pathways that are affected on loss of REPO-1 in the splicing factor dependent longevity mutants are the same pathways whose genes show splicing differences in the LL vs SL animals. Most prominent are genes involved in lipid metabolism. These raise a lot of interesting questions for the future: 1. Are there inherent or stochastic differences in levels or activity of these splicing factors early in life? 2. Could these differences account for the variation in splicing of specific genes that we see in populations that age differently? 3. Are these splicing changes causal to the different rates of aging in an isogenic population?

6.2 Organisms exhibit variability in their response to longevity interventions

There has been little to no emphasis on studying the underlying reason why individuals respond to longevity interventions variably and if so, how can we predict their response (Perez-Matos and Mair, 2020). This is critical, since the same therapeutic treatment can be beneficial, ineffective, or worse still, harmful, depending on the sex, genotype and physiological state of the individual to which it is applied (Fig 6.2). For example, dose of pharmacological treatments administered, or DR have very different effects on lifespan in different genotypes (Lucanic et al., 2017; Mitchell et al., 2016; Wilkie et al., 2020). This interaction of diet and genotype could explain the underlying cause why two longitudinal studies on rhesus monkeys undergoing DR showed different effects on lifespan rhesus monkeys (Mattison et al., 2017). While the University of Wisconsin study reported a significant positive impact of reduced caloric intake on survival, the National Institute on Aging (NIA) study showed there was no significant survival benefit. In other studies, DR does not provide longevity benefits or is minimally effective in some rodent strains (Harper et al., 2006; Turturro et al., 1999; Weindruch and Walford, 1988). Indeed, in some mice strains, DR can be deleterious (Barrows and Roeder, 1965; Fernandes et al., 1976; Forster et al., 2003; Harrison and Archer, 1987; Liao et al., 2010). These studies together indicate that lifespan extension on DR may not be a universal phenomenon.

Besides inter-genotype variation to longevity interventions, there is a high degree of variation that also exists within an isogenic population. For example, in laboratory grown wildtype *C. elegans*, or inbred *Drosophila* and mouse strains, high variance exists both for lifespan itself and response to DR/DR mimetics. Indeed, for interventions such as methionine restriction, the median lifespan of mice and rats is substantially increased, there is a subpopulation that die sooner than their non-restricted counterparts (Miller et al., 2005). Furthermore, pharmacological drugs such as rapamycin have a positive effect on lifespan in both sexes of mice, however, a subpopulation of females fail to respond (Harrison et al., 2009). These examples clearly demonstrate that a *'one size fits all'* approach to anti-aging using DR and DR mimetics does not have a full translational potential and needs optimization.

My research has shown that early life activity of splicing factors REPO-1 and SFA-1 is required for efficacy of longevity interventions such as dietary restriction, reduced TORC1 and reduced ETC signaling. Furthermore, I show that modulating the activity of REPO-1 and SFA-1 early in life determines whether subsequent application of a pro-longevity intervention, in this case inhibition of RAGA-1, successfully slows aging. Interestingly, the function of these splicing factors in longevity are mediated via the nervous system. In light of these findings, there is a whole new avenue of research that opens up. Can differences in the activity of splicing factors be a predictor of an individual's response to longevity treatments? Can we tweak the function of these factors early in life and in neurons specifically to optimize health outcomes and response to pharmacological interventions? Answering these questions will bring us a step closer to personalized medicine, such that we can maximize health outcomes in every individual.

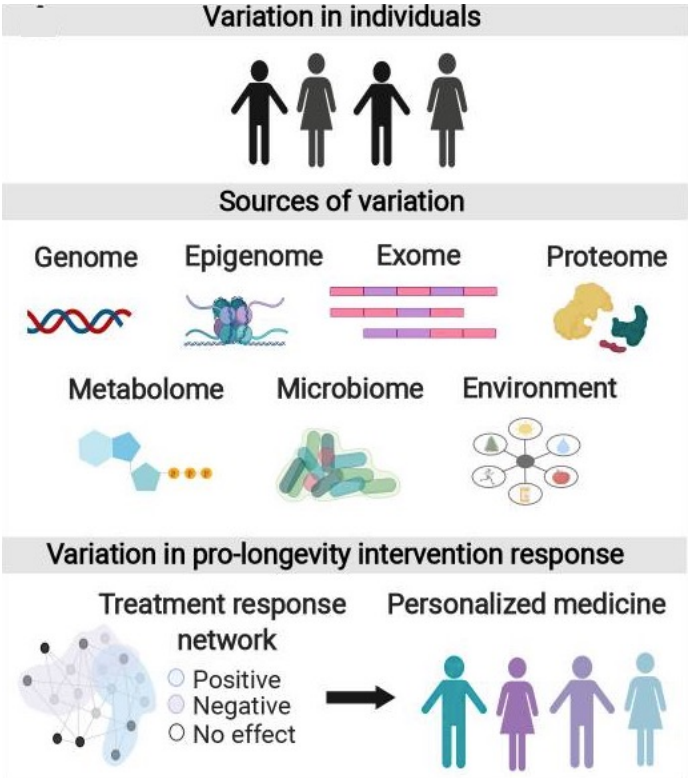

Figure 6.2: Schematic depicting sources of variation among individuals in a population.

Integrating information from all these sources using multi-omic networks will allow us to predict response of an individual to an intervention.

Figure adapted from (Perez-Matos and Mair, 2020) *(with permission).*

6.3 Precision Gerontology- The future of aging research

"If it were not for the great variability among individuals, medicine might as well be a science and not an art"- Sir William Osler, Father of Modern Medicine

As this quote suggests, understanding inter-individual variability is a major hurdle that needs to be overcome, to allow the field of medicine to transition from an art to a science. This could not be truer for aging research. Successfully translating geroscience to human application requires accurately predicting a given individual's response to a given treatment, depending on the genotype and physiology of the individual. Such an approach will allow treatments to be assigned to every human in a personalized way, maximizing health benefits.

The first step toward this end is to identify biological variables that predict individual-specific optimal aging interventions in model organisms. Only with this knowledge will we be able to provide the foundation for a personalized medicine approach for healthy aging therapeutics in humans (**Figure 6.2**). RNA splicing fidelity is one such biological variable that needs to be studied further. Differences in the activity of splicing factors and expression of different splice variants of certain genes can be robust biomarkers to predict the rate of aging and health outcomes to various interventions in *C. elegans*. If conserved in mammals, this raises important questions about how we design and implement anti-aging therapeutics.

Final summary

My Ph.D. work demonstrates that activity of splicing factors REPO-1 and SFA-1 are required for interventions such as dietary restriction, reduced TORC1 and reduced ETC function, to extend lifespan. However, it is not essential for longevity from reduced insulin signaling. I utilized these splicing factor dependent and independent longevity pathways to define changes that are coupled to their effect on lifespan. Changes to lipid metabolism was a common signature on loss of splicing factors. Interestingly, REPO-1 and SFA-1 activity modulate lipid levels in the SF-dependent mutants and bind to POD-2 (Acetyl CoA Carboxylase 1) mRNA directly. Suggesting a causal link between lipid remodeling and response to treatment, REPO-1, SFA-1, and POD-2 specifically modulate efficacy of the same pro-longevity mutations. Lastly, I show that modulating the activity of REPO-1 and SFA-1 early in life determines whether subsequent application of a pro-longevity intervention in middle/late life successfully slows aging.

CHAPTER 7

Materials and Methods

7.1 Source for *C. elegans* strains

Wild type N2 strain and transgenic strains, unless otherwise noted, were directly obtained from Caenorhabditis Genetics Center (CGC). The *C. elegans* strains used for this work are listed below.

Table 7.1: *C. elegans* strains used for this study, their genotype and source

Strain Name	Genotype	Notes	Source
N2 Bristol	Wild type	-	CGC
DA1116	*eat-2(ad1116)II.*	-	CGC
VC222	*raga-1(ok386)II.*	-	CGC
RB1206	*rsks-1(ok1255)III.*	-	CGC
MQ130	*clk-1(qm30)III.*	-	CGC
MQ887	*isp-1(qm150)IV.*	-	CGC
MQ1333	*nuo-6(qm200)I.*	-	CGC
TJ1052	*age-1(hx546)II.*	-	CGC
CF1041	*daf-2(e1370)III.*	-	Kenyon lab via the Dillin lab
TJ356	*daf-16p::daf-16a/b::GFP + rol-6(su1006)*	DAF-16 overexpressor	CGC
WBM499	*raga-1(ok386)II.*	6X outcrossed	Mair Lab
SJ4100	*zcIs13 V. [hsp-6::GFP]*	*hsp-6* transcriptional reporter	CGC
SJ4058	*zcIs9 V. [hsp-60::GFP + lin-15(+)]*	*hsp-60* transcriptional reporter	CGC
WBM392	*wbmIs31[acs-2p::GFP + rol-6(su1006)*	*acs-2* transcriptional reporter	Mair Lab
WBM941	*isp-1(qm150) IV; wbmIs31[acs-2p::GFP + rol-6(su1006)*	MQ887 X WBM392	Mair Lab
WBM942	*isp-1(qm150)IV; zcIs9 V.*	MQ887 X WBM4058	Mair Lab
WBM948	*isp-1(qm150)IV; zcIs13 V.*	MQ887 X WBM4100	Mair Lab
WBM1186	*repo-1(wbm28)IV.*	3XFLAG::REPO-1 (CRISPR)	Mair Lab
WBM1118	*sfa-1(wbm32)IV.*	3xFLAG::SFA-1 (CRISPR)	Mair Lab
WBM960	*repo-1(wbm14)IV.*	REPO-1::GFP (CRISPR)	Mair Lab
WBM1101	*sfa-1(wbm31)IV.*	wrmScarlet::SFA-1 (CRISPR)	Mair Lab
WBM1117	*repo-1(wbm14)IV.; sfa-1(wbm31)IV.*	WBM960 X WBM1101	Mair Lab
KH2235	*lin-15(n765)ybIs2167[eft-3p::ret-1E4E5(+1)E6-GGS6-mCherry+ eft-3p::ret-1E4E5(+1)E6(+2)GGS6-GFP+lin-15(+)+pRG5271Neo]X.*	*ret-1* splicing reporter worm	Gift from H. Kuroyanagi
WBM1312	*raga-1(ok386)II. ; repo-1(wbm63)IV. [GFP::repo-1]*	*raga-1(ok386)* control for tissue specificity	Mair Lab

WBM1313	*raga-1(ok386) II; repo-1(wbm63) IV [GFP::repo-1]; wbmIs87[eft-3p::3XFLAG::repo-1(genomic)::wrmScarlet::unc-54 3'UTR, *wbmIs67]*	*raga-1(ok386)* + whole body *repo-1* rescue	Mair Lab
WBM1314	*raga-1(ok386) II; repo-1(wbm63) IV [GFP::repo-1]; wbmIs104[rab-3p::3XFLAG::repo-1cDNA::wrmScarlet::rab-3 3'UTR, *wbmIs68*	*raga-1(ok386)* + neuronal *repo-1* rescue	Mair Lab
WBM1315	*aga-1(ok386) II; repo-1(wbm63) IV [GFP::repo-1]; wbmIs105[myo-3p::3XFLAG::repo-1cDNA::wrmScarlet::unc-54 3'UTR, *wbmIs63]*	*raga-1(ok386)* + muscle *repo-1* rescue	Mair Lab

7.2 Routine worm culture

Worms were routinely grown and maintained on standard sterilized nematode growth media (NGM) plates that were seeded with *E. coli* (OP50-1). *E. coli* bacteria were cultured overnight in LB at 37°C, after which 100 µl of liquid culture was seeded on plates to grow for 2 days at room temperature.

7.3 Preparation of Nematode Growth Medium (NGM) plates

MEDIACLAVE 10 (INTEGRA) was used for the preparation of NGM plates for worm culturing. The process is semi-automated and described below:

1. Add 12 g NaCl, 10 g Bacto-peptone and 80 g Agar-agar in the MEDIACLAVE cuvette. Add 3730 ml of MilliQ water to the cuvette and begin the standard run.

2. Sterilize the media at 121℃ for 60 minutes.

3. Hold the media at 50℃. Sterile supplements are added at this time since they are heat sensitive. Add 100 ml 1 M Potassium phosphate buffer pH 6 (for 2L: combine 216.6 g monobasic potassium phosphate (KH_2PO_4), 71.2 g dibasic potassium phosphate (K_2HPO_4) and water, adjust pH to 6.0 and autoclave to sterilize), 4 ml 1M $CaCl_2$, 4 ml 1M $MgSO_4$ and 4 ml 5mg/ml cholesterol (dissolved in ethanol).

Note: For plates where RNAi is used, the worms are grown on *E. coli* HT115 bacteria that are Ampillicin/Carbenicillin resistant. Therefore, when making NGM plates, 4 ml 100 mg/ml carbenicillin is added along with the supplements.

4. Allow the supplements to mix with automatic stirring for 20 minutes (use this time to load plates onto the MEDIAJET for automatic pouring).

5. Use sterilized tubing that connects the MEDIACLAVE cuvette to the MEDIAJET (INTEGRA) automatic dispenser. Dispense the media to 6 cm diameter (10 cm diameter in some cases) sterile petri dishes.

6. Plates are left at room temperature overnight to allow them to solidify. They are transferred to 4℃ the next day and can be stored for up to 3 months. Plates are removed from the cold room 24-48 hours before they need to be used.

7.4 Preparation of bacterial food source

For routine maintenance of *C. elegans*, streptomycin-resistant *E. Coli* strain OP50-1 from CGC is used. OP50-1 frozen glycerol stocks are used to streak on LB plates containing 100 µg/ml streptomycin and colonies were allowed to form overnight at 37℃. Single colonies were inoculated to LB broth without antibiotics to either grow overnight at 37℃ or over a few days at room temperature. 100 µl OP50-1 cultures were seeded to the center of 6 cm NGM plates. These plates are incubated at room temperature for 2 days before putting worms on them. The thick bacterial lawn attracts worms to the middle of the plate. For 10 cm NGM plates, 500 µl OP50-1 cultures is used and spread all over the plate using a sterilized spreader. Plates with bacteria can be stored at 4℃ for up to 1 month.

7.5 Maintaining *C. elegans* stocks for experiments

C. elegans stocks are kept at 20℃. However, for *daf-2(e1370)* strains, worms are grown at 15℃ upto the L4 stage and then shifted to 20℃ to prevent dauer arrest. Worm larvae can survive complete starvation for up to a few months in the dauer state. However, starvation can significantly affect physiology and lifespan and due to epigenetic changes, this effect can last for multiple generations (Rechavi et al., 2014). Therefore, stocks are generally kept fed for at least 2-3 generations before experiments. Furthermore, fresh thaw of frozen worm stocks is requested after worms have been in culture for more than 3 months to avoid genetic drifts. To maintain *C. elegans* stocks, a few worms of different stages were transferred to new NGM plates seeded with OP50-1 every 3 to 4 days, using a platinum worm pick. The tip of the worm pick is sterilized

on a Bunsen burner after every transfer and cooled down before picking more worms. This is done to prevent contaminants from growing on plate surfaces and more importantly, to prevent the cross-contamination of worm strains of different genotypes.

7.6 Freezing *C. elegans*

C. elegans can be frozen in media containing glycerol and stored for years in -80℃ freezer or liquid nitrogen. When strains are received from an external source or new strains are generated via crosses, CRISPR or other methods, they should be frozen down immediately to avoid genetic drifting. Every three months, strains are thawed again from these frozen stocks to prevent genetically drifted strains in our working cultures thus improving the reproducibility between experiments. Two types of freezing media are used:

- Liquid freezing media- It gives better viability and are better for long-term storage
- Soft agar freezing media- It allows for multiple thaws from one vial and is therefore better for working stocks.

Following are the steps followed to freeze down a *C. elegans* strain:

1. Ensure worm strain is not contaminated with any other bacteria or fungus prior to freezing. It is easy to spot contaminations as other bacteria have different colours (yellow, brown) and textures (watery, spotted) and fungi have mycelial growth.

2. Set up worm cultures to obtain large enough populations for freezing:

For integrated or mutant strains, e.g., worms generated through CRISPR (where the whole population has the same genotype):

Chunk 1/3 of a 60 mm NGM plate of worms and transfer it to an OP50-1 seeded 100 mm NGM plate worm side down. Prepare 3 such plates.

For strains with extrachromosomal transgenes (wherein only a subset of the population carries the transgene):

Pick 50 transgenic worms to an OP50-1 seeded 100 mm NGM plate. Prepare 3 such plates.

3. Keep these plates incubated at 20°C until the worms have grown, laid eggs, and the bacterial lawn has been used up leading to arrested L1s. Freshly starved young larvae (L1-L2 stage) survive freezing best. For some mutants that take a longer time to develop (e.g., *clk-1(qm130)*), it takes much longer for these big plates to starve out.

4. Gently unscrew the cap of a soft agar freezing media hallway and place it in microwave until it melts, then place it in a 37°C water bath to cool down. 37°C allows for the agar to stay liquefied and at the same time, can be tolerated by larvae during the freezing procedure.

5. Wash the worms from the first plate by adding 10 ml M9 buffer. Swirl the plate gently in a circular motion to suspend the worms in the liquid. Transfer the solution to the next plate and continue collecting the worms in the same manner. If required, using an additional 4-5 ml of M9 to wash any residual worms off the three plates.

6. Once the final plate is collected transfer the worms to the labeled 15 ml conical tube and centrifuge to pellet in a clinical centrifuge at 2500 rpm for one minute at RT. Aspirate the supernatant taking care not to disturb the pellet. Make sure to not use speeds higher than 2500 rpm as the goal is to wash out any/most bacteria and pellet only the worms.

7. Add 3ml M9 Buffer to the pellet and then incubate the 15ml tube on ice for 15-30 minutes. Take care to not leave the worms on ice for more than an hour.

8. Remove the soft agar freezing media from the 37°C water bath and allow to cool briefly on the bench.

9. Resuspend the worms on ice by gently inverting the tube.

10. Using sterile technique and working close to a Bunsen flame, aliquot 0.5 ml of worm suspension to each cryovial for liquid freezing media and 1 ml to each cryovial for soft agar freezing media.

11. Add 0.5 ml of liquid freezing media to each vial with 0.5 ml of worm suspension, invert the vials several times to mix and place on ice. Next add 1 ml of soft agar freezing media to each vial with 1 ml of worm suspension, quickly invert the vial several times to mix and immediately place on ice for the soft agar to solidify. Make sure this is done quickly as the soft agar freezing media tends to solidify quickly. The worm

and the freezing media are re-suspended well to ensure that it is homogenous. It would allow for better recovery while thawing and ensure that there are worms in each thaw.

12. Transfer vials to a room temperature cryopreservation freezing container. Place the container in the −80°C freezer overnight. This container allows the temperature to drop gradually at 1°C/minute which allows proper freezing. The next day, the vials are transferred to their permanent freezer locations.

7.7 Thawing *C. elegans* frozen stocks

For thawing worm strains from a soft agar stock, use a sterile 1000 µl pipette tip and scoop around the edge of the vial and remove 1/4 of the frozen solution onto an OP50-1 seeded NGM plate, then return the vial immediately to its storage box in the −80°C freezer. The liquid thaws on the plate, so once it dries up, check for sufficient larvae on the plate in the thaw. Allow the worms to recover by putting the plate in 20°C.

When needed, stocks with liquid freezing media can be thawed at room temperature and the entire content poured onto a 60 mm NGM plate with bacteria.

7.8 Bleaching *C. elegans*

Bleaching is a procedure which allows worms to dissolve leaving behind only fertilized eggs. This is routinely used to clean up *C. elegans* cultures contaminated with unwanted fungi or bacteria, to shift worm cultures from one bacterial food source to other or to obtain a synchronized population. A population containing many gravid adults is the best stage for bleaching. The steps are as follows:

1. Wash gravid adult worms from a 60 mm or 100 mm NG plate by adding 5 ml or 10 ml M9 buffer respectively. Swirl the plate gently in a circular motion to suspend the worms in the liquid. 2. Transfer the worms to a 15 ml conical tube and centrifuge to pellet in a clinical centrifuge at 2500 rpm for one minute at room temperature. Aspirate the supernatant taking care not to disturb the pellet.

3. Wash the pellet with 15 ml M9 buffer to remove residual bacteria by inverting the tube several times.

4. Centrifuge to pellet at 2500 rpm for 1 minute at RT.

5. Aspirate the wash and add bleach solution. Use 5 ml bleach if you started from a 60 mm plate or 10 ml bleach if you started from a 100 mm plate.

6. Incubate for 2-5 minutes at RT. Vortex vigorously every 30 seconds and monitor closely for the release of eggs under a dissecting microscope. Once all the worms have dissolved, move to the centrifugation step immediately.

7. Once the worms dissolve and the eggs are released centrifuge at 2500 rpm for one minute at RT to pellet the eggs.

8. Wash the pellet three times with 15 ml M9 buffer. Centrifuge at 2500 rpm for 1 minute between washes to pellet the eggs.

9. After the final wash aspirate most of the supernatant leaving some M9 buffer with the pellet. Depending on the concentration of eggs, it can be diluted in more or less M9 buffer.

10. Pipette the eggs to NGM plates with desired food source.

7.9 RNA interference (RNAi) in *C. elegans*

That double-stranded RNA (dsRNA) can be used to degrade mRNAs of any specific gene of interest was first discovered by Andrew Fire and Craig Mello in *C. elegans*, for which they were awarded the Nobel Prize in Physiology or Medicine in 2006. Although Fire and Mello initially used an injection method to introduce dsRNA (Timmons and Fire, 1998), it was later discovered that RNAi can be performed by feeding *C. elegans* with bacteria engineered to express double-stranded RNA (dsRNA) (Sijen et al., 2001; Timmons and Fire, 1998). This was done by optimizing the feeding method by using *E. Coli* strain HT115 strain which lacks RNaseIII, an enzyme that degrades most dsRNAs. Based on this system, two genome-scale RNAi libraries are currently available, generated by Julie Ahringer lab (Ahringer, 2006) and Marc Vidal lab (Rual et al., 2004). While the Ahringer library was made from genomic DNA, the Vidal library was constructed from the worm ORFome.

For RNAi clones that are available in the Ahringer and Vidal library, the appropriate bacteria were streaked out and sequence-verified before use. RNAi construct for *sfa-1* was obtained from the Ahringer RNAi and sequence verified. The *repo-1* RNAi that was not obtained from the libraries was made by cloning the first 403 bases of the *repo-1* gene into the L4440 vector using PCR of *repo-1* gene from cDNA, restriction digestion and ligation into the L4440 vector. RNAi experiments were done using *E.coli* HT115 bacteria on standard NGM plates containing 100µg/ml Carbenicillin. HT115 bacteria expressing RNAi constructs were grown overnight in LB supplemented with 12.5µg/ml Tetracycline and 100µg/ml Carbenicillin. The plates were seeded with 100 µl of the bacterial culture 48 hours before use. Respective dsRNA expressing HT115 bacteria were induced by adding 100µl IPTG (100mM) 1-2 hours before introducing worms to the plate. RNAi was induced from hatch or at Day 1 of adulthood as specified. Worms grown on empty vector HT115 RNAi bacteria are represented as control.

Table 7.2: RNAi constructs used for the study and their sequences

repo-1$_{FL}$ RNAi	NNNNNNNNNNNNNNNNTAGGGCGATTGGGTACCTCAATAGTACGGCTGATCATCGAGTCGTTCCAATTT GAATGCGACTTGTAAGAAGAATTGCTTCGTGTCTTTGTTCCACATCGTCCAAAATTTTTCAGATTTGTCAAC TTCTCTTGATGGAATTTTGAATCCAATCGTTTCATACGGCTCAGCAGCAAACAAGAGGTATTGCCATCTCTT GTCTGGAGGCTGAATCTTTTGCTCATAAGCAGACATAAATCGATGACGTGGCGCAATACCGTCAGCAATCT CCGGATAATCAATTTGGAAGAGAAGTGCTTGCTGGCCAGCTCCTGGATCACGTTCTTTTGTTACCTTGTATC CAGGACGTCCGATTTTCACAAACTTTTTAGTTTCAACTGCAGCTTTCTGTGGAGCTGGTAGAAATGGTTGTT CAGATTGTTCTTTAGCGGCACGCCGTGCAAGATTCGCTTGATGCTTCTTTCCTTGTGTATGTGCCAAATAAG ATCCTTCATTGTGGTGAAGAGTAAGACACAGCTTGCATTCGTACGTTCCAATGTGATTTCGCATGAAATAC GGATCCTTTTGAAGATCAATTGTCTCTAGAGCCAACTGGCGGAGCCGTTCCCGTCGATCAACACCAGCATC GGCGGCCGAAGCCACTCCTCCGCTTCCCGTTTTTCCTCCAGCTCTGTTCTGAAAGTCCATGCTAGCCATGGA ACCGGTGGATCCACTAGTTCTAGAGCGGCCGCCACCGCGGTGGAGCTCGAATTCATCGATGATATCAGATC TGCCGGTCTCCCTATAGTGAGTCGTATTAATTTCGAANAAGCCAGGTTGCTTCCTCGCTCACTGACTCGCTG CGCTCGGTCGTTCGGCTGNGGCGAGCGGTATCAGCTCACTCAANGNNGGTAATANGGTTATCCNNNNAAT CAGGGGANANGCNNNAANAACATGTGAGCAAANGCCAGCAANNNCAGNANNGTAAAAGGCCGCGNTGCT GGNNTTTTCCNNNGGCTCCGNCCCCCNGACGAGCNTNNNNNN
repo-1$_{short}$ RNAi (or *repo-1* RNAi)	NNNNNNNNNNNNNNNNNNNNGGGCGATTGGGTACCGGAAGAGAAGTGCTTGCTGGCCAGCTCCTGGATC ACGTTCTTNNNNNNNCTTGNATCCAGGACGTCCGATTTTCACAAACTTTTTAGTTTCAACTGCAGCTTTCTG TGGAGCTGGTAGAAATGGTTGTTCAGATTGTTCTTTAGCGGCACGCCGTGCAAGATTCGCTTGATGCTTCTT TCCTTGTGTATGTGCCAAATAAGATCCTTCATTGTTGTGAAGAGTAAGACACAGCTTGCATTCGTACGTTCC AATGTGATTTCGCATGAAATACGGATCCTTTTGAAGATCAATTGTCTCTAGAGCCAACTGGCGGAGCCGTT CCCGTCGATCAACACCAGCATCGGCGGCCGAAGCCACTCCTCCGCTTCCCGTTTTTCCTCCAGCTCTGTTCT GAAAGTCCATGCTAGCCATGGAACCGGTGGATCCACTAGTTCTAGAGCGGCCGCCACCGCGGTGGAGCTC GAATTCATCGATGATATCAGATCTGCCGGTCTCCCTATAGTGAGTCGTATTAATTTCGATAAGCCAGGTTGC TTCCTCGCTCACTGACTCGCTGCGCTCGGTCGTTCGGCTGCGGCGAGCGGTATCAGCTCACTCAAAGGCGG TAATACGGTTATCCACAGAATCAGGGGATAACGCAGGAAAGAACATGTGAGCAAAAGGCCAGCAAAAGG CCAGGAACCGTAAAAAGGCCGCGTTGCTGGCGTTTTTCCATANGCTCCGCCCCCCTGACGAGCATCACAAA AATCGACGCTCAAGTCAGANGTGGCGAAACCCGACAGGACTATAAAGATACCAGGCGTTTCCCCCTGGAA GCTCCCTCGTGCGCTCTCCTGTTCCGACCCTGCCGCTTACCGGATACCTGTCCGCCTTTCTCCCTTCGGGAA GCGTGGCGNNTTTNTCNNANNNNNNCACNNNGNANGGTATCTCANTNCGGNGTAGGTCGTTCGCNNCAAG CTGGGNTGNGTGCACGAANCCCCCNTTCAGCCNNACNNCTGCGCCTTATCCGGTAACTATCGTNTTGNNNT CCNACCCNGNANNA

rbm-34 RNAi	NNNNNNNNNNNNNNNTANNGGCGATTGGGTACCCTATGCCATCAGACGTCCCTTCTTTGCAGCCTTCTTC TTTGCAATGGCTTTCTTCGCTGACTTCTTCAAGGCACGACGATCATTTTGCTCAGTTGTTCTTTCTTTTTTGG TGGAGAACTTGAACTTGTGCAATTTTCCAGTAATTTCATTCTGGTTCTTCTTTCCGTGAGATGTTCGCTTTTT AGCAGTTTGGATCTTCGTCAAATGTCCCTTCTTCATAACTTTTGTAATGCGCAAGTCGCGTTTTTCCATTTTG ATAGTCTCCATGCTCAATGCAAGACTCACAGAAGAATCTTGTTTGAAATTGACAAACGCGAATCCTTTTCC CTTTCCAGTATCTTTATCTCTGACAATTCTGACAGCCTCGACAGGTCCGATTTGTGCAGAGAAAAAAGTAAT GAGAGCATCTTCGGTAATCTCGAACGGCAAGTTTCCAACAAAAATGGCCATATCCTTTCCAAATTCTTTCTT CTTACTTCCAACTTTGTCAACACGAATCACATGATCGTCCAGCTTGGTTCCATTGTACTTCAGAGCTTTCTC CACTGATTCTTCTGCTCCGAATTTCACATAGAACGTGAGAGAACTCTGTTTGTCATTCAATTTTCCTGTCAA ATGAGTGACTCGTTTCGTCAATTTCTCATTCGCAGGAAGCAGATTTCTCATACGGACAGAGGAAATAGTTC CAAAGTCGGAGAAAATTCGACGGACTGATTTCTCGTTCATTGTCAATGGCATATTTCCAACAAAAACAGTC AGAGCATTTTCAGCAGCTGAAGCACGTGCATTTGACTTTTGAAGAGTTCTATTCTCTCTTTGCTTCGTTCTGT CTCGCTTTCCTTCCTTATTTTCATCTTTTTTCTCTTCTCCTTCTGTTNCNNNGCAACTTCTTCAGCAGCAGCAG CAGCATCAGCTNCNTCTCTTCNTCANCTTTTTTTTGGATCATGCTTTCTTCNTNNNTTTTCAATNACTTTATC TNCCNNNNNANTTCCTNNNNACTGCTGCNNCTTCTGACN
sfa-1 RNAi (Ahringer Library)	TAGGGCGATTGGGTACCGGGCCCCCCCTCGAGGTCGACGGTATCGATAAGCTTGATTTGGAACAGTTGAGA CATGAGAAAATTCAAGCTTTATTGAAGATTAATCCGAATTTCAAACCGCCCGCTGACTATCGGTATATATA TAGGAAAATTTGAATTTTTCCGGCAAAAATGCGAGTTTTTGGTGAAAAATCACAGATTTTCAGAGTTTTCG GCTGAAAATTTGACCTTTTTCGCTGCAAATGTGTGATTCGGCTGAAAAATTCATTTTCAGCAATATTTAGCT TGAAACTACCGATTTTTTTGTTGAAAATCATTTAAAATTTCCGGATTTTCCGTTAAAAGTTGGAAATTCTTC AAATTTTTGCCCTTTGAATTTCGGCTAAAATTTGACCGAAAACACTAGAATTTTAAGCTGAAAACTGGATA AATTCCAGAAATTTGAACAATTGAGGTTTTATGGGATTTTTACGGATTTTTGACAAAAAAAACGGTAGTTTT CAAGCTGAAAATTGCTGTGAATAAATTTTTAAAATCTGAAACTCCAAAAATCTGTGATTTTTCACCAAAAA CTCGCATTTTTGCCTAAGAAATTCAAATTTTAAGCGTAAATTATAATTTTTGCAATAAAATATCTAAAATTT CAATTTTTTTCAGTGCTCCAAACATCCGTCTACACGACAAAGTCTGGATTCCCCAGGAACAATTTCCTGATC TCAATTTTGTCGGCCTACTCATTGGTCCACGTGGAAATACGCTGAAAAGCTTGGAAGCTGAAACTGGAGCC AAGATTATTATCAGAGGAAAAGGATCTATAAAAGAGGGAAAATTGACGAATCGACTCGGACCGATGCCTG GNGAAAATGAGCCATTACATGCATATGTAACTGGAACTGATATGAATGTTATCAAAAAAGCATGTGAGAA NATTAAACAAGTGATTGCTGAAGCCACTGCTCTGCCGGANACATGAGCTCAGGAAGCTGCAACTGANANA CTCGCACTGTTGAATGGAACTTTCCGACCGGANGATTTNGCAAA

7.10 Genetic Crosses

C. elegans sex is determined by the number of X chromosomes: hermaphrodites have two and males have one X chromosome (Nigon and Dougherty, 1949). While *C. elegans* strains are mostly maintained as self-fertilizing hermaphrodite cultures, males are particularly useful for crosses (see next section on how to generate males). Wild type N2 male stocks are routinely maintained by picking 3 L4 larvae and 5 males to a new NGM plate with food. For crosses, 1-3 hermaphrodites are transferred alongwith 8-10 males in a plate with very little bacteria placed at the center of the lawn. This maximizes the worms to find each other increasing the chances of mating. After 3-4 days of mating, few F1 generation progeny are singled out and allowed to self-fertilize. Another 3-4 days later, F2 generation progeny are singled out. Progeny are picked at L4 stage or earlier to prevent them from having undergone crosses with males in the plate. F2s are allowed to self-fertilize for 2-3 days before being lysed for genotyping.

7.11 Making male worms for crosses

To make male worms, first set the bacterial incubator at 30°C. Put 4 L4s in an OP50 plate. Set 3 such plates. Keep in the 30°C incubator for 4-6 hours. Remove the three plates at time points 4, 5 and 6 hours respectively and put them in the 20°C incubator. You will expect to see 1% population of males in your F1 progeny. Cross males with N2 hermaphrodites to get a 50% N2 male population.

7.12 Genotyping

Worms are individually lysed in 5 µl single worm lysis buffer (30 mM Tris pH 8, 8 mM EDTA, 100 mM NaCl, 0.7% NP40, 0.7% Tween-20). Add proteinase K to 100 µg/ml just before use. Incubate worm in lysis buffer for 60 minutes at 60˚, then at 15 minutes at 95℃ to inactivate proteinase K. 1 µl lysate was used as template for PCR reactions with the right genotyping primers that will produce bands of different sizes for distinguishing wild type and mutant alleles.

7.13 Microinjection

Microinjection is a useful technique to introduce foreign DNA/RNA/protein to modify the *C. elegans* genome. It can be used to create transgenic animals using generate extrachromosomal arrays or by CRISPR-Cas9 genome editing (see next section).

Capillaries are heated and pulled to generate a pointed tip using a flaming/brown micropipette puller (Sutter Instrument, P-1000). Miniprepped DNA or CRISPR mixes are made and centrifuged and the supernatant is loaded into the needles. This is done to eliminate any particle or debris in the mix that could possibly clog needle tip. 0.5 µl-1 µl DNA solution is loaded to each needle. The loading is monitored under the dissection scope to make sure a substantial amount of the injection mix has filled the needle. It takes roughly 2-4 minutes. Gravid Day 1 adult worms with distinct gonads are the perfect stage for microinjection. To get this stage, L4s are picked onto fresh plates the day before injection. The adult worm is mounted on a 2% agarose pad with a drop of halocarbon oil. The mix is injected into the gonads using FemtoJet Express

(Eppendorf) following standard procedures (Evans, 2006). Following injection, the animals are recovered in M9 and each individual animal that is injected is isolated into a new plate to monitor transgenic progeny.

7.14 CRISPR-Cas9 genome editing

All CRISPR edits were performed using the CRISPR protocol developed by (Paix et al., 2015). Briefly, homology repair templates were amplified by PCR using primers that introduced a minimum stretch of 35 bp homology arms flanking the site of insertion at both ends. The CRISPR injection mix contained 2.5 µl tracrRNA (4 µg/µl), 0.6 µl *dpy-10* crRNA (2.6 µg/µl), 0.5 µl target gene crRNA (2.6 µg/µl), 0.25 µl *dpy-10* ssODN (500 ng/µl), homology repair template (200 ng/µl final in the mix), 0.375 µl Hepes pH 7.4 (200mM), 0.25 µl KCl (1M) and RNase free water to make up the volume to 8 µl. 2 µl purified Cas9 (12 µg/µl) was added at the end, mixed by pipetting, spun for 2 min at 13000 rpm and incubated at 37ºC for 10 minutes. *dpy-5* was used as a co-injection marker instead of *dpy-10* in case the edits were made on Chromosome II. Mixes were microinjected into the germ line of day 1 adult hermaphrodites using standard protocol. Screening worms and genotyping was performed as described earlier (Silva-García et al., 2019). Worms generated using CRISPR were outcrossed at least six times before being used for experiments to remove the co–injection marker phenotype and other off-target edits.

7.15 Lifespan assays

All worms were kept fed for at least three generations after thawing on OP50-1 bacteria to minimize transgenerational effects of starvation on lifespan (Rechavi et al., 2014). For lifespan performed on HT115 bacteria, gravid adult worms were bleached from OP50-1 to HT115 and allowed to grow on HT115 for one generation. The gravid adults on HT115 were used to do a timed egg lay on control or RNAi bacteria to obtain synchronized populations. Day 1 of lifespan is defined as the day worms start to lay eggs. Populations were scored at least once every two days: animals that have eggs hatched internally (bagging), desiccated on the walls of petri dishes or “exploded” with significant portions of internal tissues hanging outside of the cuticle, or desiccated on the walls of the plate, were censored from statistical analyses. Death was

marked when animals displayed no movement of any part of their body and did not respond gentle prodding on the head and tail at least three times. In the cases where the drug 5-fluoro-2'-deoxyuridine (FUDR) is used to prevent internal hatching (for example to grow *eat-2(ad1116)*), plates were seeded with bacteria, allowed 24 hours to grow and 100 µl of 1 mg/mL FUDR solution was seeded on top of the bacteria lawn for each plate. FUDR was allowed 24 hours to diffuse before plates were used. Since FUDR is light sensitive, plates are covered when resting at room temperature. For experiments where both FUDR and IPTG had to be used, IPTG was added on bacterial lawns, allowed to dry and FUDR was added one day before plate use. On the day of worm transfer and 4-5 hours prior to use, these plates were again re-induced with IPTG. After all worms are marked dead, the survival data are analyzed with GraphPad Prism 9 and statistical significance was determined with Log-rank (Mantel-Cox) test.

7.16 RNA isolation and cDNA synthesis

Total RNA was extracted using Qiazol (QIAGEN), column purified by RNeasy mini kit (QIAGEN) according to manufacturer's instructions. cDNA was synthesized using SuperScript® VILO Master mix (Invitrogen).

7.17 Quantitative RT-PCR

StepOne Plus instrument from Applied Biosystems was used to perform real-time qPCR experiments following the manufacturer's instructions. The following Taqman assays from Life Technologies were used: *repo-1* (Ce02465496_g1), *rbm-34* (Ce02465498_g1), *acs-2* (Ce02486192_g1), *sod-3* (Ce02404518_gH), *fat-3* (Ce02458252_g1), *cpt-5* (Ce02419317_g1), *fat-7* (Ce02477067_g1). For each qPCR reaction, ~5ng of cDNA was used. Relative expression differences were calculated with the comparative 2ΔΔCt method using Y45F10D.4 (Ce02467253_g1) as the endogenous control. For each gene in each strain, fold-change relative to the average of wild type control group was calculated and statistical significance evaluated using Welch's t test. GraphPad Prism 9 was used for all statistical analysis and graph plotting.

7.18 Semi-quantitative RT-PCR of *tos-1* to visualize alternative splicing event

tos-1 was amplified using PCR conditions and primers as described in (Heintz et al., 2017). Apex Taq RED (Genesee Scientific) was used for amplification. 1 Kb Plus DNA ladder (Invitrogen) was used as molecular weight reference. Following PCR, samples were resolved on a 2% EtBr-stained agarose gel. Gels were imaged on ChemiDoc MP (BioRad).

7.19 Microscopy

For DIC and fluorescence imaging of REPO-1::GFP and wrmScarlet::SFA-1 at different stages, worms were anesthetized in 0.1 mg/ml tetramisole in 1X M9 buffer on empty NGM plates and mounted on 2% agarose pads on glass slides. They were imaged using the Apotome.2-equipped Imager M2 microscope with an Axiocam camera. For imaging of *acs-2*, *hsp-6* and *hsp-60* transcriptional reporters, anaesthetized worms were placed on NGM plates without bacteria until no movement was detectable, aligned to groups accordingly and subsequently imaged on a Zeiss Discovery V8 microscope equipped with an Axiocam camera.

7.20 Western Blotting and Quantification

3XFLAG::*repo-1* worms were egg laid on *E. coli* HT115 bacteria to get a synchronized population of worms. To age them up until Day 15, worms were transferred on days 1, 2, 3, 5 and 8 to separate them from their progeny. For Day 1, Day 5, Day 10 and Day 15 samples, approximately 200 adults per sample were collected in triplicates in M9 buffer and snap frozen in liquid nitrogen. For larval stages, approximately 40 animals were made to egg lay over a 12-14 hour period on each plate. 10 such plates were pooled after 24 or 48 hours to get one replicate of L1-L2 or L3-L4 stage sample respectively. To make worm lysates, RIPA buffer with protease inhibitors (Sigma #8340) were added and samples were lysed via sonication at Amplitude 60 10sec ON / 10sec OFF for a total of 3 times (Qsonica Q700) and this complete cycle was repeated 3 times. SDS-PAGE was performed by running 20 µg of protein per lane on a 4-

12% TrisGlycine gradient gel (Thermo Fisher Scientific, #XP04122BOX). Proteins were transferred to Nitrocellulose membranes (BioRad # 162-0112) and blocked with 5% BSA in TBST. They were stained with Ponceau-S Stain, 0.1% Solution (G Biosciences #89167-800) and imaged. Ponceau was washed off with 1XTBST and blots were incubated with primary antibody ANTI-FLAG M2 mouse monoclonal (Sigma Aldrich #F1804, 1:2000). They were then washed in 1XTBST and probed with secondary anti-HRP linked mouse antibody (Cell Signaling #7076, 1:5000). Blots were developed using ECL substrate (GE Healthcare # 95038-560). Bands were visualized using a Gel Doc system (Bio Rad) and Image Lab software (Version 4.1). Blots were stripped using Stripping Buffer (Thermofisher # PI46430) according to manufacturer's guidelines and re-probed with beta actin (Abcam, #8226, 1:1000). Quantification of the bands was done using ImageJ (Version 1.52a) and plotted using GraphPad Prism 9.

7.21 RNA-Sequencing

Libraries were prepared using Roche Kapa stranded mRNA HyperPrep sample preparation kits from 100ng of purified total RNA according to the manufacturer's protocol. The finished dsDNA libraries were quantified by Qubit fluorometer, Agilent TapeStation 2200, and RT-qPCR using the Kapa Biosystems library quantification kit according to manufacturer's protocols. Uniquely indexed libraries were pooled at an equimolar ratio and sequenced on an Illumina NextSeq500 with paired-end 75bp reads by the Dana-Farber Cancer Institute Molecular Biology Core Facilities.

7.22 Differential Gene Expression Analysis

All samples were processed using an RNA-seq pipeline implemented in the bcbio-nextgen project (https://bcbio-nextgen.readthedocs.org/en/latest/). Raw reads were examined for quality issues using FastQC (v0.11.8) (http://www.bioinformatics.babraham.ac.uk/projects/fastqc/) to ensure library generation and sequencing were suitable for further analysis.

To perform additional quality checks of the data, all reads were aligned to Wormbase assembly WBcel235, release WS272 of the *C. elegans* genome (Project PRJNA13578 (N2 strain)) using STAR (v.

2.6.1d) (Dobin et al., 2013). Alignments were checked for evenness of coverage, rRNA content, genomic context of alignments (for example, alignments in known transcripts and introns), complexity and other quality checks using a combination of FastQC, Qualimap (García-Alcalde et al., 2012), (http://doi.org/10.1093/bioinformatics/bts503), MultiQC (https://github.com/ewels/MultiQC) and custom tools.

To quantitate the reads corresponding to each transcript, quasi alignment was performed using Salmon (v. 0.14.2) (Patro et al., 2017), outputting the transcripts Per Million (TPM) measurements per isoform. Differential expression at the gene level was called with DESeq2 (Love et al., 2014), using counts per gene estimated from the Salmon quasi alignments by tximport. The differential effect of *repo-1* knockdown on the mutants *raga-1(ok386)*, *eat-2(ad1116)*, and *clk-1(qm30)* relative to *age-1(hx546)* was explored using the design formula: ~ repo1_effect + treatment + repo1 effect: treatment.

The DEGReport (Pantano, 2019) (http://lpantano.github.io/DEGreport/) package was used to identify gene clusters that change similarly upon knockdown of repo-1 using a hierarchical correlation clustering approach. UpSet plots of shared differentially expressed genes between analyses were generated using the UpSetR R package (Conway et al., 2017). Groups of DE genes with similar expression changes with *repo-1* knockdown in REPO-1 RNA-Seq identified by DEGReport were examined for enrichment using WormCat (Holdorf et al., 2020).

Genome and transcriptome reference files and annotations download links:

Genome: ftp://ftp.wormbase.org/pub/wormbase/releases/WS272/species/c_elegans/PRJNA13758/c_elegans.PRJNA13758.WS272.genomic.fa.gz

Transcriptome: ftp://ftp.wormbase.org/pub/wormbase/releases/WS272/species/c_elegans/PRJNA13758/c_elegans.PRJNA13758.WS272.canonical_geneset.gtf.gz

Annotations: ftp://ftp.wormbase.org/pub/wormbase/releases/WS272/species/c_elegans/PRJNA13758/annotation/

7.23 SRS microscopy imaging, *C. elegans* sample preparation and image quantification

For the SRS microscope system, pulsed Pump (tunable from 790 to 990 nm) and Stokes (1045 nm) beams were provided by Insight X3 femtosecond laser (Spectra-Physics), and spatiotemporally overlapped by a Spectral Focus Timing and Recombination Unit (SF-TRU, Newport). The intensity of Stokes beam is modulated at 20 MHz by an electro-optic modulator (EOM, 4103, New Focus). Overlapping pump and Stokes beams were emitted from the port of SF-TRU and coupled into a multi photon laser scanning microscope (FVMPE-RS, Olympus). After passing through the sample, the forward going Pump and Stokes beams were collected by an air condenser. A flip mirror was used to direct the transmitted laser to a photodiode module, which includes a telescope to relay and change the beam size to fit the area of the photodiode, as well as an optical filter to remove the modulated Stokes beam and let the pump beam transmit for the detection of stimulated Raman loss signal. The output current from the photodiode was terminated, filtered, and demodulated by a lock-in amplifier (SRS Detection Module, APE) at 20 MHz to ensure shot noise-limited detection sensitivity. The lock-in amplifier output was then fed into the analog box of FVMPE-RS microscope system to process the SRS signal. For lipid imaging, CH_2 signals were detected at 2845 cm^{-1}. To achieve this, pump beam was set at 805 nm and the delay stage was positioned at 33.550 nm. For both pump and Stokes beams, 10% laser power was used. A 20x air objective (UPlanSAPO, 0.75 N.A., Olympus) was used for imaging. The microscope was controlled by Olympus Fluoview software. SRS microscopy images were quantified using ImageJ software (NIH). Polygon selection tool was used to select the area to be quantified and average pixel intensity was calculated with the "analyze-measure" command. After subtracting the background intensity, all measurements were averaged to obtain mean and standard deviation. In each imaging session, approximately 20-30 worms were immobilized with 1% sodium azide on 2% agarose pads on glass microscope slides and 10-20 worms, which have anterior intestine in focus, were imaged. Mutant lipid levels were normalized to those of wild-

type worms and relative SRS signals are shown in box plots. Wild-type and control worms were bleached on plates with HT115 bacteria and their progeny were used for adult-egg laying on plates with HT115 bacteria transformed with either empty L4440 vector or vector carrying RNAi against *sfa-1* or *repo-1*. Embryos were grown at 20°C, on these plates, until larval L4 stage, when they are synchronized again and imaged 24 hours later.

7.24 Enhanced Crosslinking Immunoprecipitation (eCLIP) in MEFs and Worms

eCLIP was performed by Eclipse Bioinnovations Inc (San Diego, www.eclipsebio.com) according to the published eCLIP protocol (Van Nostrand et al., 2016). For each replicate (N=2), 20 million MEFs were UV crosslinked (UVC-515 Ultralum) at 400 mJoules/cm2 with 254-nm radiation, and snap frozen in liquid nitrogen. Cells were lysed and treated with RNase I to fragment RNA as previously described. SF1 (Bethyl: Cat No. A303-213A, Lot No. A303-213A-1) and SF3A2 (Bethyl: Cat No. A304-821A, Lot No. A304-821A-1) antibodies were used for immunoprecipitation of the proteins respectively. Only the region from 65 kDa to 140 kDa was excised for eCLIP. RNA adapter ligation, immunoprecipitation-western blotting, reverse transcription, DNA adapter ligation and PCR amplification were performed as previously described.

For *C. elegans* eCLIP (N=1), 50,000 worms or 50uL packed worms (~1mg of total protein) was grown. Worms were obtained from an egg lay of CRISPR tagged 3XFLAG::SFA-1 (WBM1118) and 3XFLAG::REPO-1 (WBM1186) on 10 cm plates seeded with HT115 bacteria. At Day 1 of adulthood, they were transferred to a 15 ml centrifuge tube in M9+0.01% Tween and washed gently 3 times with 10mL M9 at room temperature. They were resuspended in 5 ml fresh M9 and transferred to NGM plates without bacteria. After the worms dispersed uniformly, the plates were placed on leveled ice, plate lid removed followed by crosslinking (UVC-515 Ultralum) at 254-nm UV with an energy setting of 500 mJoules/cm2. Immobilized worms were transferred to a 2mL round bottom microcentrifuge tube using M9 and spun for 30 seconds at 3,000xg. Excess M9 was aspirated out and the worm pellet flash frozen in

liquid nitrogen. Monoclonal Anti-FLAG M2 antibody (Sigma: Cat No. F1804-1MG, Lot No. SLBX2256) was used for immunoprecipitation of FLAG::SFA-1 and FLAG::REPO-1 and eCLIP was performed by excising the 80-155kDa region for SFA-1 and 32-115kDa for REPO-1.

7.25 Caloric Restriction of young/old mice and isolation of mouse tissue

The CR mice experiments were done in collaboration with Dr. Anne Lanjuin and Dr. Caroline Heintz. Four cohorts of mice, 5 in each group, were obtained from the National Institute of Aging. They were aged 4 and 18 months of age. Half of the mice from each age group were fed an *ad libitum* diet, whereas the other half was on a 40% calorie restricted diet since their 16th week of age. After they arrived the HSPH mouse facility, they were kept on this same diet and allowed to acclimatize to the new environment for a month before being sacrificed for tissue collection. *Ad libitum* (AL) mice had access to food all the time. CR mice were fed one pellet per day between 6-8 AM (between 7:30am-8am generally), which amounted to ~60% of calories consumed by AL mice. The cages were changed after every 8-10 days.

At the time of dissection, mice were aged 5 months and 19 months respectively. On the day of dissection, CR mice were fed by 8AM. After they finished eating their food by 10 AM, food was removed from all the groups of mice including the AL group. After 6 hours of food removal, dissections were done. The mice weights were recorded first. It was followed by euthanizing the mice for 3 minutes in a CO_2 chamber. It was followed by cervical dislocation. Immediately after, cardiac puncture was performed, and blood was pulled using a syringe and then put in Sarstedt microfuge Z gel tubes (Catalog No.50-809-211). The blood stayed in tubes at RT 15 mins, then spun 10mins at 10,000 rpm (RT). The serum was collected from the top of tube and flash frozen in liquid nitrogen. Simultaneously, tissue dissections were done. We collected various mouse tissues including hypothalamus and separate regions of the brain, gastrocnemius and soleus muscle, gonadal and inguinal fat pads, heart, testes, the pituitary gland and serum. All samples were snap frozen in liquid nitrogen at stored at -80°C. Moreover, primary dermal fibroblasts were cultured from mouse

tails isolated from the different groups by Dr. Porsha Howell. Dissection of each mouse took approximately 20 minutes.

7.26 Isolation of RNA from Mouse Tissue

For isolation of RNA from mouse tissues, the Qiagen RNeasy Plus Universal Mini Kit (Cat No.: 73404) was used. The steps followed are listed below (adapted from the Qiagen RNeasy Plus Universal Mini Kit Protocol Book):

1. Excise the tissue sample from the animal or remove it from storage. Determine the amount of tissue. We used 30 ng of liver and muscle tissue that was cut from the stock tube using a scalpel in dry ice (to prevent thawing). For the hypothalamus enriched brain region, we used the whole tissue.
2. Place the tissue in a suitably sized vessel containing 900 µl QIAzol Lysis Reagent.
   Generally, round-bottomed tubes allow more efficient disruption and homogenization than conical-bottomed tubes.
3. Place the tip of the disposable probe into the vessel and operate the TissueRuptor at full speed until the lysate is uniformly homogeneous (usually 20–40 s).
   We used the VWR Pellet Mixer (hand-held battery-operated homogenizer) (Cat #47747-370) and the VWR Disposable Pestles (Cat #47747-358) for liver sample. For tougher tissue like brain and muscle, we used the TissueRuptor with steel probes (borrowed from Brendan Manning lab)
   Note: *To avoid damage to the TissueRuptor and disposable probe during operation, make sure the tip of the probe remains submerged in the buffer. Foaming may occur during homogenization, especially of brain tissue. If this occurs, let the homogenate stand at room temperature for*
   2–3 min until the foam subsides before continuing with the procedure.
   Note: *Incomplete homogenization leads to significantly reduced RNA yields and can cause clogging of the RNeasy spin column.*
4. Place the tube containing the homogenate on the benchtop at room temperature (15–25°C) for 5 min.
   This step promotes dissociation of nucleoprotein complexes.

5. Add 100 µl gDNA Eliminator Solution. Securely cap the tube containing the homogenate, and shake it vigorously for 15 s.

   Addition of gDNA Eliminator Solution will effectively reduce genomic DNA contamination of the aqueous phase, making further treatment with DNase unnecessary.

6. Add 180 µl chloroform. Securely cap the tube containing the homogenate and shake it vigorously for 15 s.

   Thorough mixing is important for subsequent phase separation.

7. Place the tube containing the homogenate on the benchtop at room temperature for 2–3 min.
8. Centrifuge at 12,000 x g for 15 min at 4°C. After centrifugation, heat the centrifuge to room temperature (15–25°C) if the same centrifuge will be used in the later steps of this procedure.

   After centrifugation, the sample separates into 3 phases: an upper, colorless, aqueous phase containing RNA; a white interphase; and a lower, red, organic phase. For tissues with an especially high fat content, an additional, clear phase may be visible below the red, organic phase. The volume of the aqueous phase should be approximately 600 µl.

9. Transfer the upper, aqueous phase (usually 600 µl) to a new microcentrifuge tube (not supplied).
10. Add 1 volume (usually 600 µl) of 70% ethanol and mix thoroughly by pipetting up and down. Do not centrifuge. Proceed immediately to step 11.

    Note: *The volume of lysate may be less than 600 µl due to loss during homogenization and centrifugation. Precipitates may be visible after addition of ethanol. Resuspend precipitates completely by vigorous shaking and proceed immediately to step 11.*

11. Transfer up to 700 µl of the sample to a RNeasy Mini spin column placed in a 2 ml collection tube (supplied). Close the lid gently, and centrifuge for 15 s at ≥8000 x g (≥10,000 rpm) at room temperature (15–25°C). Discard the flow-through.
12. Repeat step 11 using the remainder of the sample. Discard the flow- through.
13. Add 700 µl Buffer RWT to the RNeasy spin column. Close the lid gently, and centrifuge for 15 s at ≥8000 x g (≥10,000 rpm) to wash the membrane. Discard the flow-through.

14. After centrifugation, carefully remove the RNeasy spin column from the collection tube so that the column does not contact the flow-through. Be sure to empty the collection tube completely.

    Note: *Buffer RWT is supplied as a concentrate. Ensure that ethanol is added to Buffer RWT before use.*

15. Add 500 µl Buffer RPE to the RNeasy spin column. Close the lid gently, and centrifuge for 15 s at ≥8000 x g (≥10,000 rpm) to wash the membrane. Discard the flow-through.

    Note: Buffer RPE is supplied as a concentrate. Ensure that ethanol is added to Buffer RPE before use.

16. Add 500 µl Buffer RPE to the RNeasy spin column. Close the lid gently, and centrifuge for 2 min at ≥8000 x g (≥10,000 rpm) to wash the membrane.

    The long centrifugation dries the spin column membrane, ensuring that no ethanol is carried over during RNA elution. Residual ethanol may interfere with downstream reactions.

    Note: After centrifugation, carefully remove the RNeasy spin column from the collection tube so that the column does not contact the flow-through. Otherwise, carryover of ethanol will occur.

17. **Optional**: Place the RNeasy spin column in a new 2 ml collection tube (supplied) and discard the old collection tube with the flow- through. Close the lid gently, and centrifuge at full speed for 1 min.

    Perform this step to eliminate any possible carryover of Buffer RPE, or if residual flow-through remains on the outside of the RNeasy spin column.

18. Place the RNeasy spin column in a new 1.5 ml collection tube (supplied). Add 30–50 µl RNase-free water directly to the spin column membrane. Close the lid gently. To elute the RNA, centrifuge for 1 min at ≥8000 x g (≥10,000 rpm).

19. For accurate values, measure absorbance in 10 mM Tris·Cl, pH 7.5. Pure RNA has an A260/A280 ratio of 1.9–2.1 in 10 mM Tris·Cl, pH 7.5.

7.27 NanoString of mouse RNA samples

Creating hybridization mix:

1. Invert hybridization buffer to mix and spin down.
2. Thaw Reporter CodeSet at room temperature, invert to mix and spin down.
3. Add 70 µl of the hybridization buffer to the Reporter CodeSet, invert to mix, spin down. This is the Master mix.
4. Set up Hybridization reaction in PCR tubes: To each tube, add 8 µl of Mastermix, 1.5-5µl of sample, and add rest of RNase free buffer to bring the total volume of each reaction to 13 µl.

For our experiments, the RNA concentrations to run were standardized and it was found that 150 ng of RNA gave good binding densities. We therefore made a 30 ng/µl dilution of RNA and used 5 µl to add to the hybridization reaction.

5. To each tube, add 2 µl of Capture ProbeSet.
6. Cap the tubes, mix by inverting (do not vortex), briefly spin down and incubate in a pre-heated thermocycler at 65°C.
7. Incubate reactions for at least 16 hours. Maximum hybridization time should not exceed 48 hours. Ramp reactions down to 4°C and process the following day.

Loading samples for Nanostring run:

1. Remove cartridge from -20°C and equilibrate to room temperature for 15 minutes.
2. Remove hybridized samples from the thermocycler; do not let samples remain at room temperature for longer than 15 minutes before initializing a run.
3. Briefly spin down hybridized samples.
4. Bring sample volume to 35 µL by adding 20 µl of RNAse-free water or hybridization buffer.
5. Load 30-35 µL of each sample into the cartridge (we used a volume of 32µl). Maximum cartridge volume is 35 µL for each lane.
6. Hold pipette perpendicular to cartridge, insert the tip into the loading port.

7. Depress the plunger to the second stop, creating an air bubble.
8. Remove the pipette from the cartridge BEFORE releasing the plunger.
9. Load 32 µL water for empty lanes with no samples.
10. Wipe away excess liquid from the surface of the cartridge with a KimWipe or similar lint-free wipe.
11. Apply transparent seal over the sample loading ports.
12. Visually inspect that there are no empty lanes and loading ports have been sealed with tape.
13. Remove protective green seal from the reagent ports.
14. Take your cartridge to the nCounter Sprint Profiler instrument (in Sarah Fortune's Lab space) and place the cartridge into the cartridge drawer. Ensure the cartridge is aligned in the proper orientation and fully seated in the cartridge tray. Also ensure that instrument calibration is up-to-date.
15. Start your run.

Data were then analyzed using nSolver 4.0 software on the desktop.

List of reagents and composition:

Nematode Growth Media (NGM)

12 g NaCl

10 g Bacto-peptone

80 g Agar-agar

3730 ml of MilliQ

Autoclave at 121℃ for 60 minutes; hold the media at 50℃ and then add supplements

Supplements:

100 ml 1 M Potassium phosphate buffer pH 6

4 ml 1M $CaCl_2$

4 ml 1M $MgSO_4$

4 ml 5mg/ml cholesterol (dissolved in ethanol)

4 ml 100 mg/ml carbenicillin (if making NG Carb plates for seeding *E. coli* HT115 for RNAi experiments)

1 M Potassium phosphate buffer pH 6

216.6 g monobasic potassium phosphate (KH_2PO_4)

71.2 g dibasic potassium phosphate (K_2HPO_4)

1.8 L water

adjust pH to 6.0

Make up volume to 2L

Autoclave to sterilize

Liquid freezing media

5.8 g sodium chloride

50 ml 1M potassium phosphate buffer pH 6

300 ml glycerol

1L water

Autoclave to sterilize

Soft agar freezing media

2.9 g sodium chloride

3.4 g monobasic potassium phosphate (KH2PO4)

4.4 g dibasic potassium phosphate (K2HPO4)

150 ml glycerol

400 ml water

Adjust pH to 6.0 and make up volume to 500 ml

Aliquot 50 ml to bottles

0.2 g agar to each bottle and stir to resuspend

Autoclave to sterilize

M9 buffer

3 g KH_2PO_4

6 g Na_2HPO_4

5 g NaCl

1 ml 1 M $MgSO_4$

1L MilliQ water

Autoclave to sterilize

Chapter 8

Appendix

Appendix I- Supplemental data figures

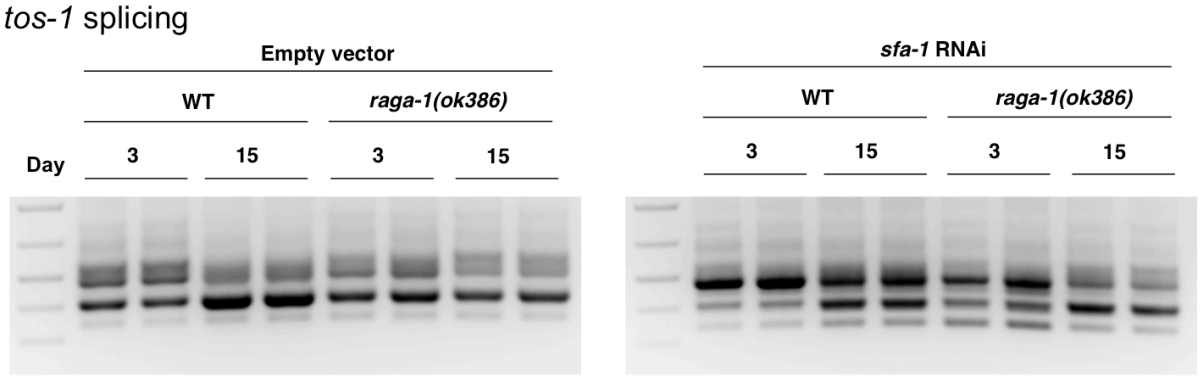

Figure 8.1 Youthful splicing of *tos-1* is preserved with age in TORC1 mutant *raga-1(ok386)* but is reversed with *sfa-1* RNAi.

tos-1 splicing pattern in *raga-1(ok386)* mutants at day 3 and 15 of adulthood with *sfa-1* RNAi (2 biological replicates shown).

Data published in (Heintz et al., 2017).

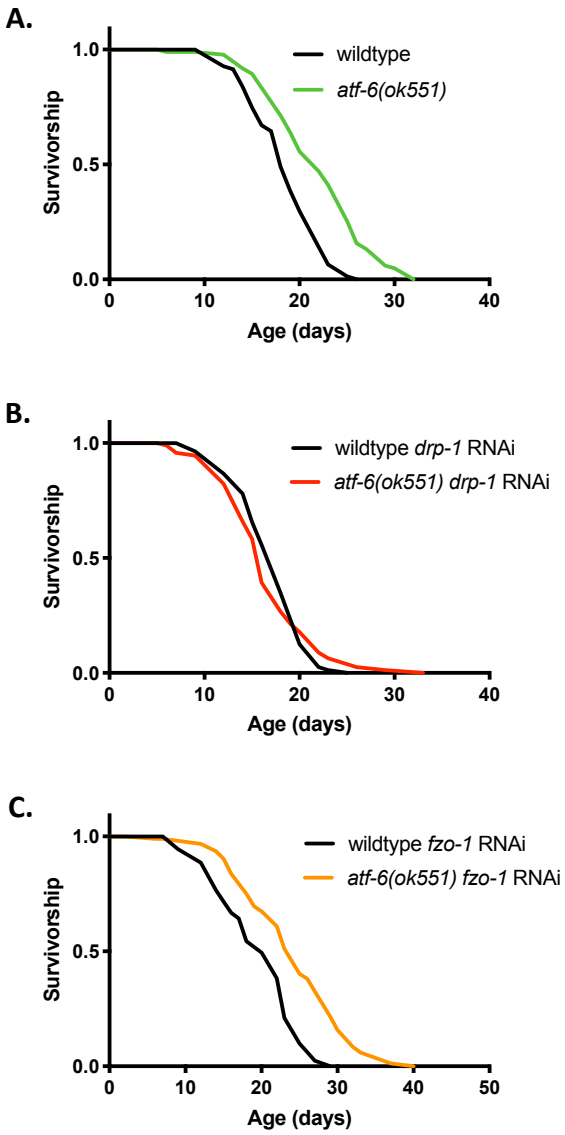

Figure 8.2: Mitochondrial fission is required for longevity in *atf-6* mutants.

Lifespan analysis of wildtype and *atf-6(ok551)* worms fed A. control bacteria and dsRNA for the mitochondrial fission machinery B. *drp-1* and fusion machinery C. *fzo-1* (n = 100 per condition).

Data published in (Burkewitz et al., 2020).

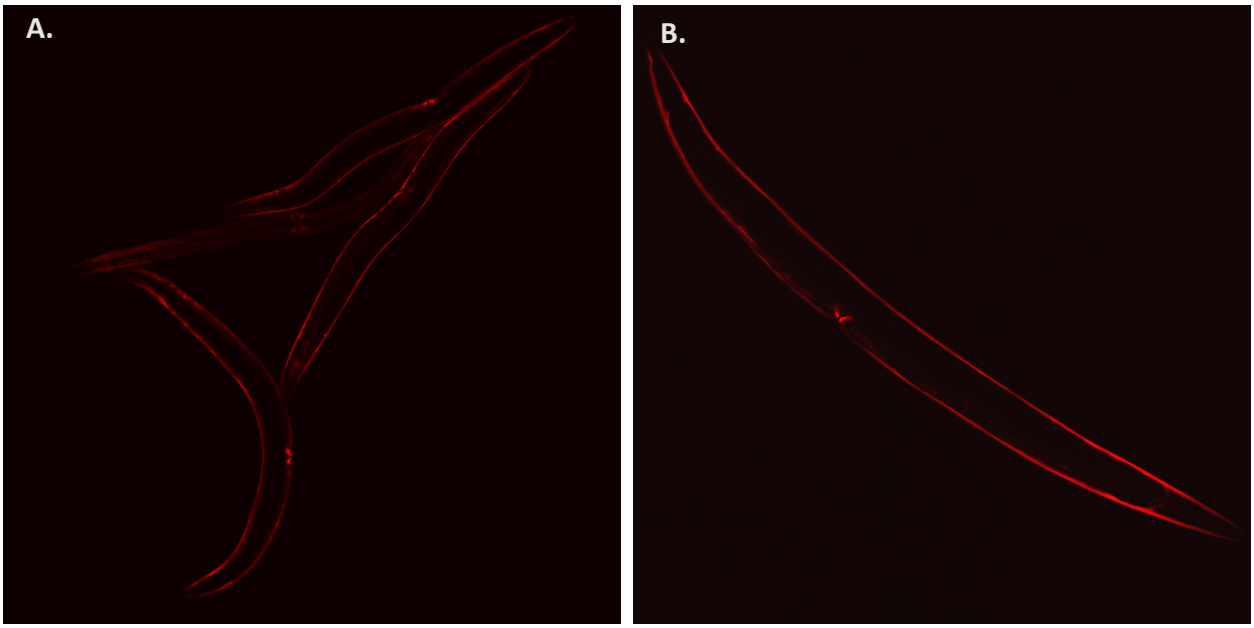

Figure 8.3: Validation of the muscle SKI LODGE system by single-copy insertion of wrmScarlet.

SKI LODGE strain expressing muscle-specific *myo-3p* promoter driving cassette (Chromosome I) was tested by knock-in of wrmScarlet construct using microinjection to confirm tissue-specific expression. Images of anaesthetized worms captured on a fluorescence scope at A. 10X and B. 20X magnification.

Data published in (Silva-García et al., 2019).

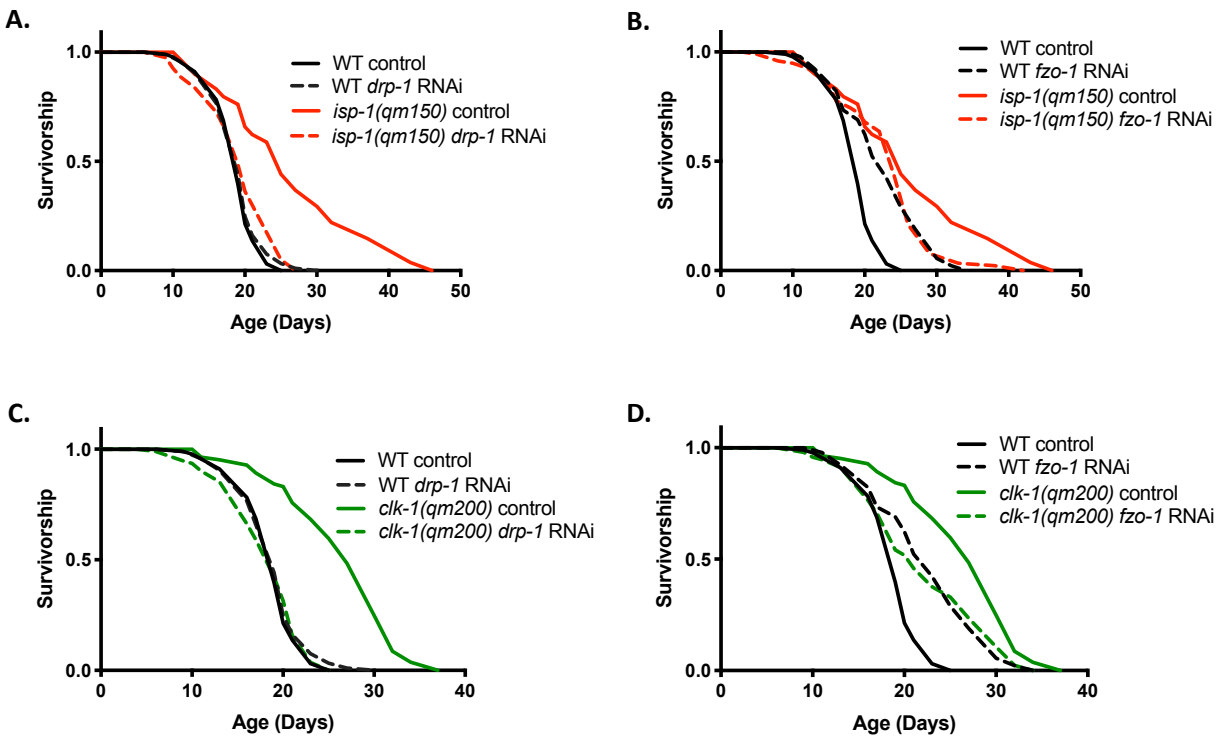

Figure 8.4: Mitochondrial fission and fusion is required for longevity in electron transport chain mutants.

A,B. Lifespan analysis of wildtype and *isp-1(qm150)* on *drp-1* and *fzo-1* RNAi.

C,D. Lifespan analysis of wildtype and *clk-1(qm200)* on *drp-1* and *fzo-1* RNAi

Note that *fzo-1* RNAi increases wildtype median lifespan. However, ETC mutants are not able to further extend lifespan of *fzo-1* RNAi treated worms. n=100 per condition.

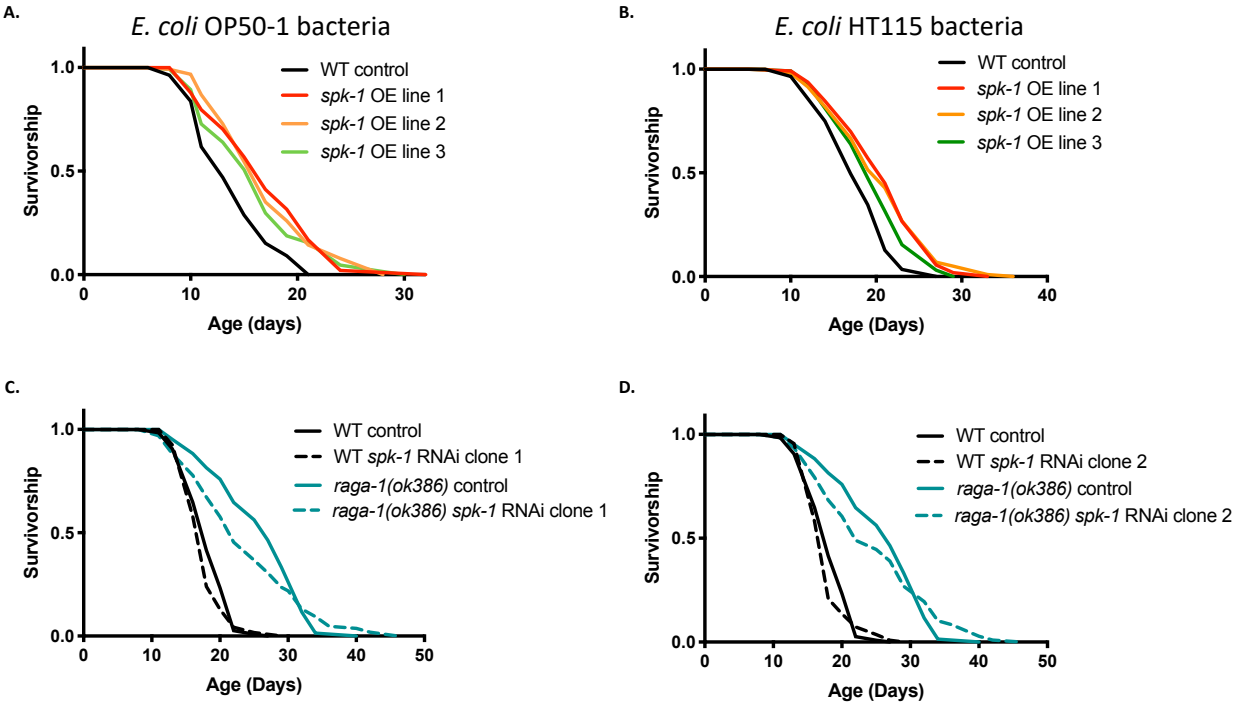

Figure 8.4: Role of splicing factor kinase *spk-1* in *C. elegans* longevity.

A,B. Lifespan analysis of wildtype N2 and *spk-1* overexpressor strains (extrachromosomal arrays expressing *eft-3p::spk-1cDNA (isoform a)::SL2::mCherry::unc-54* 3'UTR) on *E. coli* OP50-1 and HT115 bacteria as food source.

C,D. Lifespan analysis of wildtype and *raga-1(ok386)* on two different clones of *spk-1* RNAi obtained from the Vidal library.

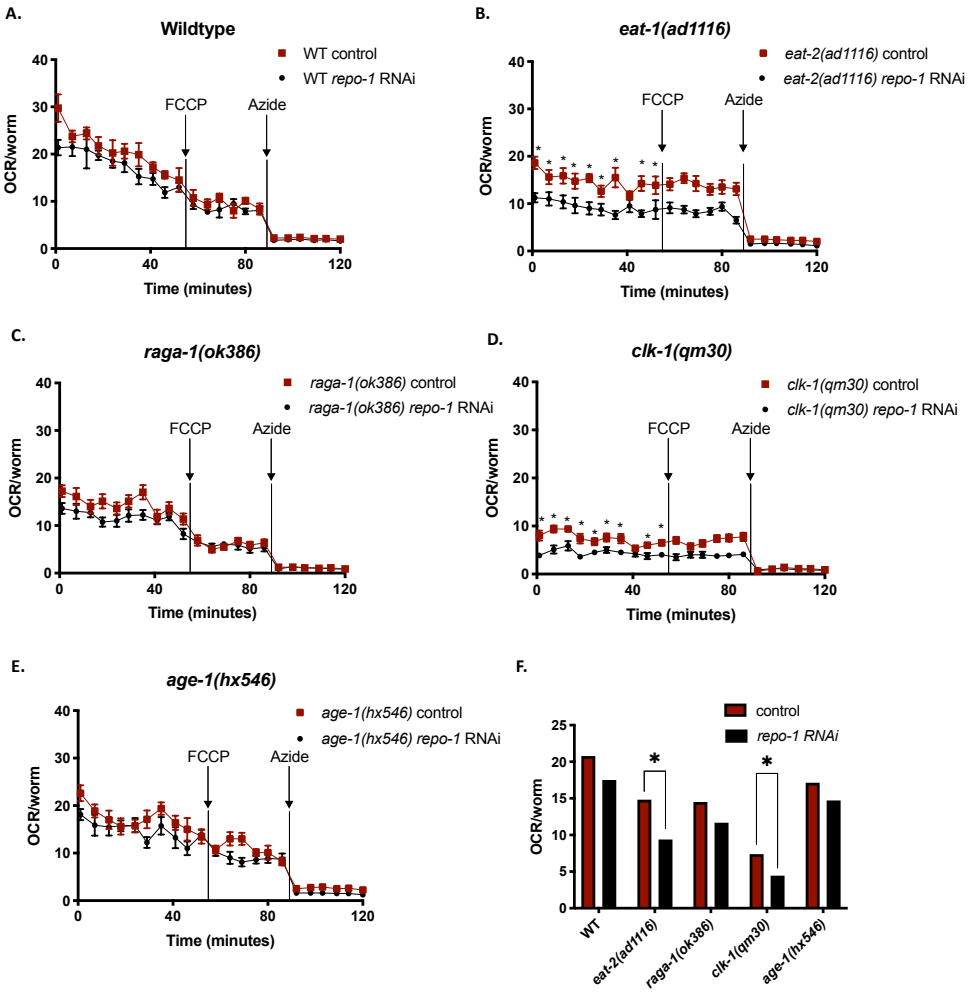

Figure 8.5: Effect of *repo-1* knockdown on basal respiration of wildtype and long-lived mutants in *C. elegans.*

Seahorse analysis of wildtype and long-lived mutants on fed on control bacteria and *repo-1* RNAi from hatch and OXPHOS measured at Day 1. Drugs used were FCCP and sodium azide to measure basal and maximal respiration and spare respiratory capacity. Note: FCCP failed to increase respiration in our experiment. Basal respiration was significantly different on *repo-1* RNAi in *eat-2(ad1116)* and *clk-1(qm30)* worms.

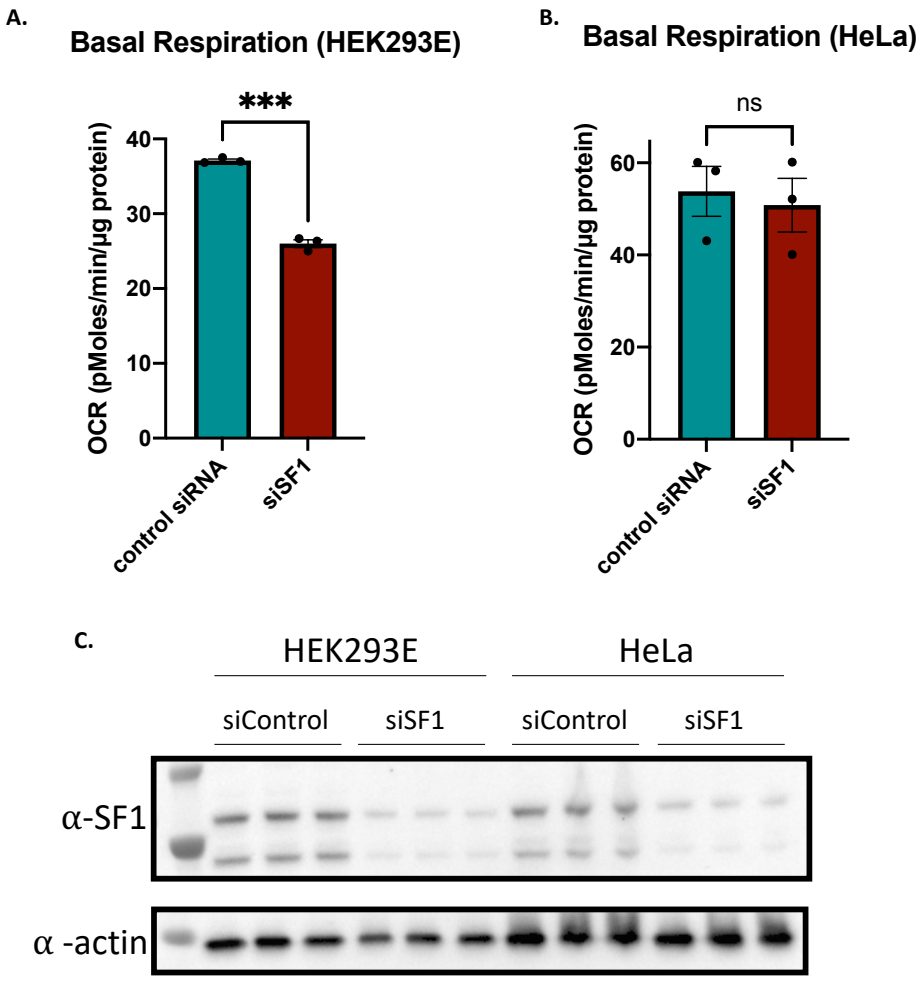

Figure 8.6: Effect of SF1 knockdown on basal respiration of HEK293E and HeLa cells.

A, B. Basal OCR measured using Seahorse in HEK293E and HeLa cells. (****P≤0.0001, ***P≤0.001, **P≤0.01, *P≤0.05; ns P>0.05). P-values calculated with unpaired, two-tailed Welch's t-test.

C. Western blot confirming knockdown of SF1 in the two cell lines 48 hours post treatment with siSF1.

Appendix II- Supplemental data tables

Table 8.1: 620 genes that respond differentially on loss of *repo-1* in *eat-2(ad1116)*, *raga-1(ok386)* and *clk-1(qm30)* compared to wildtype N2 worms.

2L52.1	C08A9.10	col-135	dpy-31	F55B11.2	jac-1	ncam-1	R12A1.3	T06D8.10	unc-83
aat-3	C08B6.4	col-143	dyc-1	F55B11.3	K04C1.5	ncx-3	R12E2.15	T07A9.14	ung-1
abcf-2	C08G9.2	col-160	eat-6	F55G11.4	K07C11.7	nduo-1	R74.2	T07D1.2	utp-20
abhd-3.2	C09F5.1	col-165	ebax-1	F56A4.2	K08E4.3	nduo-3	repo-1	T09B4.5	vab-23
abu-14	C11E4.6	col-178	eef-1G	F56D2.3	K10C2.12	ndx-6	rfc-1	T12B5.15	vha-6
abu-8	C14B9.2	col-181	efl-3	F57A8.1	K10D6.2	nep-2	rgl-1	T13F3.6	W02D9.6
AC8.4	C15H9.9	col-184	eftu-2	F58G6.3	K11H12.6	nfki-1	rhgf-1	T13H5.4	W03F9.4
acd-1	C16B8.2	col-19	egl-19	F59B1.2	K12H4.3	nfm-1	rhgf-2	T14B1.1	W05F2.4
acdh-2	C16H3.3	col-20	eif-3.B	F59C12.3	kars-1	nhr-119	rpc-2	T16G1.2	W06F12.2
acdh-3	C17C3.15	col-42	enol-1	far-2	kat-1	nhr-41	rpl-24.2	T19A5.3	wago-4
acdh-9	C17E4.20	col-74	ephx-1	far-8	kin-32	nhx-6	rpt-3	T19B10.2	Y102A11A.5
acl-12	C18C4.7	col-8	eppl-1	fars-3	klp-20	nid-1	rrf-2	T19B4.3	Y105E8B.9
acox-1.2	C23H3.2	col-80	eps-8	fat-1	kynu-1	nkcc-1	rsf-1	T20D4.7	Y119D3B.14
acp-6	C26B9.3	col-93	eri-12	fat-3	lam-1	nlp-39	ruvb-1	T21B6.3	Y119D3B.21
acs-11	C26F1.1	col-98	exc-15	fat-7	lam-2	nlp-40	ruvb-2	T22B11.4	Y15E3A.4
acs-20	C27A7.5	comt-3	exc-4	fbf-2	lbp-1	npl-4.2	sad-1	T24B8.4	Y37D8A.2
acs-3	C29F5.1	cpn-1	exc-6	fbxa-115	lbp-2	npp-11	sel-7	T24B8.5	Y38E10A.14
act-5	C30G12.2	cpr-5	F09E10.1	fbxa-72	ldb-1	npp-7	sem-4	T27A10.6	Y39B6A.10
aex-3	C33D9.13	cpr-6	F10D11.6	fbxb-101	lec-3	nrde-1	set-19	taf-4	Y39G10AR.11
agmo-1	C33G3.4	cpsf-3	F10G2.1	feh-1	lec-4	nsy-1	set-30	tag-151	Y39H10A.6
agt-1	C35A5.3	cpt-5	F10G8.8	fhod-1	lec-5	osm-11	sex-1	tag-196	Y41G9A.10
agxt-1	C35E7.5	crb-1	F11E6.3	flcn-1	lec-9	osm-7	sftb-1	tag-241	Y41G9A.5
ajm-1	C35E7.6	crn-3	F13D11.4	fmo-1	lect-2	pab-2	shc-2	tag-273	Y42G9A.3
alfa-1	C36E8.1	csq-1	F13H10.5	fntb-1	let-268	pals-23	shn-1	tag-297	Y43F8B.3
alh-9	C39B5.2	ctb-1	F13H8.5	gars-1	let-391	pat-9	sipa-1	tag-343	Y47G6A.19
aman-1	C44C10.9	ctbp-1	F14B6.3	gei-15	let-805	pck-2	skn-1	tag-65	Y47G6A.22
ampd-1	C48E7.1	ctc-1	F14B8.5	gpa-17	let-858	pcp-2	skr-20	tba-4	Y48E1B.8
anmt-2	C48E7.6	cth-1	F15B9.10	gpb-2	lfi-1	pes-8	skr-3	tba-7	Y4C6B.5
apl-1	C52E12.1	cth-2	F17A9.4	grd-3	lgc-22	pfd-1	slc-25A10	tbc-7	Y51H7C.1
asb-1	cab-1	ctsa-3.1	F17A9.5	grd-5	lgx-1	pgk-1	slo-1	tep-1	Y53C10A.5
asd-2	cacn-1	ctsa-4.2	F18E3.12	grh-1	lim-8	pgp-5	slt-1	tln-1	Y53F4B.20
asfl-1	cam-1	cus-2	F19B2.5	grl-10	lin-12	pgp-9	smd-1	tni-1	Y53F4B.25
asp-4	capg-1	cut-3	F19F10.11	gst-10	lin-14	phat-1	smo-1	tnt-2	Y53H1B.2
atgp-1	cdc-5L	cutl-16	F19F10.9	H11E01.3	lin-45	pho-11	sna-1	tofu-2	Y54E10A.17
athp-2	cdh-1	cutl-23	F21A3.3	H20J04.4	lips-3	pho-7	snpc-1.1	top-2	Y54G2A.45
attf-2	cdh-5	cutl-29	F21C10.7	H24G06.1	lntl-1	phy-2	snpc-1.3	try-10	Y54G2A.75
attf-6	cdk-11.1	cutl-9	F22B8.7	haf-7	lpd-7	plrg-1	snpc-4	tsp-14	Y57G11B.5
B0001.5	cdk-12	cwn-1	F25B4.7	hars-1	lpr-4	pmp-4	snr-2	ttbk-7	Y59E9AL.36
B0205.14	cec-7	cyc-2.1	F25E2.2	hbl-1	lrch-1	pmt-2	snr-3	ttn-1	Y64G10A.7
B0303.11	ceh-32	cyn-6	F26A10.2	hex-2	lsy-13	ppm-1.D	snr-4	ttr-18	Y65B4A.2
B0353.1	ceh-34	cyp-25A1	F26F12.3	hil-2	lys-7	pqn-22	snr-7	ttr-2	Y66D12A.19
B0464.6	ceh-37	cyp-42A1	F26F12.4	hil-3	M02H5.8	prg-1	snrp-200	twk-31	Y69H2.3
B0495.7	ceh-43	cysl-1	F32D1.5	hil-7	M03C11.8	pro-2	snx-6	txdc-12.1	Y6D1A.2
bam-2	ceh-86	D1086.6	F32D8.4	hpo-15	M03D4.4	prom-1	somi-1	uaf-2	Y71A12B.12
bbs-5	cest-17	D1086.7	F35E12.6	hpo-34	M03F8.3	prp-21	sorb-1	ugt-12	Y71F9AL.8
bckd-1A	cest-25	dao-5	F35G12.5	hpo-6	M153.1	prp-31	sox-2	ugt-23	Y71H2AM.15
bcl-11	cex-1	dbt-1	F37H8.5	hum-6	mab-7	prp-4	spd-2	ugt-26	Y73E7A.8
BE0003N10.3	cfz-2	dct-18	F39H11.1	ifb-1	mafr-1	ptl-1	spon-1	ugt-28	Y92H12BR.2
best-21	chd-1	ddx-15	F40H7.12	igcm-1	mca-2	ptp-1	spp-17	ugt-29	Y97E10C.1
best-26	clec-186	ddx-17	F41F3.3	igcm-4	mcu-1	ptr-16	spp-2	ugt-41	ZC190.4
blmp-1	clec-209	deb-1	F41G3.3	iglr-3	mig-1	ptr-23	strm-1	ugt-47	ZC247.2
bus-19	clec-265	del-6	F42A10.5	imb-1	mig-17	pyk-1	sup-12	ugt-63	zfh-2
C01F1.3	clec-56	dex-1	F44A2.5	insc-1	mig-6	pyp-1	syd-2	unc-1	ZK1053.4
C01G6.3	clh-1	dhs-25	F44E2.4	inx-12	mltn-9	R02F11.1	syf-1	unc-112	ZK1058.3
C02B10.3	clip-1	dhs-3	F45E1.4	inx-13	mnp-1	R02F2.1	syg-1	unc-115	ZK1320.9
C02F5.14	cnc-8	dhs-5	F46C8.3	inx-2	mog-5	R05A10.3	syg-2	unc-120	ZK1321.4
C04F12.5	coel-1	disl-2	F48E3.8	inx-3	mrp-2	R07B7.2	sym-2	unc-2	ZK180.5
C05C10.3	col-101	dlg-1	F53B3.5	inx-5	mrp-8	R07E3.6	syx-16	unc-27	ZK287.4
C05D10.4	col-103	dnj-9	F53F4.11	ipgm-1	mth-1	R07E5.19	T01B6.1	unc-37	ZK512.2
C05D9.3	col-106	dpf-2	F54D1.6	irg-4	myo-3	R08D7.1	T01D3.3	unc-53	ZK546.5
C05E11.3	col-122	dpy-18	F54D5.5	irx-1	myo-5	R08F11.1	T02G5.7	unc-6	zmp-2
C06E7.4	col-124	dpy-27	F54F7.2	ivns-1	nars-1	R08F11.4	T05B11.4	unc-82	ztf-13

Table 8.2: Shared eCLIP targets of SF1 and SF3A2 in MEFs.

Peak cutoff was set at log2foldchange>2, -log10(P-value)>2. Data from reproducible peaks in two biological replicates.

2410002F23Rik	Ccnd2	Eif4a1	Hmgb2	Mvk	Plec	Slc25a36	Tnpo1	Ythdf3
Abcc5	Ccnl1	Eif4b	Hmgcr	Mycbp2	Plekha5	Slc35b3	Tnrc18	Zc2hc1a
Abce1	Ccnl2	Eif4enif1	Hnrnpa1	Myef2	Plekhh2	Slc3a2	Tns2	Zc3h7a
Acaca	Ccnt2	Eif4g2	Hnrnpa2b1	Myl6	Pnisr	Slc4a7	Top2a	Zeb1
Actr3	Cd2ap	Eif5	Hnrnpa3	Myo10	Postn	Slmap	Tpm2	Zfc3h1
Adam9	Cdc123	Eno1	Hnrnpd	Myo9a	Ppm1b	Smc4	Tpp2	Zfhx3
Adgrg6	Cdk1	Ep300	Hnrnpdl	Myof	Ppp1r12a	Smc5	Tra2b	Zfp148
Adgrl1	Cdk4	Epb41l2	Hnrnph1	Naa16	Ppp2r2a	Smchd1	Trio	Zfp207
Aebp1	Cep170	Eps15l1	Hnrnpk	Naa25	Ppp3cb	Smg1	Trip12	Zfp532
Agtpbp1	Cfl2	Erbin	Hnrnpu	Nap1l1	Ppp4r2	Snd1	Trpm7	Zfp638
Ahctf1	Chd2	Esyt2	Hp1bp3	Ncam1	Prkci	Snhg1	Trrap	Zfp948
Ahcyl1	Clasp2	Evc	Hspa9	Ncor1	Prpf39	Matr3	Ttc14	Zmynd8
Ahr	Clk1	Ewsr1	Hspg2	Neat1	Psap	Socs5	Ttc3	Zwint
Akap11	Clk4	Eya4	Huwe1	Nedd4	Psmd14	Son	U2af1	Zyx
Akt3	Cnn3	F3	Il1rl1	Nf1	Psme4	Sparc	U2af2	Zzz3
Angpt1	Cnot1	Fam91a1	Il6st	Nfat5	Pspc1	Sptan1	Ubap2	mmu-mir-125b-1
Ank	Cnot7	Far1	Immt	Nfkbiz	Ptbp2	Sptbn1	Ubap2l	mmu-mir-18a
Ankrd10	Col11a1	Fbln2	Ints6	Nfx1	Ptcd3	Sqle	Ube2d3	mmu-mir-19a
Ankrd17	Col1a2	Fbn2	Ints7	Nipbl	Ptma	Srcap	Ube2i	mmu-mir-23b
Ankrd28	Col3a1	Fgf7	Ipo8	Nktr	Pum2	Srek1	Ubp1	mmu-mir-301a
Anxa1	Col5a1	Fgfr1	Kansl2	Nmd3	Rab2a	Srrm1	Ubr3	tRNA-Gly-CCC-1-2
Aopep	Col5a2	Fhl3	Kirrel	Nono	Racgap1	Srrm2	Ubr4	tRNA-His-GTG-2-8
Ap1g1	Col6a1	Fip1l1	Kmt2e	Nop56	Ranbp2	Srsf1	Ubr5	tRNA-Ile-AAT-1-7
Araf	Col6a2	Flna	Kpnb1	Npepps	Rbfox2	Srsf10	Uhrf2	tRNA-Thr-AGT-2-1
Arglu1	Cpsf6	Flnb	Ktn1	Npm1	Rbm25	Srsf11	Usp14	
Arhgef40	Cpsf7	Fmnl3	Lamp2	Nptn	Rbm26	Srsf3	Usp24	
Asap1	Crebzf	Fmr1	Laptm4a	Nsfl1c	Rbm3	Srsf5	Usp34	
Asph	Csde1	Fn1	Larp4b	Nup153	Rbm39	Srsf6	Usp36	
Atad2	Csf1	Fndc3a	Lmbrd1	Oasl2	Rbpj	Ssbp1	Usp7	
Atp13a3	Csnk1a1	Fnip2	Lmo7	Oga	Rcc2	Stat2	Utrn	
Atp2b1	Cspp1	Foxp1	Lrch3	Ogt	Rictor	Stxbp3	Vapa	
Atp2c1	Cyp51	Fubp1	Lrp1	Orc4	Rnf213	Taf15	Vcan	
Atp6v0c	Dab1	Fus	Lrp6	Otud4	Rpl10	Tardbp	Vcl	
Atrx	Dab2	Fxr1	Luc7l	Pan3	Rpl17	Tbc1d31	Wac	
Atxn1	Dazap1	Gas5	Luc7l2	Pbx1	Rpl9	Tbc1d5	Wapl	
Azin1	Ddr2	Gls	Lyst	Pcm1	Rprml	Tbce	Washc1	
Bclaf1	Ddx46	Gm17066	Macf1	Pdcd6ip	Rrbp1	Tbl1x	Washc4	
Best3	Dhx36	Gm22685	Malat1	Pdgfrb	Rsrc2	Tbl1xr1	Wdr26	
Birc6	Dld	Gm22951	Map4k3	Pdlim7	Sc5d	Tcerg1	Wdr43	
Bora	Dleu2	Gm23744	Map4k4	Pds5a	Sec24b	Tcf4	Wls	
Bptf	Dlg1	Gm25106	Mat2a	Pds5b	Sec31a	Tent2	Wnk1	
Brd2	Dnajc13	Gm26652	Matr3|Snhg4	Phf20l1	Sec61a2	Tex10	Wsb1	
Brwd1	Dnm1	Gm42664	Mbnl1	Phip	Setd5	Thoc1	Wtap	
C430049B03Rik	Dnm2	Gnl3	Mbnl2	Phka2	Setdb1	Thoc2	Wwc2	
Cald1	Dnm3os	Gtf2a2	Mdm2	Phldb1	Sf1	Thrap3	Wwp2	
Caprin1	Dock7	Gulp1	Meaf6	Picalm	Sf3b3	Tia1	Xpo1	
Cbfb	Dst	H2az1	Mettl26	Pja2	Sfswap	Tial1	Xpo4	
Cblb	Dzip1	Hltf	Mme	Pkd1	Ska2	Timp3	Xpo6	
Ccar1	Ecpas	Hmga2	Mtbp	Pkd2	Slc20a1	Tmem245	Xpot	
Ccdc88a	Eif3a	Hmgb1	Mtdh	Plcg1	Slc25a3	Tnks	Ythdc1	

Table 8.3: Shared eCLIP targets of SFA-1 and REPO-1 in *C. elegans*.

Peak cutoff was set at log2foldchange>1, -log10(P-value)>1. Data obtained from one biological replicate.

Shared targets	Unique REPO-1 targets				Unique SFA-1 targets					
alh-8	B0491.5	cchl-1	let-767	sqd-1	B0379.1	T02G5.7	Y82E9BR.17	fust-1	osm-3	sygl-1
atx-2	C18E9.4	cdc-25.1	lin-45	srap-1	C12D8.1	T04A6.1	Y82E9BR.19	fzr-1	par-1	syx-16
C04G6.12	C23H5.8	ced-10	mdh-2	stt-3	C16A3.5	T04A8.7	ZC262.2	gei-17	parg-1	tRNA-Lys-CTT-1-12
C16D9.11	C25H3.9	cel-mir-8191	mdt-9	sucl-2	C18H9.6	T05H10.1	ZK484.3	gfat-1	pas-5	tRNA-Pro-TGG-6-1
ctc-2	C50D2.8	cey-3	mesp-1	tRNA-Ile-TAT-1-1	C27H6.5	T07A9.14	ZK484.9	gfat-2	pod-1	tRX-000006
D1086.10	F07H5.4	clec-50	mir-2214	tRNA-Ser-AGA-2-2	C42C1.11	T08G11.1	ZK643.5	gld-3	pqn-22	tRX-000026
F31F7.1	F27D4.1	col-147	mrpr-1	tRNA-Ser-TGA-6-1	C46C2.8	T10B9.11	ZK829.7	glh-2	pqn-53	tac-1
F56D5.4	F37C4.5	col-98	mtch-1	tRNA-Thr-TGT-1-5	C51F7.3	T10C6.6	ZK994.7	gls-1	pqn-70	tag-10
fln-1	F45F2.10	cpr-5	myo-1	tRX-000019	C56A3.6	T19B4.8	acdh-1	gpcp-2	pqn-83	tcer-1
H06I04.9	H28O16.1	ctb-1	nduo-1	tRX-000059	D1086.7	T27A3.9	acs-2	grsp-1	prp-6	tlk-1
H09I01.2	H34I24.2	ctc-1	nduo-2	tbb-1	E04F6.8	T28B11.1	alh-11	gsr-1	ptc-1	top-2
ima-3	MTCE.13	ctf-4	nep-17	tcc-1	F07H5.5	T28D6.10|T2	alh-6	hcf-1	rab-11.1	tpi-1
ketn-1	MTCE.13|MTCE.14	cyb-2.2	nfx-1	tkt-1	F08H9.10	T28H10.3	atf-7	hecd-1	rab-5	tpxl-1
mak-1	MTCE.20	cyn-5	nhr-97	tufm-1	F10G7.9	W04D2.7	atn-1	hif-1	rad-23	ttn-1
MTCE.8	MTCE.28	dhhc-6	nlp-36	ubc-25	F12F6.1	Y105E8A.25	bca-2	him-1	rbm-5	ttr-50
oma-1	MTCE.30	dlat-1	nmt-1	ubq-1	F12F6.11	Y106G6D.7	ccch-1	hlh-30	rbpl-1	uaf-1
pck-1	MTCE.33	dld-1	nog-1	ubql-1	F13H10.8	Y111B2A.12	cco-2	hrpf-1	ret-1	ubl-1
pck-2	MTCE.8|MTCE.9	dnj-13	npa-1	ucr-1	F19H8.6	Y119D3B.12	cct-5	hrpu-1	rig-6	ubr-5
pod-2	MTCE.9	dod-23	npp-12	uev-1	F21D5.1	Y14H12B.2	ceh-44	idh-1	rnh-1.0	unc-116
prg-2	R07H5.8	eef-2	npp-18	unc-54	F28B3.6	Y17G7B.10	clec-84	ifet-1	rnp-1	unc-43
rpl-3	R13H4.2	egl-45	npp-9	vgln-1	F28D9.4	Y17G7B.20	clp-1	ifg-1	rpl-17	unc-49
rpn-13	T07C4.3	enol-1	nrd-1	vha-19	F28F8.10	Y17G7B.21	cng-1	ile-1	rpl-22	unc-89
rps-13	T09B4.5	epc-1	oaz-1	vha-2	F29C4.2	Y24D9A.10	col-103	isp-1	rpn-1	upb-1
rps-20	T12E12.1	far-6	ostb-1	vhp-1	F38E11.14	Y37E3.1	col-142	kin-1	rps-17	vab-10
rrn-3.1	T13C2.6	fasn-1	pam-1		F39G3.3	Y37H9A.5	cpb-3	kin-18	rps-4	vha-3
sams-3	T19D12.2	fbxl-1	par-5		F53H1.1	Y41E3.1	cpz-1	lat-1	rsd-6	vms-1
sfa-1	T26A8.6	gck-1	pbs-2		F55F8.3	Y48G8AL.10	cyc-1	lea-1	rsp-1	wago-1
snrp-200	Y39A3CL.7	gpdh-2	pbs-7		F56A8.3	Y53G8AR.9	daf-16	let-711	rsp-7	wago-4
T06D8.11	Y41D4A.5	gpi-1	pdi-1		F57C9.4	Y54G2A.50	ddx-17	lev-11	saps-1	xrep-4
tos-1	Y54F10AM.5	grd-3	pisy-1		F59E12.6	Y55F3AM.3	dhc-1	lid-1	sax-7	zip-8
tRNA-Leu-TAG-1-2	Y94H6A.8	gta-1	pptr-1		K07C10.6	Y57E12AL.1	dhhc-2	lin-5	scav-2	zyg-11
tRNA-Lys-CTT-1-1	ZK228.4	his-67	pyc-1		K07C5.4	Y57G11C.11	dig-1	lpd-3	set-2	
tRNA-Lys-CTT-1-9	aars-2	hpd-1	repo-1		K07H8.10	Y57G11C.9	eel-1	mbtr-1	skr-1	
tRNA-Ser-AGA-2-1	alh-9	hphd-1	rme-2		K08D12.6	Y59C2A.3	egg-2	mca-3	sls-2.16	
tRNA-Ser-TGA-1-1	asp-10	hrdl-1	rnp-7		K08E3.5	Y61A9LA.3	eif-3.D	mdt-15	sls-2.2	
tRNA-Thr-CGT-3-1	asp-5	hrpk-1	rnr-1		K09F6.10	Y65B4A.6	emb-9	mig-6	sls-2.8	
tRX-000018	asp-6	imb-3	rpia-1		K09F6.6	Y69H2.7	emc-2	mnk-1	sma-10	
tRX-000022	atp-4	imp-1	rpl-11.1		M01H9.3	Y71D11A.7	emr-1	ncbp-2	sms-1	
unc-22	bath-20	inf-1	rpl-41.1		M04F3.2	Y71G10AL.1	eri-6	ncx-2	smy-10	
unc-52	bath-44	kin-10	sams-4		MTCE.14	Y73B6A.6	ero-1	nhr-274	spk-1	
Y17G7B.8	bckd-1B	kin-19	spd-2		R12B2.6	Y75B8A.24	etr-1	nono-1	sqv-2	
Y39E4B.6	cap-2	laf-1	spd-5		R53.4	Y75B8A.6	fbp-1	nos-2	sup-39|mir-1831	
Y82E9BR.2	cbp-1	lec-5	spn-4		T01H3.2	Y79H2A.3	frm-1	nuo-5	sup-6	

Appendix III- Abbreviations

DR: Dietary Restriction

C. elegans: *Caenorhabditis elegans*

bDR: Bacterial Liquid Dietary Restriction

sDR: Solid Plate Dietary Restriction

BD: Bacterial Deprivation

IF: Intermittent Fasting

AMPK: AMP-activated Protein Kinase

TOR: Target of Rapamycin

TORC1: Target of Rapamycin Complex 1

S6K: Ribosomal Protein S6 Kinase

FOXO: Forkhead box O

UPR: Unfolded Protein Response

mtUPR: Mitochondrial Unfolded Protein Response

CRISPR: Clustered Regularly Interspaced Short Palindromic Repeats

TFEB: Transcription Factor EB

SF1: Splicing Factor 1

BBP: Branchpoint Binding Protein

REPO-1: Reversed Polarity (in early embryos) 1

SRSF: Serine/arginine-rich Splicing Factor

SL: Short life expectancy

LL: Long life expectancy

NIA: National Institute of Aging

REFERENCES

Adusumalli S, Ngian Z, Lin W, et al. (2019) Increased intron retention is a post-transcriptional signature associated with progressive aging and Alzheimer's disease. *Aging Cell*. DOI: 10.1111/acel.12928.

Ahringer J (2006) *Reverse Genetics*. WormBook.

Apfeld J, O'Connor G, McDonagh T, et al. (2004) The AMP-activated protein kinase AAK-2 links energy levels and insulin-like signals to lifespan in C. elegans. *Genes & development* 18(24): 3004–3009.

Barrows CH and Roeder LM (1965) The Effect of Reduced Dietary Intake on Enzymatic Activities and Life Span of Rats. *Journal of Gerontology*. DOI: 10.1093/geronj/20.1.69.

Bazopoulou D, Knoefler D, Zheng Y, et al. (2019) Developmental ROS individualizes organismal stress resistance and lifespan. *Nature* 576(7786). Nature Publishing Group: 301–305.

Bennett CF and Kaeberlein M (2014) The mitochondrial unfolded protein response and increased longevity: Cause, consequence, or correlation? *Experimental Gerontology*. DOI: 10.1016/j.exger.2014.02.002.

Bhadra M, Howell P, Dutta S, et al. (2020) Alternative splicing in aging and longevity. *Human genetics* 139(3): 357–369.

Bishop NA and Guarente L (2007) Two neurons mediate diet-restriction-induced longevity in C. elegans. *Nature*. DOI: 10.1038/nature05904.

Bjedov I, Toivonen JM, Kerr F, et al. (2010) Mechanisms of life span extension by rapamycin in the fruit fly Drosophila melanogaster. *Cell metabolism* 11(1): 35–46.

Blaustein M, Pelisch F, Tanos T, et al. (2005) Concerted regulation of nuclear and cytoplasmic activities of SR proteins by AKT. *Nature Structural & Molecular Biology*. DOI: 10.1038/nsmb1020.

Blüher M, Kahn BB and Kahn CR (2003) Extended longevity in mice lacking the insulin receptor in adipose tissue. *Science* 299(5606): 572–574.

Brandhorst S and Longo VD (2016) Fasting and Caloric Restriction in Cancer Prevention and Treatment. *Metabolism in Cancer*. DOI: 10.1007/978-3-319-42118-6_12.

Burkewitz K, Weir HJM and Mair WB (2016) AMPK as a Pro-longevity Target. *Experientia. Supplementum* 107: 227–256.

Burkewitz K, Feng G, Dutta S, et al. (2020) Atf-6 Regulates Lifespan through ER-Mitochondrial Calcium Homeostasis. *Cell Reports*. DOI: 10.1016/j.celrep.2020.108125.

Chang J-W, Zhang W, Yeh H-S, et al. (2015) mRNA 3′-UTR shortening is a molecular signature of mTORC1 activation. *Nature Communications*. DOI: 10.1038/ncomms8218.

Chang J-W, Yeh H-S, Park M, et al. (2019) mTOR-regulated U2af1 tandem exon splicing specifies transcriptome features for translational control. *Nucleic Acids Research*. DOI: 10.1093/nar/gkz761.

Chen D, Thomas EL and Kapahi P (2009) HIF-1 modulates dietary restriction-mediated lifespan extension via IRE-1 in Caenorhabditis elegans. *PLoS genetics* 5(5): e1000486.

Chen D, Li PW-L, Goldstein BA, et al. (2013) Germline Signaling Mediates the Synergistically Prolonged Longevity Produced by Double Mutations in daf-2 and rsks-1 in C. elegans. *Cell Reports*. DOI: 10.1016/j.celrep.2013.11.018.

Chetty R, Stepner M, Abraham S, et al. (2016) The Association Between Income and Life Expectancy in the United States, 2001-2014. *JAMA*. DOI: 10.1001/jama.2016.4226.

Clancy DJ (2001) Extension of Life-Span by Loss of CHICO, a Drosophila Insulin Receptor Substrate Protein. *Science*. DOI: 10.1126/science.1057991.

Colman RJ, Anderson RM, Johnson SC, et al. (2009) Caloric restriction delays disease onset and mortality in rhesus monkeys. *Science* 325(5937): 201–204.

Colman RJ, Mark Beasley T, Kemnitz JW, et al. (2014) Caloric restriction reduces age-related and all-cause mortality in rhesus monkeys. *Nature Communications*. DOI: 10.1038/ncomms4557.

Conway JR, Lex A and Gehlenborg N (2017) UpSetR: an R package for the visualization of intersecting sets and their properties. *Bioinformatics* 33(18): 2938–2940.

Corsi AK (2015) A Transparent window into biology: A primer on Caenorhabditis elegans. *WormBook*. DOI: 10.1895/wormbook.1.177.1.

Curran SP and Ruvkun G (2005) Lifespan regulation by evolutionarily conserved genes essential for viability. *PLoS Genetics*. DOI: 10.1371/journal.pgen.0030056.eor.

Curtis R, O'Connor G and DiStefano PS (2006) Aging networks in Caenorhabditis elegans: AMP-activated protein kinase (aak-2) links multiple aging and metabolism pathways. *Aging cell* 5(2). Wiley: 119–126.

Dillin A, Hsu A-L, Arantes-Oliveira N, et al. (2002) Rates of behavior and aging specified by mitochondrial function during development. *Science* 298(5602): 2398–2401.

Dirks AJ and Leeuwenburgh C (2006) Caloric restriction in humans: potential pitfalls and health concerns. *Mechanisms of ageing and development* 127(1): 1–7.

Dobin A, Davis CA, Schlesinger F, et al. (2013) STAR: ultrafast universal RNA-seq aligner. *Bioinformatics* 29(1): 15–21.

Durieux J, Wolff S and Dillin A (2011) The cell-non-autonomous nature of electron transport chain-mediated longevity. *Cell* 144(1): 79–91.

Escorcia W, Ruter DL, Nhan J, et al. (2018) Quantification of Lipid Abundance and Evaluation of Lipid Distribution in Caenorhabditis elegans by Nile Red and Oil Red O Staining. *Journal of Visualized Experiments*. DOI: 10.3791/57352.

Escoubas CC, Silva-García CG and Mair WB (2017) Deregulation of CRTCs in Aging and Age-Related Disease Risk. *Trends in genetics: TIG* 33(5): 303–321.

Fernandes G, Yunis EJ and Good RA (1976) Influence of diet on survival of mice. *Proceedings of the National Academy of Sciences*. DOI: 10.1073/pnas.73.4.1279.

Fontana L and Partridge L (2015) Promoting health and longevity through diet: from model organisms to humans. *Cell* 161(1): 106–118.

Forster MJ, Morris P and Sohal RS (2003) Genotype and age influence the effect of caloric intake on mortality in mice. *The FASEB Journal*. DOI: 10.1096/fj.02-0533fje.

Friedman DB and Johnson TE (1988) A mutation in the age-1 gene in Caenorhabditis elegans lengthens life and reduces hermaphrodite fertility. *Genetics* 118(1): 75–86.

Fujita K, Mondal AM, Horikawa I, et al. (2009) p53 isoforms Δ133p53 and p53β are endogenous regulators of replicative cellular senescence. *Nature Cell Biology*. DOI: 10.1038/ncb1928.

García-Alcalde F, Okonechnikov K, Carbonell J, et al. (2012) Qualimap: evaluating next-generation sequencing alignment data. *Bioinformatics* 28(20): 2678–2679.

Geiss GK, Bumgarner RE, Birditt B, et al. (2008) Direct multiplexed measurement of gene expression with color-coded probe pairs. *Nature Biotechnology*. DOI: 10.1038/nbt1385.

Goldman DP, Cutler D, Rowe JW, et al. (2013) Substantial health and economic returns from delayed aging may warrant a new focus for medical research. *Health affairs* 32(10): 1698–1705.

Greer EL, Banko MR and Brunet A (2009) AMP-activated protein kinase and FoxO transcription factors in dietary restriction-induced longevity. *Annals of the New York Academy of Sciences* 1170(1). Wiley: 688–692.

Haley-Zitlin V and Richardson A (1993) Effect of dietary restriction on DNA repair and DNA damage. *Mutation Research/DNAging*. DOI: 10.1016/0921-8734(93)90023-v.

Hansen M, Taubert S, Crawford D, et al. (2007) Lifespan extension by conditions that inhibit translation in Caenorhabditis elegans. *Aging cell* 6(1): 95–110.

Hansen M, Chandra A, Mitic LL, et al. (2008) A role for autophagy in the extension of lifespan by dietary restriction in C. elegans. *PLoS genetics* 4(2). Public Library of Science (PLoS): e24.

Harper JM, Leathers CW and Austad SN (2006) Does caloric restriction extend life in wild mice? *Aging Cell*. DOI: 10.1111/j.1474-9726.2006.00236.x.

Harries LW, Hernandez D, Henley W, et al. (2011) Human aging is characterized by focused changes in gene expression and deregulation of alternative splicing. *Aging Cell*. DOI: 10.1111/j.1474-9726.2011.00726.x.

Harrison DE and Archer JR (1987) Genetic Differences in Effects of Food Restriction on Aging in Mice. *The Journal of Nutrition*. DOI: 10.1093/jn/117.2.376.

Harrison DE, Strong R, Sharp ZD, et al. (2009) Rapamycin fed late in life extends lifespan in genetically heterogeneous mice. *Nature*. DOI: 10.1038/nature08221.

Heestand BN, Shen Y, Liu W, et al. (2013) Dietary restriction induced longevity is mediated by nuclear receptor NHR-62 in Caenorhabditis elegans. *PLoS genetics* 9(7): e1003651.

Heintz C, Doktor TK, Lanjuin A, et al. (2017) Corrigendum: Splicing factor 1 modulates dietary restriction and TORC1 pathway longevity in C. elegans. *Nature* 547(7664): 476.

Henderson ST and Johnson TE (2001) daf-16 integrates developmental and environmental inputs to mediate aging in the nematode Caenorhabditis elegans. *Current biology: CB* 11(24): 1975–1980.

Holdorf AD, Higgins DP, Hart AC, et al. (2020) WormCat: An Online Tool for Annotation and Visualization of Caenorhabditis elegans Genome-Scale Data. *Genetics* 214(2): 279–294.

Holly AC, Melzer D, Pilling LC, et al. (2013) Changes in splicing factor expression are associated with advancing age in man. *Mechanisms of Ageing and Development*. DOI: 10.1016/j.mad.2013.05.006.

Holzenberger M, Dupont J, Ducos B, et al. (2003) IGF-1 receptor regulates lifespan and resistance to oxidative stress in mice. *Nature* 421(6919): 182–187.

Honjoh S, Yamamoto T, Uno M, et al. (2009) Signalling through RHEB-1 mediates intermittent fasting-induced longevity in C. elegans. *Nature* 457(7230): 726–730.

Houthoofd K, Braeckman BP, Lenaerts I, et al. (2002) No reduction of metabolic rate in food restricted Caenorhabditis elegans. *Experimental gerontology* 37(12): 1359–1369.

Jia K and Levine B (2007) Autophagy is required for dietary restriction-mediated life span extension in C. elegans. *Autophagy* 3(6): 597–599.

Jia K, Chen D and Riddle DL (2004) The TOR pathway interacts with the insulin signaling pathway to regulateC. eleganslarval development, metabolism and life span. *Development*. DOI: 10.1242/dev.01255.

Jiang K, Patel NA, Watson JE, et al. (2009) Akt2 Regulation of Cdc2-Like Kinases (Clk/Sty), Serine/Arginine-Rich (SR) Protein Phosphorylation, and Insulin-Induced Alternative Splicing of PKCβII Messenger Ribonucleic Acid. *Endocrinology*. DOI: 10.1210/en.2008-0818.

Johnson SC, Rabinovitch PS and Kaeberlein M (2013) mTOR is a key modulator of ageing and age-related disease. *Nature*. DOI: 10.1038/nature11861.

Kaeberlein TL, Smith ED, Tsuchiya M, et al. (2006) Lifespan extension in Caenorhabditis elegans by complete removal of food. *Aging Cell*. DOI: 10.1111/j.1474-9726.2006.00238.x.

Kapahi P, Zid BM, Harper T, et al. (2004) Regulation of lifespan in Drosophila by modulation of genes in the TOR signaling pathway. *Current biology: CB* 14(10): 885–890.

Kapahi P, Chen D, Rogers AN, et al. (2010) With TOR, Less Is More: A Key Role for the Conserved Nutrient-Sensing TOR Pathway in Aging. *Cell Metabolism*. DOI: 10.1016/j.cmet.2010.05.001.

Katewa SD, Demontis F, Kolipinski M, et al. (2012) Intramyocellular Fatty-Acid Metabolism Plays a Critical Role in Mediating Responses to Dietary Restriction in Drosophila melanogaster. *Cell Metabolism*. DOI: 10.1016/j.cmet.2012.06.005.

Keikhaee MR, Nash EB, O'Rourke SM, et al. (2014) A semi-dominant mutation in the general splicing factor SF3a66 causes anterior-posterior axis reversal in one-cell stage C. elegans embryos. *PloS one* 9(9): e106484.

Kenyon C (2011) The first long-lived mutants: discovery of the insulin/IGF-1 pathway for ageing. *Philosophical transactions of the Royal Society of London. Series B, Biological sciences* 366(1561): 9–16.

Kenyon C, Chang J, Gensch E, et al. (1993) A C. elegans mutant that lives twice as long as wild type. *Nature* 366(6454): 461–464.

Klass MR (1977) Aging in the nematode Caenorhabditis elegans: major biological and environmental factors influencing life span. *Mechanisms of ageing and development* 6(6): 413–429.

Krämer A (1992) Purification of splicing factor SF1, a heat-stable protein that functions in the assembly of a presplicing complex. *Molecular and cellular biology* 12(10): 4545–4552.

Kuroyanagi H, Watanabe Y, Suzuki Y, et al. (2013) Position-dependent and neuron-specific splicing regulation by the CELF family RNA-binding protein UNC-75 in Caenorhabditis elegans. *Nucleic acids research* 41(7): 4015–4025.

Lakowski B and Hekimi S (1998) The genetics of caloric restriction in Caenorhabditis elegans. *Proceedings of the National Academy of Sciences of the United States of America* 95(22): 13091–13096.

Lamming DW (2005) HST2 Mediates SIR2-Independent Life-Span Extension by Calorie Restriction. *Science*. DOI: 10.1126/science.1113611.

Lapierre LR, De Magalhaes Filho CD, McQuary PR, et al. (2013) The TFEB orthologue HLH-30 regulates autophagy and modulates longevity in Caenorhabditis elegans. *Nature communications* 4: 2267.

Larson-Meyer DE, Heilbronn LK, Redman LM, et al. (2006) Effect of calorie restriction with or without exercise on insulin sensitivity, β-cell function, fat cell size, and ectopic lipid in overweight subjects. *Diabetes care* 29(6). Am Diabetes Assoc: 1337–1344.

Latorre E, Ostler EL, Faragher RGA, et al. (2019) FOXO1 and ETV6 genes may represent novel regulators of splicing factor expression in cellular senescence. *The FASEB Journal*. DOI: 10.1096/fj.201801154r.

Lee BP, Pilling LC, Emond F, et al. (2016) Changes in the expression of splicing factor transcripts and variations in alternative splicing are associated with lifespan in mice and humans. *Aging cell* 15(5): 903–913.

Lee BP, Pilling LC, Bandinelli S, et al. (2019) The transcript expression levels of HNRNPM, HNRNPA0 and AKAP17A splicing factors may be predictively associated with ageing phenotypes in human peripheral blood. *Biogerontology*. DOI: 10.1007/s10522-019-09819-0.

Lee G, Zheng Y, Cho S, et al. (2017) Post-transcriptional Regulation of De Novo Lipogenesis by mTORC1-S6K1-SRPK2 Signaling. *Cell* 171(7): 1545-1558.e18.

Lee RY, Hench J and Ruvkun G (2001) Regulation of C. elegans DAF-16 and its human ortholog FKHRL1 by the daf-2 insulin-like signaling pathway. *Current biology: CB* 11(24): 1950–1957.

Lev I, Bril R, Liu Y, et al. (2018) Inter-generational Consequences for Growing C.elegans in Liquid. *bioRxiv*. DOI: 10.1101/467837.

Liao C-Y, Rikke BA, Johnson TE, et al. (2010) Genetic variation in the murine lifespan response to dietary restriction: from life extension to life shortening. *Aging Cell*. DOI: 10.1111/j.1474-9726.2009.00533.x.

Lin K, Hsin H, Libina N, et al. (2001) Regulation of the Caenorhabditis elegans longevity protein DAF-16 by insulin/IGF-1 and germline signaling. *Nature genetics* 28(2): 139–145.

López-Otín C, Blasco MA, Partridge L, et al. (2013) The hallmarks of aging. *Cell* 153(6): 1194–1217.

Love MI, Huber W and Anders S (2014) Moderated estimation of fold change and dispersion for RNA-seq data with DESeq2. *Genome biology* 15(12): 550.

Lucanic M, Plummer WT, Chen E, et al. (2017) Impact of genetic background and experimental reproducibility on identifying chemical compounds with robust longevity effects. *Nature communications* 8: 14256.

Ma L and Robert Horvitz H (2009) Mutations in the Caenorhabditis elegans U2AF Large Subunit UAF-1 Alter the Choice of a 3′ Splice Site In Vivo. *PLoS Genetics*. DOI: 10.1371/journal.pgen.1000708.

Ma L, Tan Z, Teng Y, et al. (2011) In vivo effects on intron retention and exon skipping by the U2AF large subunit and SF1/BBP in the nematode Caenorhabditis elegans. *RNA* 17(12): 2201–2211.

Mair W and Dillin A (2008) Aging and survival: the genetics of life span extension by dietary restriction. *Annual review of biochemistry* 77: 727–754.

Mair W, Goymer P, Pletcher SD, et al. (2003) Demography of dietary restriction and death in Drosophila. *Science* 301(5640): 1731–1733.

Mair W, Morantte I, Rodrigues APC, et al. (2011) Lifespan extension induced by AMPK and calcineurin is mediated by CRTC-1 and CREB. *Nature* 470(7334). Nature Publishing Group: 404–408.

Mana MD, Kuo EY-S and Yilmaz ÖH (2017) Dietary Regulation of Adult Stem Cells. *Current Stem Cell Reports*. DOI: 10.1007/s40778-017-0072-x.

Matai L, Sarkar GC, Chamoli M, et al. (2019) Dietary restriction improves proteostasis and increases life span through endoplasmic reticulum hormesis. *Proceedings of the National Academy of Sciences*. DOI: 10.1073/pnas.1900055116.

Mattison JA, Roth GS, Mark Beasley T, et al. (2012) Impact of caloric restriction on health and survival in rhesus monkeys from the NIA study. *Nature* 489(7415). Nature Publishing Group: 318–321.

Mattison JA, Colman RJ, Beasley TM, et al. (2017) Caloric restriction improves health and survival of rhesus monkeys. *Nature communications* 8: 14063.

Mazin P, Xiong J, Liu X, et al. (2013) Widespread splicing changes in human brain development and aging. *Molecular systems biology* 9: 633.

McCay CM, Crowell MF and Maynard LA (1935) The Effect of Retarded Growth Upon the Length of Life Span and Upon the Ultimate Body Size: One Figure. *The Journal of nutrition* 10(1). Oxford Academic: 63–79.

McKenna T, Rosengardten Y, Viceconte N, et al. (2014) Embryonic expression of the common progeroid lamin A splice mutation arrests postnatal skin development. *Aging Cell*. DOI: 10.1111/acel.12173.

Melendez A (2003) Autophagy Genes Are Essential for Dauer Development and Life-Span Extension in C. elegans. *Science*. DOI: 10.1126/science.1087782.

Miller RA, Buehner G, Chang Y, et al. (2005) Methionine-deficient diet extends mouse lifespan, slows immune and lens aging, alters glucose, T4, IGF-I and insulin levels, and increases hepatocyte MIF levels and stress resistance. *Aging cell* 4(3): 119–125.

Mitchell SJ, Madrigal-Matute J, Scheibye-Knudsen M, et al. (2016) Effects of Sex, Strain, and Energy Intake on Hallmarks of Aging in Mice. *Cell metabolism* 23(6): 1093–1112.

National Center for Health Statistics (US) (2011) *Health, United States, 2010: With Special Feature on Death and Dying*. Hyattsville (MD): National Center for Health Statistics (US).

Nigon V and Dougherty EC (1949) Reproductive patterns and attempts at reciprocal crossing of Rhabditis elegans maupas, 1900, and Rhabditis briggsae Dougherty and nigon, 1949 (Nematoda: Rhabditidae). *Journal of Experimental Zoology*. DOI: 10.1002/jez.1401120307.

Okkema PG and Krause M (2005) Transcriptional regulation. *WormBook: the online review of C. elegans biology*: 1–40.

O'Rourke EJ and Ruvkun G (2013) MXL-3 and HLH-30 transcriptionally link lipolysis and autophagy to nutrient availability. *Nature Cell Biology*. DOI: 10.1038/ncb2741.

Paix A, Folkmann A, Rasoloson D, et al. (2015) High Efficiency, Homology-Directed Genome Editing in Caenorhabditis elegans Using CRISPR-Cas9 Ribonucleoprotein Complexes. *Genetics* 201(1): 47–54.

Pani G (2015) Neuroprotective effects of dietary restriction: Evidence and mechanisms. *Seminars in cell & developmental biology* 40: 106–114.

Panowski SH, Wolff S, Aguilaniu H, et al. (2007) PHA-4/Foxa mediates diet-restriction-induced longevity of C. elegans. *Nature* 447(7144): 550–555.

Pantano L (2019) DEGreport: Report of DEG analysis. *New Jersey, NJ: R package version* 1(0).

Papsdorf K and Brunet A (2019) Linking Lipid Metabolism to Chromatin Regulation in Aging. *Trends in Cell Biology*. DOI: 10.1016/j.tcb.2018.09.004.

Passacantilli I, Frisone P, De Paola E, et al. (2017) hnRNPM guides an alternative splicing program in response to inhibition of the PI3K/AKT/mTOR pathway in Ewing sarcoma cells. *Nucleic Acids Research*. DOI: 10.1093/nar/gkx831.

Patro R, Duggal G, Love MI, et al. (2017) Salmon provides fast and bias-aware quantification of transcript expression. *Nature methods* 14(4). Nature Publishing Group: 417–419.

Pellacani C, Bucciarelli E, Renda F, et al. (2018) Splicing factors Sf3A2 and Prp31 have direct roles in mitotic chromosome segregation. *eLife* 7. DOI: 10.7554/eLife.40325.

Perez-Matos MC and Mair WB (2020) Predicting longevity responses to dietary restriction: A stepping stone toward precision geroscience. *PLoS genetics*.

Raj B and Blencowe BJ (2015) Alternative Splicing in the Mammalian Nervous System: Recent Insights into Mechanisms and Functional Roles. *Neuron* 87(1): 14–27.

Rea SL (2005) Metabolism in the Caenorhabditis elegans Mit mutants. *Experimental gerontology* 40(11): 841–849.

Rea SL, Wu D, Cypser JR, et al. (2005) A stress-sensitive reporter predicts longevity in isogenic populations of Caenorhabditis elegans. *Nature genetics* 37(8). Nature Publishing Group: 894–898.

Rea SL, Ventura N and Johnson TE (2007) Relationship Between Mitochondrial Electron Transport Chain Dysfunction, Development, and Life Extension in Caenorhabditis elegans. *PLoS Biology*. DOI: 10.1371/journal.pbio.0050259.

Rechavi O, Houri-Ze'evi L, Anava S, et al. (2014) Starvation-induced transgenerational inheritance of small RNAs in C. elegans. *Cell* 158(2): 277–287.

Redman LM and Ravussin E (2011) Caloric restriction in humans: impact on physiological, psychological, and behavioral outcomes. *Antioxidants & redox signaling* 14(2): 275–287.

Rhoads TW, Burhans MS, Chen VB, et al. (2018) Caloric Restriction Engages Hepatic RNA Processing Mechanisms in Rhesus Monkeys. *Cell metabolism* 27(3): 677-688.e5.

Robida-Stubbs S, Glover-Cutter K, Lamming DW, et al. (2012) TOR signaling and rapamycin influence longevity by regulating SKN-1/Nrf and DAF-16/FoxO. *Cell metabolism* 15(5): 713–724.

Rodríguez SA, Grochová D, McKenna T, et al. (2016) Global genome splicing analysis reveals an increased number of alternatively spliced genes with aging. *Aging cell* 15(2): 267–278.

Rual J-F, Ceron J, Koreth J, et al. (2004) Toward improving Caenorhabditis elegans phenome mapping with an ORFeome-based RNAi library. *Genome research* 14(10b). Cold Spring Harbor Lab: 2162–2168.

Ruetenik A and Barrientos A (2015) Dietary restriction, mitochondrial function and aging: from yeast to humans. *Biochimica et biophysica acta* 1847(11): 1434–1447.

Sanidas I, Polytarchou C, Hatziapostolou M, et al. (2014) Phosphoproteomics Screen Reveals Akt Isoform-Specific Signals Linking RNA Processing to Lung Cancer. *Molecular Cell*. DOI: 10.1016/j.molcel.2013.12.018.

Schreiber MA, Pierce-Shimomura JT, Chan S, et al. (2010) Manipulation of behavioral decline in Caenorhabditis elegans with the Rag GTPase raga-1. *PLoS genetics* 6(5): e1000972.

Sedensky MM and Morgan PG (2006) Mitochondrial respiration and reactive oxygen species in mitochondrial aging mutants. *Experimental gerontology* 41(3): 237–245.

Seo K, Choi E, Lee D, et al. (2013) Heat shock factor 1 mediates the longevity conferred by inhibition of TOR and insulin/IGF-1 signaling pathways in C. elegans. *Aging cell* 12(6). Wiley: 1073–1081.

Sheaffer KL, Updike DL and Mango SE (2008) The Target of Rapamycin Pathway Antagonizes pha-4/FoxA to Control Development and Aging. *Current Biology*. DOI: 10.1016/j.cub.2008.07.097.

Sijen T, Fleenor J, Simmer F, et al. (2001) On the Role of RNA Amplification in dsRNA-Triggered Gene Silencing. *Cell*. DOI: 10.1016/s0092-8674(01)00576-1.

Silva-García CG, Lanjuin A, Heintz C, et al. (2019) Single-Copy Knock-In Loci for Defined Gene Expression in Caenorhabditis elegans. *G3* 9(7): 2195–2198.

Stilling RM, Benito E, Barth J, et al. (2014) De-regulation of gene expression and alternative splicing affects distinct cellular pathways in the aging hippocampus. *Frontiers in Cellular Neuroscience*. DOI: 10.3389/fncel.2014.00373.

Swindell WR (2009) Genes and gene expression modules associated with caloric restriction and aging in the laboratory mouse. *BMC Genomics*. DOI: 10.1186/1471-2164-10-585.

Tabrez SS, Sharma RD, Jain V, et al. (2017) Differential alternative splicing coupled to nonsense-mediated decay of mRNA ensures dietary restriction-induced longevity. *Nature Communications*. DOI: 10.1038/s41467-017-00370-5.

Tanackovic G and Krämer A (2005) Human splicing factor SF3a, but not SF1, is essential for pre-mRNA splicing in vivo. *Molecular biology of the cell* 16(3): 1366–1377.

Tatar M (2001) A Mutant Drosophila Insulin Receptor Homolog That Extends Life-Span and Impairs Neuroendocrine Function. *Science*. DOI: 10.1126/science.1057987.

Timmons L and Fire A (1998) Specific interference by ingested dsRNA. *Nature*. DOI: 10.1038/27579.

Tollervey JR, Wang Z, Hortobagyi T, et al. (2011) Analysis of alternative splicing associated with aging and neurodegeneration in the human brain. *Genome Research*. DOI: 10.1101/gr.122226.111.

Tóth ML, Sigmond T, Borsos E, et al. (2008) Longevity pathways converge on autophagy genes to regulate life span in Caenorhabditis elegans. *Autophagy* 4(3): 330–338.

Tullet JMA, Hertweck M, An JH, et al. (2008) Direct inhibition of the longevity-promoting factor SKN-1 by insulin-like signaling in C. elegans. *Cell* 132(6): 1025–1038.

Turturro A, Witt WW, Lewis S, et al. (1999) Growth Curves and Survival Characteristics of the Animals Used in the Biomarkers of Aging Program. *The Journals of Gerontology Series A: Biological Sciences and Medical Sciences*. DOI: 10.1093/gerona/54.11.b492.

Van Nostrand EL, Pratt GA, Shishkin AA, et al. (2016) Robust transcriptome-wide discovery of RNA-binding protein binding sites with enhanced CLIP (eCLIP). *Nature methods* 13(6). Nature Publishing Group: 508–514.

Vellai T, Takacs-Vellai K, Zhang Y, et al. (2003) Influence of TOR kinase on lifespan in C. elegans. *Nature*. DOI: 10.1038/426620a.

Wang MC, Min W, Freudiger CW, et al. (2011) RNAi screening for fat regulatory genes with SRS microscopy. *Nature Methods*. DOI: 10.1038/nmeth.1556.

Wang Y and Tissenbaum HA (2006) Overlapping and distinct functions for a Caenorhabditis elegans SIR2 and DAF-16/FOXO. *Mechanisms of Ageing and Development*. DOI: 10.1016/j.mad.2005.09.005.

Watts JL and Ristow M (2017) Lipid and Carbohydrate Metabolism in Caenorhabditis elegans. *Genetics* 207(2): 413–446.

Weindruch R and Walford RL (1988) *The Retardation of Aging and Disease by Dietary Restriction*. C.C. Thomas.

Weir HJ, Yao P, Huynh FK, et al. (2017) Dietary Restriction and AMPK Increase Lifespan via Mitochondrial Network and Peroxisome Remodeling. *Cell metabolism* 26(6): 884-896.e5.

Wilkie SE, Mulvey L, Sands WA, et al. (2020) Strain-specificity in the hydrogen sulphide signalling network following dietary restriction in recombinant inbred mice. *GeroScience*. DOI: 10.1007/s11357-020-00168-2.

Yuan Y, Kadiyala CS, Ching T-T, et al. (2012) Enhanced energy metabolism contributes to the extended life span of calorie-restricted Caenorhabditis elegans. *The Journal of biological chemistry* 287(37): 31414–31426.

Zhang Y, Lanjuin A, Chowdhury SR, et al. (2019) Neuronal TORC1 modulates longevity via AMPK and cell nonautonomous regulation of mitochondrial dynamics in C. elegans. *eLife* 8. DOI: 10.7554/eLife.49158.

Zhou Z, Qiu J, Liu W, et al. (2012) The Akt-SRPK-SR axis constitutes a major pathway in transducing EGF signaling to regulate alternative splicing in the nucleus. *Molecular cell* 47(3): 422–433.